Resource Management In 3G Systems Employing Smart Antennas

by

Shakheela H. Marikar

Thesis submitted to the Faculty of the

Virginia Polytechnic Institute and State University

in partial fulfillment of the requirements for the degree of

MASTER OF SCIENCE

in

Electrical Engineering

Approved:

Dr. Luiz A. DaSilva

Dr. Jeffrey H. Reed

Dr. Annamalai Annamalai

January 2002

Blacksburg, VA

Resource Management in 3G Systems Employing Smart Antennas

Shakheela H. Marikar

(Abstract)

Modern mobile communication systems will provide enhanced high-speed data, multimedia, and voice services to mobile users. The integration of such heterogeneous traffic types implies that the network must provide differentiated Quality of Service (QoS). Beam forming techniques have been proposed to increase the spectral efficiency of the wireless channel. Using beamforming in the network will lead to intra-cell handoffs within the cell due to user mobility. In a commercially deployed next generation cellular system, it is likely that beam forming and QoS guarantees to the users will co-exist. In this work we propose a resource allocation and management scheme tailored for a network that employs smart antennas in support of a heterogeneous user mix.

Resource management in a wireless system should take care of channel impairments and non-ideal antenna patterns. Mobile users moving from one beam to the other give rise to resource reallocation issues. Depending on the scatterer distribution in the cell, the Angle of Arrival (AoA) of the users will also change, affecting the interference pattern in the cell. In a system with data and multimedia users, some of the users are likely to be elastic in their demands for bandwidth. In this work, we propose a resource allocation and management scheme tailored for systems with smart antennas having heterogeneous users. The algorithm works by comparing the received power in the beams. Elasticity of user requirement for data services is exploited to provide adaptive QoS, thereby reducing the call dropping probability due to user mobility.

Simulation results showing the channel and Multiple Access Interference (MAI) effects on system performance are presented. The effect of channel coding to provide Bit Error Rate (BER) guarantees is studied. We also show the throughput advantage obtained using the resource management algorithms. It is also seen that the throughput of the system

increases for a user population having a higher elasticity. A modified resource allocation algorithm to reduce the blocking probability of the calls is presented and performance verified using simulation. The probability of call dropping in an unmanaged system due to user mobility is shown. Our studies show that using managed system the call drop probability can be minimized.

ACKNOWLEDGMENTS

First and foremost, I am thankful to God, the most gracious most merciful for all he has gifted me with. It is His plan and my belief in him that helped me finish this work.

My sincere appreciation goes to my academic advisor, Dr. Luiz A. DaSilva for his professional guidance and advice throughout my tenure in Virginia Tech. He has vastly improved my engineering and technical writing skills. I am grateful to my committee members Dr. Jeffrey H. Reed and Dr. Annamalai Annamalai for their help and suggestions.

Many a times, my conversation with my fellow researchers especially Fakhrul Alam, Ramesh Chembil Palat, Carl Fossa, Ran Gozali, Raqibul Mostafa, Vikash Srivastava and Yu Lei had been insightful in the methodology of research and furthering my knowledge in communication theory. I would like to thank them for their time and helpful suggestions. My association with MPRG for the past one and a half years has been a positive and an enriching experience. I am grateful towards all my fellow researchers and the staff of MPRG for making my stay at Virginia Tech a memorable one. This work was supported by LGE. I wish to thank them for the financial support.

I thank my parents for their love and affection. They taught me the importance of education and always encouraged me to work harder and better to achieve what I want. It was my husband Firosh who encouraged me to pursue my education even at the cost of our personal sacrifices. I wish to thank Firosh for his love, patience and confidence in me.

TABLE OF CONTENTS

CHAPTER 1 INTRODUCTION 1

1.1 REVIEW 1
1.2 MOTIVATION 4
1.3 OVERVIEW OF OUR WORK 5
1.4 CONTRIBUTION 6
1.5 THESIS OUTLINE 6

CHAPTER 2 SYSTEM MODEL 8

2.1 INTRODUCTION 8
2.2 OUTLINE OF THE MODEL 8
2.3 QOS REQUEST MODEL 9
2.4 USER LOCATION AND MOVEMENT 16
2.5 CALL ADMISSION CONTROL 18
2.6 TRANSMITTER AND RECEIVER 20
2.7 CHANNEL MODEL 21
2.7.1 Frequency Selective Fading 22
2.7.2 Effects of Doppler Spread 23
2.7.3 Rayleigh Fading 23
2.7.4 Direction of Arrival (DoA) 25
2.8 CHAPTER CONCLUSION 29

CHAPTER 3 PHYSICAL LAYER MODEL 30

3.1 INTRODUCTION 30
3.2 INTERFACES TO THE PHYSICAL LAYER 30
3.2.1 Interface to MAC Layer 31
3.2.2 Interface to RRC 31
3.3 TRANSPORT CHANNELS 31
3.4 PHYSICAL CHANNELS 33
3.4.1 DPDCH 35

3.4.2 DPCCH *36*
3.5 UPLINK TRANSMITTER 36
3.5.1 Channel Concatenation and Code block segmentation *37*
3.5.2 Channel Coding *38*
3.5.3 Physical Channel Segmentation *41*
3.5.4 Interleaving *41*
3.5.5 Spreading *42*
3.5.6 Scrambling *44*
3.5.7 Modulation *46*
3.6 UPLINK RECEIVER 47
3.6.1 Rake Receiver *49*
3.6.2 Beamforming *51*
3.6.3 2D-Rake Receiver *56*
3.6.4 De-scrambling and De-spreading *58*
3.6.5 De-Interleaving *58*
3.6.6 Convolutional Decoder *58*
3.7 CHAPTER CONCLUSION 59

CHAPTER 4 RESOURCE MANAGEMENT FOR A SMART ANTENNA NETWORK 60

4.1 INTRODUCTION 60
4.2 DIFFERENTIATING SERVICES 60
4.3 USER ELASTICITY AND SATISFACTION INDEX 62
4.4 REQUIREMENTS OF RESOURCE MANAGEMENT 64
4.4.1 Resource Management in a cellular system with omni-directional antennas *64*
4.4.2 Intra-cell handoff in a smart antenna system *64*
4.4.3 Utilizing user elasticity for resource management *66*
4.5 RESOURCE ALLOCATION FOR AN OMNI-DIRECTIONAL ANTENNA SYSTEM 67
4.5.1 Symbol Definitions: *67*
4.5.2 Algorithm: *67*
4.6 INITIAL RESOURCE ALLOCATION FOR A SMART ANTENNA SYSTEM 70

4.6.1 Constants *70*
4.6.2 Symbol Definitions: *70*
4.6.3 Algorithm Description: *71*
4.7 MODIFIED RESOURCE ALLOCATION FOR SMART ANTENNA SYSTEM 73
4.7.1 Symbol Definitions: *73*
4.7.2 Algorithm Description: *73*
4.8 RESOURCE MANAGEMENT FOR A SMART ANTENNA SYSTEM 76
4.8.1 Constants *76*
4.8.2 Symbol Definitions *76*
4.8.3 Algorithm Description: *77*
4.9 SUPPORT OF SERVICES 82
4.10 CHAPTER CONCLUSION 82
CHAPTER 5 SIMULATION RESULTS AND DISCUSSION 83
5.1 INTRODUCTION 83
5.2 EFFECT OF HETEROGENEOUS USERS IN A CELLULAR SYSTEM 83
5.2.1 Cell Capacity with different data rates *84*
5.2.2 Cell Capacity in different channels *85*
5.2.3 Cell capacity with heterogeneous users *87*
5.3 EFFECT OF CONVOLUTIONAL CODING 87
5.4 SIMULATION TIME CHART 90
5.5 DROP PROBABILITY FOR A SYSTEM WITH SMART ANTENNAS 91
5.6 RESOURCE MANAGEMENT IN AN OMNI-DIRECTIONAL ANTENNA NETWORK 93
5.7 RESOURCE MANAGEMENT MECHANISMS 95
5.8 APPLICATION OF RESOURCE MANAGEMENT TO SMART ANTENNA SYSTEM SUPPORTING HETEROGENEOUS USERS 98
5.8.1 Fully elastic users *98*
5.8.2 Inelastic Users *102*
5.9 EFFECT OF FREQUENCY OF UPDATE 103
5.10 CHAPTER CONCLUSION 105
CHAPTER 6 CONCLUSIONS AND FUTURE WORK 106

6.1 SUMMARY 106
6.2 CONCLUSIONS 107
6.3 FUTURE RESEARCH DIRECTIONS 109
6.4 CHAPTER CONCLUSION 110

BIBLIOGRAPHY 111

GLOSSARY OF ACRONYMS 116

List of Figures

Figure 2.1 Block schematics of the system model 9
Figure 2.2 UMTS QoS Architecture 12
Figure 2.3 Data rate requests by the users as a function of time. 16
Figure 2.4 Probability density function (pdf) of the direction of the random user. 17
Figure 2.5 User mobility model. 18
Figure 2.6 Block diagram of a communication system 21
Figure 2.7 Time domain plot of Rayleigh fading coefficients 24
Figure 2.8 Block diagram of channel implementation. 25
Figure 2.9 Physical Model for geometrically based single bounce circular model. 27
Figure 2.10 Geometry for the computation of AoA 28
Figure 2.11 Probability distribution of AoA. 28
Figure 3.1 Interface of the physical layer with upper layers [31] 31
Figure 3.2 Frame format of DPDCH 35
Figure 3.3 Frame format of DPCCH 36
Figure 3.4 Data flow diagram for the uplink transmitter with 10 ms transport block size 37
Figure 3.5 Connection diagram of rate 1/2 convolutional coder 39
Figure 3.6 Connection diagram of rate 1/3 convolutional coder 39
Figure 3.7 Code tree used for the generation of OVSF codes 43
Figure 3.8 Configuration of uplink scrambling sequence generator [36] 45
Figure 3.9 Spreading and scrambling of the uplink transmitted sequence 46
Figure 3.10 Data flow diagram at the receiver 48
Figure 3.11 Block diagram of a rake receiver 49
Figure 3.12 Rake receiver performance in indoor channel 50
Figure 3.13 Rake receiver performance in outdoor channel 51
Figure 3.14 Geometry of a LES antenna array [37] 52
Figure 3.15 Array factor of a linear antenna array with maxima at 45^0 53
Figure 3.16 Array factor of circular antenna array 55
Figure 3.17 Fixed beamforming network[37] 55
Figure 3.18 Two-dimensional RAKE receiver decoding for a single user 57
Figure 3.19 BER of convolutional coded and uncoded system. 59

Figure 4.1 BER for different spreading factors with normalized power 62
Figure 4.2 AoA of a user moving with a velocity of 120 kmph near the base station 65
Figure 4.3 AoA of a user moving with a velocity of 120 kmph in the periphery of the cell 65
Figure 4.4 Flow chart for simple resource allocation for omni-directional antennas 69
Figure 4.5 Flow chart for resource allocation for a smart antenna system 72
Figure 4.6 Modified resource allocation for a system with smart antennas 75
Figure 4.7. Flow chart of resource degradation section of resource management 79
Figure 4.8 Resource up-gradation section of resource management algorithm 81
Figure 5.1 Power level plot of heterogeneous users in a WCDMA system 84
Figure 5.2 BER plots for homogenous users with rate = 120 Kbps and 30 Kbps 85
Figure 5.3 BER of users with SF = 4 (Rate = 9600 Kbps) in outdoor and indoor channels 86
Figure 5.4 BER in a system with heterogeneous users 87
Figure 5.5 BER performance of the encoder for 120 kbps (Eb/N0 = 5 dB) 89
Figure 5.6 BER performance of the encoder for 3.84 Mbps (Eb/N0 = 5 dB) 89
Figure 5.7 Time chart for the simulation 90
Figure 5.8 Call drop probability in a system with smart antennas (without resource management) 92
Figure 5.9 Throughput in an omni-directional antenna system with and without resource management 93
Figure 5.10 Blocking probability of an omni-directional antenna system for a managed and unmanaged system 94
Figure 5.11 Satisfaction index of users with and without resource management 95
Figure 5.12 Beam pattern for the base station antenna 96
Figure 5.13 Plot of SI variation with location. 97
Figure 5.14 Aggregate throughput in the cell (fully elastic rates) 99
Figure 5.15 Blocking probability for the calls (fully elastic rates) 99
Figure 5.16 Drop probability for the calls (fully elastic rates) 100
Figure 5.17 Net Satisfaction Index of the users (fully elastic rates) 101
Figure 5.18 Satisfaction Index of accepted users (fully elastic rates) 101

Figure 5.19 Aggregate throughput in the cell (in-elastic rates)..... 102
Figure 5.20 Satisfaction Index of the users (in-elastic rates) 103
Figure 5.21 Throughput variation with different frequency for resource management.. 104
Figure 5.22 Satisfaction Index for different frequency of update for resource management 104
Figure 5.23 Variation in drop probability with different update intervals 105

List of Tables

Table 2.1 QoS classes defined in UMTS 11
Table 2.2 Power delay profile of indoor and outdoor channels 23
Table 3.1 Transport Channels defined in WCDMA standard 32
Table 3.2 Physical channels in the 3G standard 34
Table 3.3 DPDCH fields [32] 35
Table 3.4 Code block sizes for different coding schemes 38
Table 3.5 Data rate calculation for rate ½ coder 40
Table 3.6 Data Rate calculation for Rate 1/3 coder 40
Table 3.7 Second Interleaving pattern 41
Table 5.1 User characteristics for the example in Figure 5.13 97

Chapter 1 INTRODUCTION

Third Generation (3G) Mobile Communication systems will provide enhanced high-speed data, multimedia, and voice services to mobile users. The integration of such heterogeneous traffic types implies that the network must provide differentiated Quality of Service (QoS). However, these new services have to work in a bandwidth-limited environment. Clearly, the user mix that can be supported at any given time will be a function of QoS requirements and available bandwidth, but in general 3G systems must support much higher data rates than those typical of voice-oriented services. Studies to date have concentrated on improving spectral efficiency – accommodating more data within the same transmission bandwidth. One area that has gained considerable attention from the research community is the exploitation of the spatial domain through antenna beamforming.

Adding smart antennas at the base station enables Space Division Multiple Access (SDMA). Since this is a multiple access scheme, an important part is the Radio Resource Management (RRM). In this thesis we explore the effect of smart antenna deployment on RRM. Specifically, the impact of switched beam antennas on RRM will be explored in detail in this work.

In the next section, we will review some of the literature already available on smart antennas and resource management in order to present the background for our work. This section will also identify the area of our work and the requirement of a resource management scheme suitably tailored for a smart antenna network. Section 1.2 describes the motivation for our work. Section 1.3 introduces the work presented in this thesis and section 1.4 discusses the specific contribution of the thesis. The organization of this document is provided in section 1.5.

1.1 Review

Smart antennas and resource management are two widely researched areas. Antenna beam forming has been conventionally treated as a physical layer issue, with the research

concentrating on weight adaptation, capacity improvement and implementation issues. The impact of beam forming on the higher layers has not been adequately explored in the literature. Resource management needed to support multiple data rates in turn has typically been considered a higher layer issue, by and large studied independently of physical layer conditions such as beam patterns, channel profile, fading etc. In this thesis, we study some of the interactions between beam forming and resource management to yield capacity improvements in a wireless system supporting multiple data rates. We will describe some of the work already available in the present literature, in order to position our work.

The capacity improvement obtained with beam forming was studied by Choi *et al.* [1]. In this work, the performance and hardware complexity of adaptive antennas and switched beam antennas in a Code Division Multiple Access (CDMA) system are studied. Simulation studies conducted have shown that the switched beam antenna array outperforms the tracking beam antenna array when the desired signal is not sufficiently stronger than the interferer, since the switched beam antenna array system is much less affected by environmental parameters. However, for a strong desired signal and weaker interferers tracking beam system outperforms the switched beam system. This is attributed to the higher processing gain. The study concentrates on the comparison between switched beam and tracking beam algorithms. Single data rate users have been assumed in this work.

The performance improvement from a network perspective has been addressed in [2]. In this study, the power feasibility problem is addressed from a network-oriented approach rather than the link oriented approach. A particular power allocation is said to be feasible if transmitted power levels can be set to satisfy every user's demanded QoS [2]. Erlang capacity of a CDMA system with smart antennas is studied in this work. These performance analysis studies have been conducted from the viewpoint of a homogenous (single rate) user population.

The resource management problem has also been addressed from an omni-directional antenna point of view. Assuming the use of omni-directional antennas, resource management techniques for 3G systems are presented in [3]. This paper provides an overview of radio resource allocation schemes that are flexible and support different traffic classes. Bandwidth reservation techniques are elaborated in detail in this work, but all the algorithms in this paper use only simple omni-directional antennas. A measurement based call admission control is studied in [4]. The state of the cellular system is studied and a call admission decision is made. A bandwidth adaptation algorithm is also given in this work. Huang *et al*. [5] propose a novel adaptive resource allocation algorithm consisting of call admission control, resource reservation, and bandwidth adaptation for real-time video/audio applications. A scheduling mechanism for non-real time traffic is also presented in this paper. The algorithm takes into account the user mobility and the nature of multimedia traffic.

From this short review, we find that the beam forming and resource management in multi-rate systems have been addressed as separate areas of research. However, in a system with narrow beam forming and resource management with multiple data rates, integrating physical layer and resource management aspects can provide an added dimension to the resource management problem. To date, the published works do not explore the resource management issues of multi-rate systems as applied to a base station with smart antennas. In the present work, we study the resource management issues in a system that provides QoS guarantees with smart antennas deployed. We thoroughly model the physical layer and channel parameters – including Rayleigh fading, AoA variation due to scattering and multipath channel profile. We study the resource management from the point of view of an accepted communication standard – in this case, the 3G standard is used for modeling the QoS requirements, transmitter and receiver parameters, and communication between different modules.

We describe the relevant details related to the system model in the following chapters. Related work on different aspects of our model is reviewed along with the presentation of the model.

1.2 Motivation

The data rates supported by a 3G system can be as high as 2 Mbps, within a relatively narrow frequency band. Spectrally efficient coding techniques or spectrum enhancement techniques such as beam forming have been proposed to this end. Hence, in a commercially deployed 3G system, heterogeneous services and beam forming networks will coexist.

In a base station with smart antennas, allocating and managing resources when the users are mobile poses a new challenge. The initial resource allocation will depend on the present cell conditions, the location and channel conditions applicable to the new user and the acceptable data rates of the new user. The aim of the resource allocation scheme should be to reduce the blocking probability and to accept the user with at least the lowest data rate.

The users can move from the coverage area of one beam to another, giving rise to a condition similar to handoff between cells. With narrow beams the area covered by an individual beam is very low, hence the possibility of a user moving between beams is higher than the probability of his movement between cell boundaries. In addition to that, depending on the channel, the direction of arrival of multipath components can vary. This causes the user to interfere with multiple beams even when the line of sight direction of the user does not change. These factors make management of multiple users in a smart antenna network challenging.

In addition, the use of error correction codes can reduce the BER and thereby increase the capacity. However, the effectiveness of the error correction coding schemes for high data rates and in the presence of multipath components must be checked. This will allow us to predict the capacity of the system with coding schemes.

Since multiple services are allowed, another factor that can be used effectively is the elasticity of the users. User elasticity is the ability of the users to support different data rates, which can be adapted to the present channel and cell conditions. This provides

another dimension to the resource management problem, by adjusting the data rates of different users when the channel conditions change. By taking advantage of the user elasticity, we can fully utilize the resources, in order to increase the aggregate capacity of the system.

We can ask a few questions at this point. Can we reduce the blocking probability in the cell by taking advantage of the user elasticity? Can we decrease the drop probability of the calls arising due to the user movement between narrow beams? Are there mechanisms by which we can use the beam forming and the multi-rate of the systems to optimally allocate and use the resources in the system? Can we maximize the aggregate throughput in the cell, without increasing the BER of the users? The management scheme should attempt to address these questions taking into account the beam patterns and the multipath profile of existing users.

1.3 Overview of our work

From the above discussions, the requirement of a resource management algorithm for heterogeneous users in a smart antenna network evolves. The system must take care of interference caused by a user on multiple beams, movement of user between beams and differences in resource availability in the same cell depending on user location. The algorithm should be robust enough to work in various wireless environments having degradations such as fading, multipath, random scatter, etc.

This thesis proposes and evaluates one such resource allocation and management scheme. The key idea is to provide adaptive QoS to users depending on the characteristics of traffic currently present in the cell. Due to the spatial domain considerations introduced by smart antennas, the relative cell characteristics change as the user moves within the cell, causing a change in the QoS provided to the user in motion. In this work we propose an algorithm for resource allocation that accommodates elastic and non-elastic traffic, achieving graceful QoS degradation as users move within a cell and interfere with one another.

1.4 Contribution

Our contribution is the development and evaluation of a resource allocation and management scheme tailored to networks employing smart antennas. The evaluation of the algorithm is performed using a simulation model having an integrated medium access layer and physical layer.

We modeled the cell conditions in order to represent a real world cellular system. The user mobility is modeled as a mixture of stationary, random walk and high velocity users. Since the performance is dependent on the channel conditions, a good model of the physical layer is essential. The physical layer model incorporates the mobile transmitter, a 2D rake receiver exploiting the spatial and temporal diversity. The channel modeling considers the multipath profile and AoA of the multipath components. The physical layer passes the received power level in the beams to the higher layers to make the resource management decision. The resource allocation and management algorithm is tested on this physical layer framework.

The resource allocation and management algorithms we have proposed take advantage of the user elasticity and maximize the aggregate throughput. Through simulation studies, we show that the drop probability and blocking probability of the calls are reduced by adaptively re-allotting the resources among the different users. The increase in the aggregate throughput as compared to the system with no resource management can also be observed.

1.5 Thesis Outline

The thesis is organized as follows. In chapter 2 we give an overview of the higher layers in the 3G system, QoS requirements, and the different models used to characterize the users in the system. The elastic call generation, parameters of Wideband CDMA (WCDMA), mobile transmitter, channel modeling and base station receiver are explained in this chapter. Chapter 3 describes in detail the physical layer model used to study the resource allocation and admission protocols. The parameters pertaining to the channel are explained in this chapter. Chapter 4 presents the proposed algorithms for resource

allocation and resource management. Chapter 5 discusses the results showing the performance gain of a managed scheme and the effect of user elasticity on the overall performance. Finally we conclude the thesis with some closing remarks and directions of further research.

Chapter 2 SYSTEM MODEL

2.1 Introduction

The objective of this chapter is to introduce and explain the characteristics of the simulation model we have developed. We employ this system in the later chapters to study the feasibility and performance characteristics of our proposed resource management algorithm. The aim of the algorithm is to optimize resource allocation in a wireless network deploying smart antennas at the base station and providing differentiated services for the users. Hence the system should support spatial and temporal diversity, model a vector channel, and support service differentiation. In this chapter we develop a suitable system model that satisfies all these requirements while trying to keep complexity to a reasonable level.

2.2 Outline of the model

A top-level view of the model is shown in Figure 2.1. The resource management mechanism will operate continuously – initially to accept users to the system and later on for a constant monitoring of the system to prevent errors due to increased interference. Depending on the services the user wants to utilize, the QoS requirement generation block generates a range of data rates and maximum acceptable BER requirements. This request is passed to the base station through a dedicated control channel. Depending on resource availability, the base station allots a supportable QoS to the mobile user. The data rate of the user is adjusted to suit the allotted data rate. The data are divided into segments and channel coding is applied. The data are spread using a pseudo noise sequence for multiple access and transmitted on the channel. The receiver is modeled to employ antenna diversity, and a rake receiver is used to combine signals from the same user arriving at the receiver by following different paths. The BER of the users is determined. The resource management algorithm operates in the Media Access Control (MAC) layer of the protocol stack. The algorithm constantly monitors the system and changes the data rate of individual users so as to maintain all users within the guaranteed service level. The channel is modeled as a vector channel, which affects the amplitude,

phase and AoA of the component signals. In the following sections we will discuss each of these blocks in more detail.

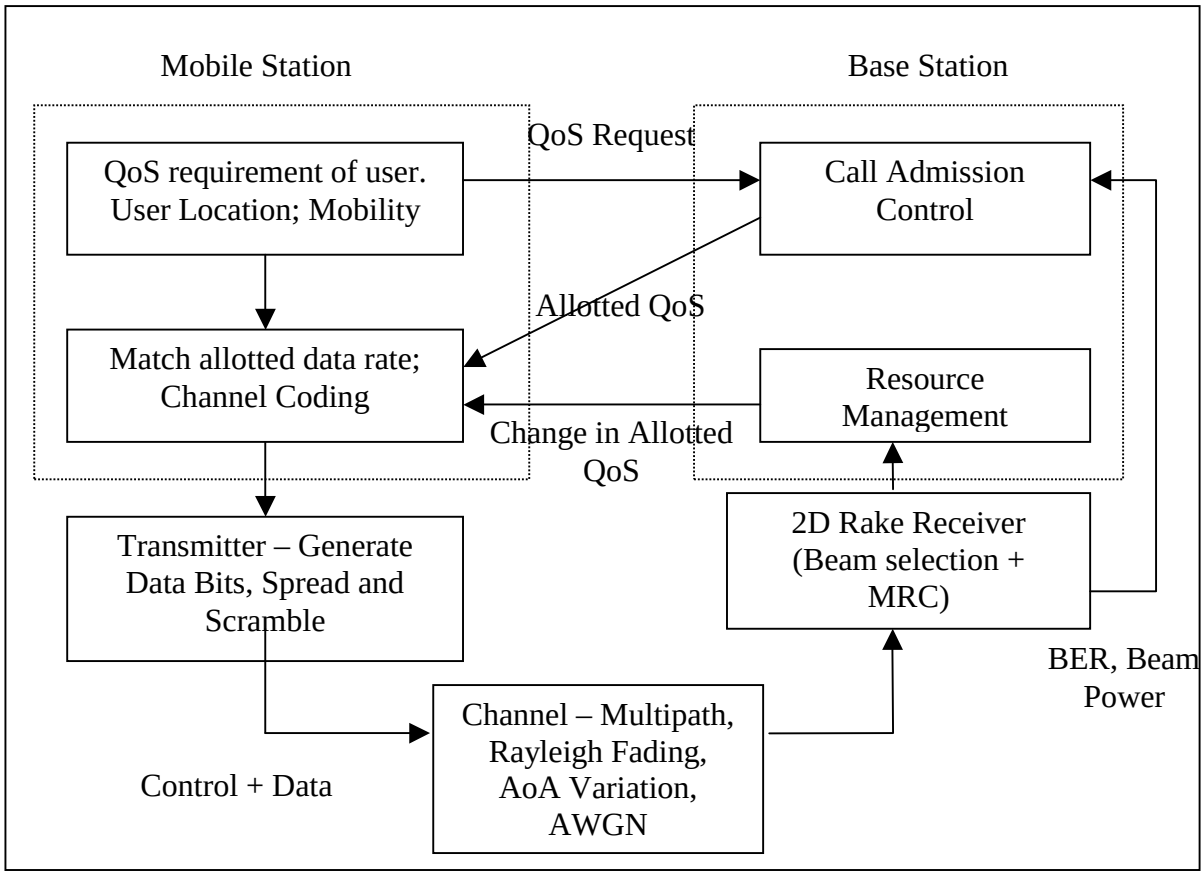

Figure 2.1 Block schematics of the system model

2.3 QoS Request Model

A major enhancement of third generation systems as compared to Second Generation (2G) systems is provisioning for QoS. QoS implies differentiation in services available to users according, for instance, to the requirements of a particular type of traffic. The traffic type can be real time voice, streaming video, video conferencing, file transfer, real time video, etc. QoS guarantees may include data rate as well as upper bounds on BER, delay and packet jitter. The parameters associated with QoS are explained below:

Data Rate: : The data rate available to the user. For instance, for real time video the data rate required will be considerably higher than for voice transmission.

BER: : Bit Error Rate expected. Errors are introduced in the transmitted data due to channel effects such as fading and interference from other users. Depending on the type of data being sent, BER requirements may vary. For example, the BER required by a file transfer system will be in the order of 10^{-6} or lower, while that required by voice traffic will be in the order of 10^{-2}. Depending on service type, a suitable error correction coding scheme can be applied to the data stream.

Delay : Delay defines the time it takes for the transmitted sequence to reach the receiver. Voice applications have much more stringent delay requirements than traditional data applications.

Packet Jitter : Considering a packet transmission, the packets arrive at the receiver after a finite delay. Depending on the route taken by the packets and/or dynamic variations in network load, the delay with which the data is received will vary contributing to packet jitter. For example, streaming video requires low jitter.

In practice, services may be differentiated by their cost to the user. It is logical that a service requiring higher bandwidth has a higher cost associated with it.

For a 3G system, services are broadly classified into four classes: conversational, streaming, interactive and background [6,7]. The main difference between these classes is how delay dependent the traffic is. Table 2.1 gives a description and basic characteristics of each class. In addition, [8] lists an additional class called “assured bandwidth class.” This is shown in italics in the table.

Table 2.1 QoS classes defined in UMTS

Class	**Fundamental Characteristics (as defined in 3G standard)**	**Characteristics**	**Example**
Conversational	- Preserves time relation (variation) between information entities of the stream - Conversational pattern (stringent and low delay)	- Real time - Very delay sensitive (end to end delay < 150 ms) - Low transfer time - Packets should arrive in order - Guaranteed bit rate	Voice Voice over IP Video Conferencing
Streaming	- Preserves time relation (variation) between information entities of the stream	- Real time - Less delay sensitive than conversational class - Packets should arrive in order - Guaranteed bit rate	Streaming Video Streaming Audio
Interactive	- Request response pattern - Preserves payload content	- Interactive traffic - Low BER requirement - Low round trip delay	Web Browsing
Background	- Destination is not expecting the data within a certain time - Preserves payload content	- Non real time - Largely delay insensitive - Packet jitter is not important	Background downloading of email. Short Message Service (SMS). Reception of measurement records. Download of databases.
Assured Bandwidth		- *Long term average throughput is assured* - *No inherent delay characteristics identified*	*Premium class web browsing* *Premium class email*

3G standardization efforts have yielded a layered service architecture whose aim is to provide end-to-end QoS guarantees to the users in the network. Figure 2.2 shows the Universal Mobile Telecommunication System (UMTS) QoS architecture [6]. From an end user's perspective, the End-to End QoS is the most important criterion. This is

divided into three parts – Terminal Equipment/Mobile Termination (TE/MT) bearer service (local to the mobile), UMTS bearer service, and external bearer service (landline bearer service). The UMTS bearer service is further classified into Radio Access Bearer Service (RAB) and Core Network Bearer Service (CN). The RAB and CN implement the optimized ways to realize the corresponding bearer service taking into account mobility and mobile subscriber profiles.

The CN effectively controls and utilizes the backbone service. The CN covers the layer 1 and layer 2 functionality and can reuse an already existing standard for the backbone [7]. The solution has lately been converging to an Internet Protocol (IP) based backbone delivering QoS based on mechanisms such as differentiated services (DiffServ) [9,10].

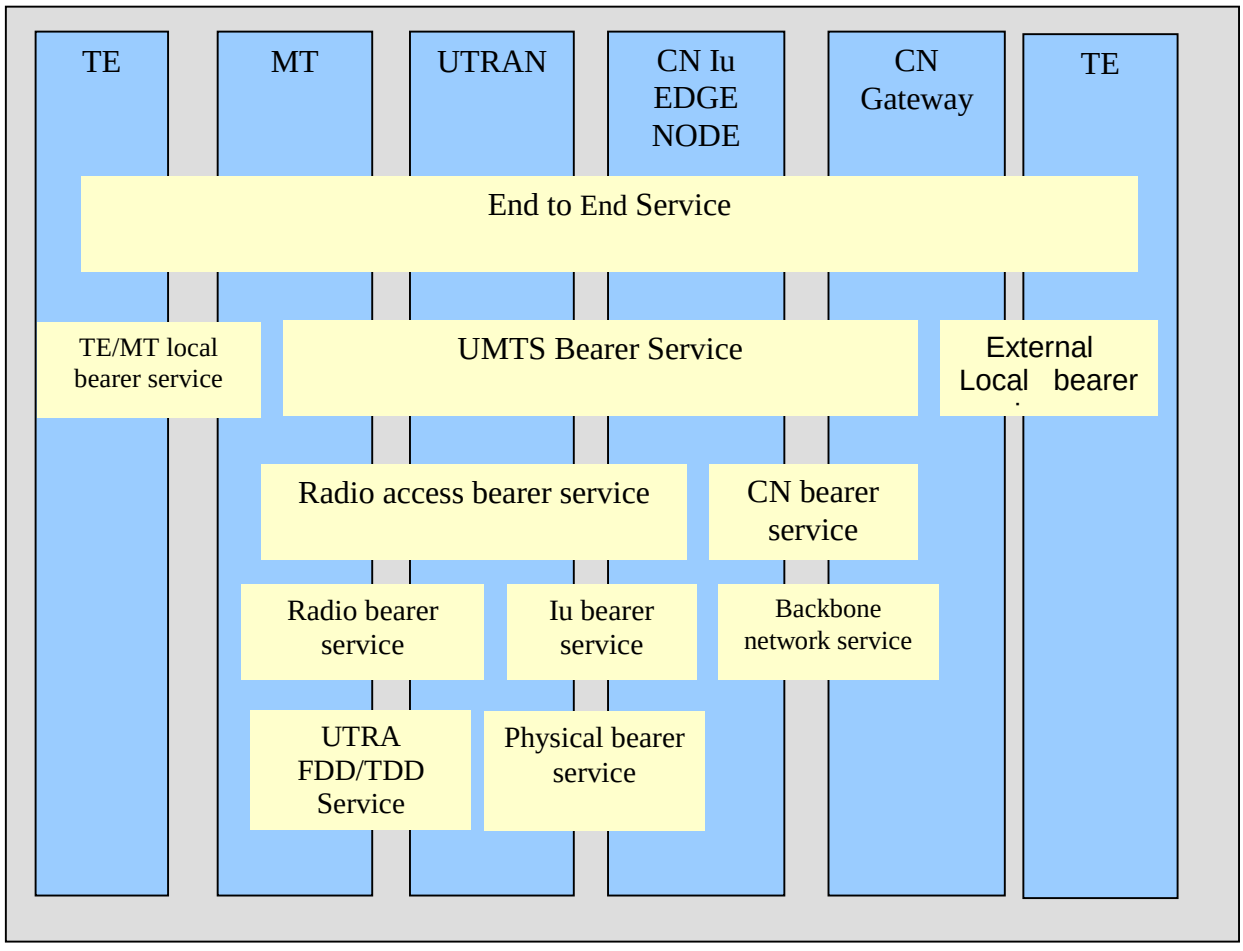

Figure 2.2 UMTS QoS Architecture

The RAB defines the physical later protocols and air interface. The functionality is to provide confidential transport of data and signaling from the TE to the MT. The RAB can be further divided into the radio interface between the Radio Access Network (RAN) and the core network (Iu) bearer service and radio bearer service. The radio bearer service or UMTS Terrestrial Radio Access Network (UTRAN) controls the radio access transport. The Iu bearer service provides transport between the UTRAN and CN. UTRAN can make use of either a Frequency Division Duplexing (FDD) or Time Division Duplexing (TDD) mode of operation. A comprehensive coverage of the UMTS network architecture can be found in [7,8, 11].

In order to provide an end-to-end QoS guarantee, all the layers in the system must have their associated QoS parameters defined. The QoS guarantees provided by the backbone network service depends on the architecture chosen. IP, Asynchronous Transfer Mode (ATM) or leased public telephone lines can be used in the backbone. The QoS parameters for the traffic classes at the various layers are listed in [6]. Some of the attributes are maximum bit rate, guaranteed bit rate, delivery order, maximum Service Data Unit (SDU) size, SDU format information, SDU error ratio, transfer delay, residual BER etc.

In our study, we look into the QoS guarantees provided by the physical layer, i.e., the radio bearer service. (Defining the radio bearer service parameters is a task of the Third Generation Partnership Project (3GPP) Radio Access Network (RAN) Workgroup (RAN WG2). As of October 2001, this document has not been published.) The radio bearer service has certain QoS attributes that must be provisioned by the lower layers. These are maximum bit rate, guaranteed bit rate, residual BER, transfer delay etc. Both connection oriented networks and connectionless networks can be supported by the physical layer. For example, the 3GPP standards define two different channels – Dedicated Physical Data Channel (DPDCH) and Physical Random Access Channel (PRACH) for connection oriented and connectionless service, respectively. Depending on the delay and jitter requirements of the system, the suitable channel can be selected. For example, for the conversational class, transmission through the PRACH cannot guarantee stringent delay and jitter requirements, and therefore real time traffic classes should be handled using

dedicated physical channels. For non-real time systems, delay can be translated in terms of BER. If the BER is high, the retransmission rate is high thereby increasing the delay.

We study data communications over a dedicated channel; hence the parameters of interest include peak data rate, guaranteed data rate and BER. One constraint is that the transmitted chip rate is a constant and spreading codes can vary only in discrete steps, restricting the raw data rates to a set of discrete rates. This is discussed in detail in Chapter 3, where we consider the physical layer characteristics of the system in greater detail.

We can define "transmission classes." A transmission class is composed of a set of usable data rates (including the peak data rate) and the BER requirement. Different transmission classes can be defined, and the mix of transmission classes depends on various factors – distribution of offices and residential areas, day of the week, time of day etc. The ratio of different classes of users as a statistical quantity can be found from traffic dimensioning [12]. The dimensioning of hybrid traffic in 3G systems can be found in [13]. The authors propose a method of dimensioning traffic based on demographic data, morphology weighting, market forecast and time dependency to develop a traffic profile. A model in which hot spots exist in different regions, giving rise to a log-normal traffic pattern is proposed in [14]. A deterministic fluid model and two stochastic models for traffic can be found in [15].

In our system we use a simplified model in which multiple transmission classes exist with a pre-defined user distribution. The user distribution for the different classes can be selected based on traffic dimensioning results. For example, if the total number of classes is N, for each class i we define a structure with elements:

Id_i	:	Identifier for the transmission class
p_i	:	Proportion of users in this transmission class
$R_{req,I} = \{R_{min,i}, R_{step1,i}, R_{step2,i} \ldots R_{max,I}\}$	:	Subset of Data Rates supported by the transmission class

$\boldsymbol{H\_Time_i}$	:	Mean holding time for the connection
$\boldsymbol{BER_i}$	:	BER requirement for the traffic class

The parameters in the definition of a transmission class characterize the user and application requirements. The minimum data rate requirement arises from the type of application – for example voice users will have a minimum data rate requirement of 9600 bps. Maximum data rate is limited by the power and processor limitations of the user handset. The maximum cost the user is prepared to pay for the service also limits the maximum data rate requirement. BER requirement is tied to the application type. The range of data rates models application elasticity. If the base station fails to provide at least a data rate $R_{min,I}$ with a BER BER_i, the call is dropped. Once a call is generated, the call continues to exist in the cell for a period of time called the hold time. The hold time of a call is a stochastic quantity, assumed to follow an exponential distribution. The mean hold time of a call is dependent on the application requirement. For example, it is reasonable to assume that a web browsing request will have a shorter mean hold time than a file transfer.

The traffic in the cell depends on the mix of different transmission classes. For any particular class mix, $\sum_{i=1}^{N} p_i = 1$. A new call has the probability p_i to be of the user transmission class *i*. Call arrivals are modeled as a Poisson process. For this purpose, the mean inter arrival time between calls has to be specified in order to model the QoS request generation. The inter arrival time between calls is also a stochastic quantity having an exponential distribution.

In Figure 2.3, the requests from a user mix with three transmission classes are shown. The proportion of requests from classes 1 through 3 is 0.5, 0.25 and 0.25, respectively. The Y-axis represents the transmission data rates requested – in a $\log_2$ format. The X-axis represents time. The mean inter-arrival time is specified as 120 time units. Depending on the resources available, the Base Station (BS) makes a decision regarding what data rate is to be provided to the user.

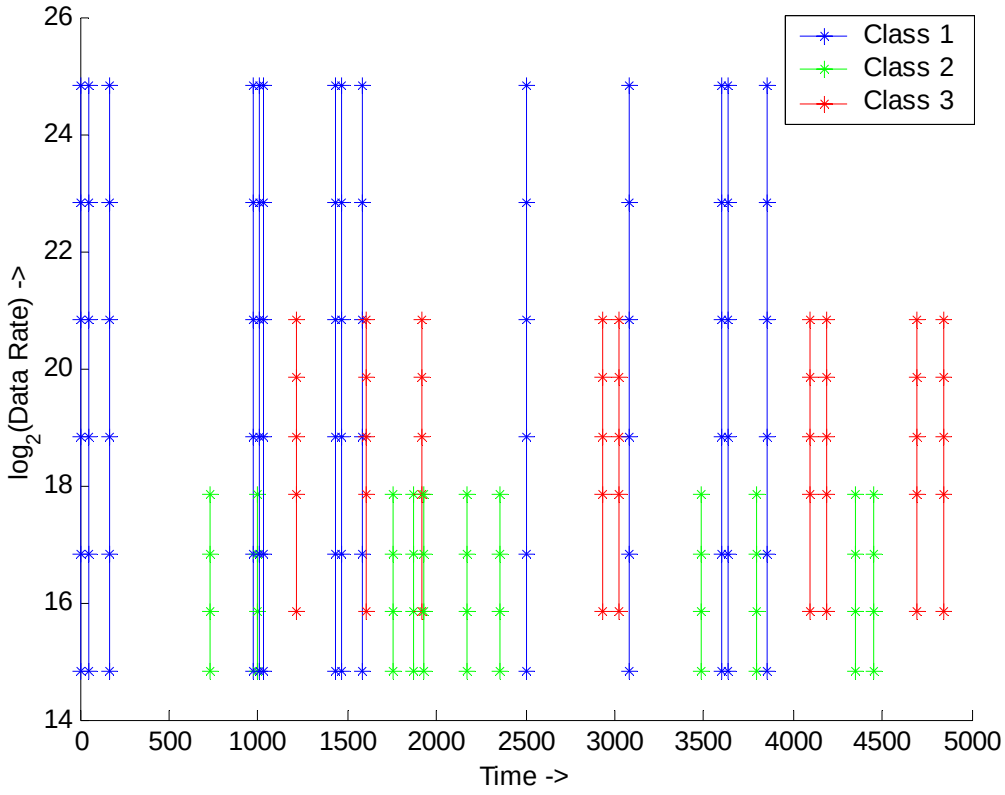

Figure 2.3 Data rate requests by the users as a function of time.

2.4 User Location and Movement

One of the important models that have to be studied and implemented is the user mobility. Since smart antennas utilize the spatial dimension for diversity combining and multiple access, accurate modeling of user movement in the cell area is important. In particular, there are two parameters of interest: (i) location of the user when the call is initiated; (ii) direction and velocity with which the user is moving.

Some previous works in Personal Communication Systems (PCS) have attempted to characterize different kinds of user movement. [16] looks into a mobility characterization based on the map of an area and predicts the movement of autonomous users over that area as well as the call patterns of the users. In [17] the mobility of the users is characterized as a modified Brownian motion. A highway pattern for one-dimensional space is modeled in [18]. The random walk approach for user mobility movement has

been proposed in [17]; this approach is used to model mobility in many PCS system studies [19]. A comprehensive mathematical treatment of user movement within the cell, also including channel holding time and average number of handovers can be found in [20].

For the present study we consider four kinds of users:

(i) Random walk users: These users move in a half cosine direction at low velocity (30 to 60 km/h). The direction of user movement is updated every 50 time slots. This model represents urban users moving in a city. The random walk users change their direction of movement at periodic intervals. The probability density function for the random walk users has a half cosine pulse shape, with the mean corresponding to the previous direction. The pdf can be expressed as given in the following equation.

$$f_{\delta}(\delta_t) = \begin{cases} K_{\delta} \cos(\delta_t - \delta_{t-1}) & \delta_{t-1} - \pi \le \delta_{t-1} \le \delta_{t-1} + \pi \\ 0 & otherwise \end{cases} \quad 2.1$$

The probability density function (pdf) of the direction is given in Figure 2.4

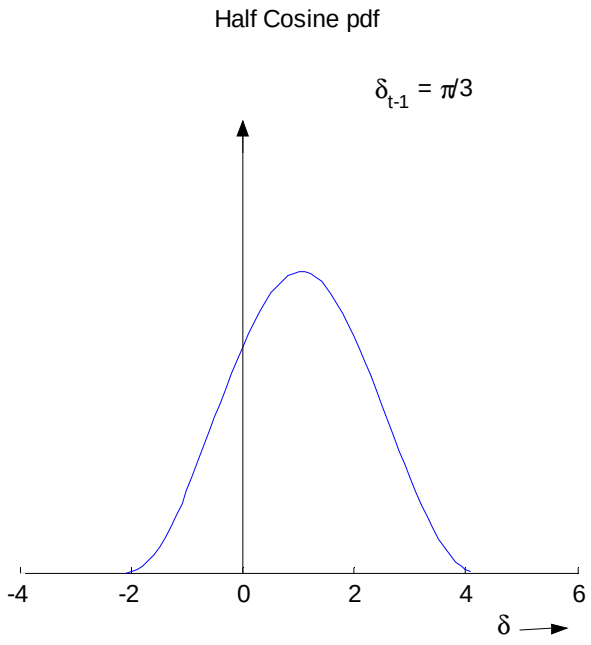

Figure 2.4 Probability density function (pdf) of the direction of the random user.

(ii) Constant Direction Users: In addition, there is another class of users present in the system having a high velocity and moving at a constant angular direction. These users emulate highway users.

(iii) Pedestrian Users: The third kind of users is pedestrian users having very low velocity and a half cosine direction of movement.

(iv) Stationary users: This class of users has zero velocity.

The mix of the users in the cell is a combination of the above classes. The call patterns and the handover between antenna beams will be different for different mixes of users. The mix of users depend on the location (random walk users will represent a significant portion of the total users in urban areas), time (random walk users peak during rush hour time), day of the week etc. For a specific mix of users, a visual representation of these different mobility types is shown in Figure 2.5.

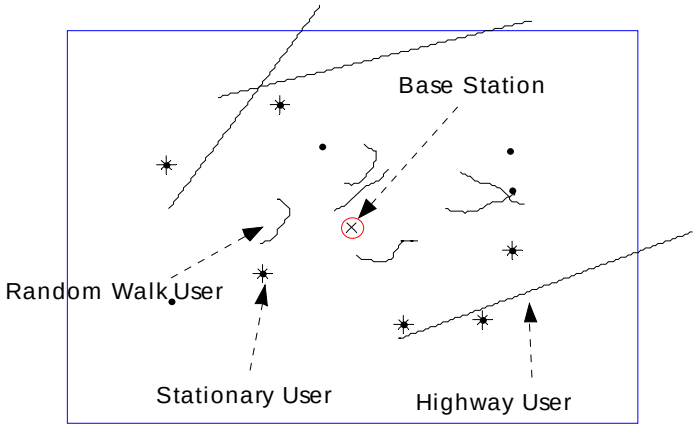

Figure 2.5 User mobility model.

2.5 Call Admission control

Multiple users co-exist in a wireless system. There are many methods for multiple access of the common wireless channel – the users can be multiplexed in time, frequency or

code leading to Time Division Multiple Access (TDMA), Frequency Division Multiple Access (FDMA) and Code Division Multiple Access (CDMA), respectively. As opposed to TDMA and FDMA schemes where resources are dedicated to individual users, CDMA can be more dynamic. For a CDMA system, users share the same frequency and time slots, but each user spreads his data with a pseudo random code. Pseudo random codes with good cross correlation properties are chosen so as to maximize the interference rejection. Thereby, CDMA is an interference-limited multiple access scheme. If all the users in the system have the same power, then the Signal to Interference and Noise Ratio (SINR) is given by Equation 2.2 where U is the total number of users.

$$SINR_i = \frac{E_b}{N_0 + \sum_{j=1\, j\neq i}^{U} E_b} = \frac{1}{\frac{1}{\left(\frac{E_b}{N_0}\right)} + (U-1)} \qquad 2.2$$

As the number of users increases, SINR level decreases and the BER of the user under consideration becomes high. If the wireless system provides differentiated services to the users, then the users will have different powers. The SINR ratio can then be written as

$$SINR_i = \frac{E_{bi}}{N_0 + \sum_{u=1 u\neq i}^{U} E_{bu}} \qquad 2.3$$

where E_{bu} is the bit energy for user j. The purpose of the call admission control block is to ensure that the SINR level of each of the users is above a given threshold.

The call admission algorithm measures the received power from the user requesting admission into the wireless network. Depending on the position and location of the user, the algorithm decides whether the user can be admitted to the system without degrading the performance of other users currently in the system. In a differentiated data rate system, the power at which the user can transmit is also decided by the call admission control. The decision is passed to the mobile station through control channels. The

algorithm must also consider the environment in which the wireless system is operating, characteristics of the base station etc.

The mobile station waits for the response from the base station regarding the data rate or power for its transmission and starts sending data or voice using the allotted channels. The next section briefly deals with the transmitter functionality.

2.6 Transmitter and Receiver

In a wireless communication system, transmission occurs from the mobile station to the base station (uplink or reverse link) and from the base station to the mobile station (downlink or forward link). In either case, the transmitted data is subjected to impairments due to the wireless channel (fading, shadowing, multipath, etc.). In addition, there is interference due to multiple access to the channel. Transmitted data must be sufficiently protected against these effects. The operations at the transmitter are suitably paired at the receiver so as to get back the data /voice that is transmitted.

The block diagram of a conventional transmitter–receiver pair is shown in Figure 2.6. The actual data sequence to be transmitted is source coded to reduce the redundancy in the sequence. Channel coding is performed on the sequence to add redundancy and thereby decrease the BER. Interleaving is performed to protect against the occurrence of burst errors. An outer layer of codes can be imposed on the system in order to reduce the error probability. Finally, the sequence is modulated, up-converted and transmitted. At the receiver, the reverse operations take place. Since the CDMA system must be protected against multiple access errors, the coded sequence must be multiplied with a pseudo noise code before transmitting. The codes can be m-sequence, gold codes, Kasami codes, etc., depending on the system characteristics – whether synchronous/asynchronous, indoor/outdoor etc. The functionality in the uplink and down link are the same; the differences are in the chipping codes used, modulation schemes etc. The first step at the receiver is to unscramble the data. Then the data is de-spread and de-interleaved. The de-interleaved data is decoded to recover the best estimate of the transmitted sequence.

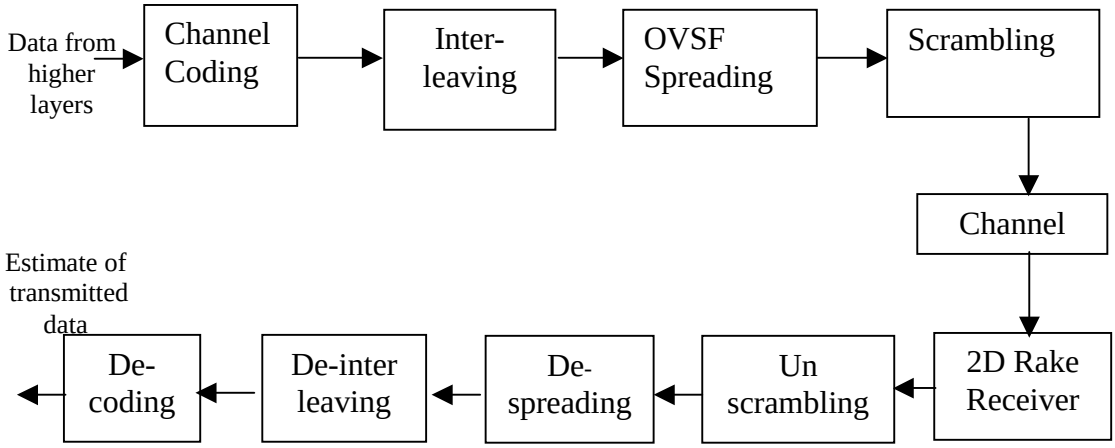

Figure 2.6 Block diagram of a communication system.

If the data arriving at the receiver can be decomposed in the time domain, rake receivers can be used. Combining beam-forming techniques to the time domain rake gives rise to a 2D-Rake receiver, yielding performance improvements. The transmitter and receiver models for WCDMA are described in detail in Chapter 3.

2.7 Channel Model

In a wireless system, the channel plays an important role in terms of the total data rate that can be supported, interference caused to other users, bit error rate, etc. The channel effects on the signal can be broadly classified into two areas: large scale path loss effects and small scale fading effects.

Large-scale fading effects are due to the distance between the transmitter and receiver and cause differences in the signal strength at the receiver. In a mobile communication system, this can lead to very undesirable effects since the signal from a Mobile Station (MS) very close to the BS can over shadow the signal from a MS very far away. Hence power control is used to bring the signal strength at the receiver to a constant value. Power control is a very important aspect of wireless systems, and numerous techniques have been proposed to deal with this issue [21,22,23]. We assume that we have a perfect power controlled system – meaning the maximum amplitude of all the signals arriving at

the receiver will be normalized irrespective of the transmitter's distance from the receiver.

The small-scale fading effects model the signal fluctuations over very short travel distances or short durations. Small-scale fading results from interference between two or more versions of the transmitted signal that arrive at the receiver at slightly different times. In our system the received signal suffers from small scale fading and the different small scale fading effects are described in the following sub-sections.

When smart antennas are used in a system, the AoA of the signals plays an important role. Various models have been proposed for modeling the AoA for different terrain conditions. Circular channel model [24] and elliptical channel model [25] represent two dimensional channel models for different terrain and scatterer conditions. We adopt the circular model, explained in detail in section 2.7.4.1.

2.7.1 Frequency Selective Fading

If the signal bandwidth is greater than the bandwidth of the channel, then the channel induces frequency selective fading. In such a case, the different multipath components that arrive at the receiver can be resolved. Hence, Inter Symbol Interference (ISI) is present and the channel acts as a linear filter.

The power of the specular components depends on the channel conditions. Various channel measurement campaigns have tabulated the power delay profiles of different kinds of channels. Measurements studies have been conducted [26] on the power distribution of the different multipath and are shown in Table 2.2. The relative delays are given in nanoseconds (ns) and the average power is in dB.

Indoor and outdoor channels have different power delay profiles. The outdoor channel is characterized by many resolvable multipath components, whereas the indoor channel has fewer resolvable multipath components. The type of channel that the signals encounter is selected based on the distance between the mobile and the base station.

Table 2.2 Power delay profile of indoor and outdoor channels

(a). Vehicular A. outdoor channel	
Relative Delay	Average Power
0	0
310	-1
710	-9
1090	-10
1730	-15
2510	-20

(b) indoor channel	
Relative Delay	Average Power
0	0
50	-3
110	-10
170	-18
290	-26
310	-32

2.7.2 Effects of Doppler Spread

In a system where there is relative motion between the transmitter and the receiver, frequency dispersion of the received signal occurs. If the Doppler spread of the channel is less than the bandwidth of the baseband signal then the signal undergoes slow fading. The Doppler spread is dependent on the velocity of the mobile and is given by

$$f_n = \frac{v}{\lambda}\cos\alpha_n \qquad 2.4$$

where f_n is the Doppler frequency, v is the relative velocity of the mobile, λ is the wavelength of the radio signal and α_n is the angular direction of mobile movement. For the WCDMA frequency range around 2GHz, a mobile moving at 120 km/hr corresponds to a Doppler spread of 223 Hz. Since this is very small compared to the bandwidth of the transmitted signal, the signal undergoes slow fading.

2.7.3 Rayleigh Fading

The specular multipath reaching the receiver is a combination of many multipath signals that cannot be resolved in the time domain. The phase additions of the signals reaching the receiver will lead to a fading envelope for the signal. The Rayleigh distribution is

used to characterize the time varying nature of the received envelope. The probability density function and Cumulative Distribution Function (CDF) of the Rayleigh distribution is given by the following equations

$$p(r) = \begin{cases} \frac{r}{\sigma^2}\exp(-\frac{r^2}{2\sigma^2}).....(0 \le r \le \infty) \\ 0.....(r < 0) \end{cases} \quad 2.5$$

$$P(R) = \Pr(r \le R) = \int_0^R p(r)dr = 1 - \exp\left(-\frac{R^2}{2\sigma^2}\right) \quad 2.6$$

From the CDF, the amount of time during which the signal experiences a deep fade can be predicted. The BER of a system without error control coding can increase significantly during this time. The Rayleigh fading coefficients are plotted in Figure 2.7. The Rayleigh fading coefficients can be generated using Clark and Gan's fading model [27]. A bank of Rayleigh fading simulators with variable gains and time delays can model frequency selective fading effects. The block diagram of the channel is given in Figure 2.8.

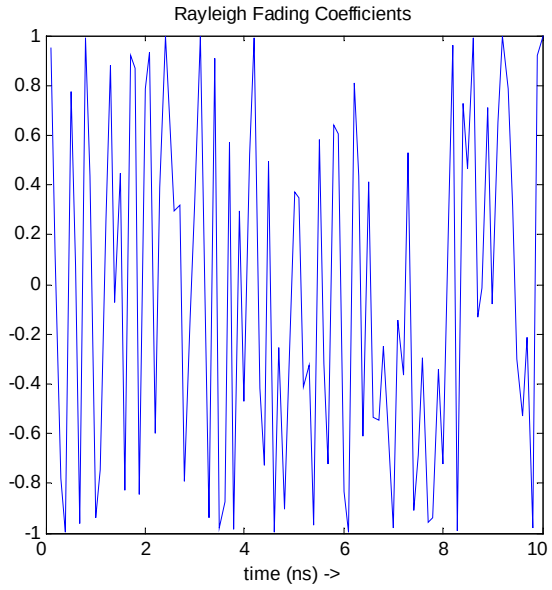

Figure 2.7 Time domain plot of Rayleigh fading coefficients

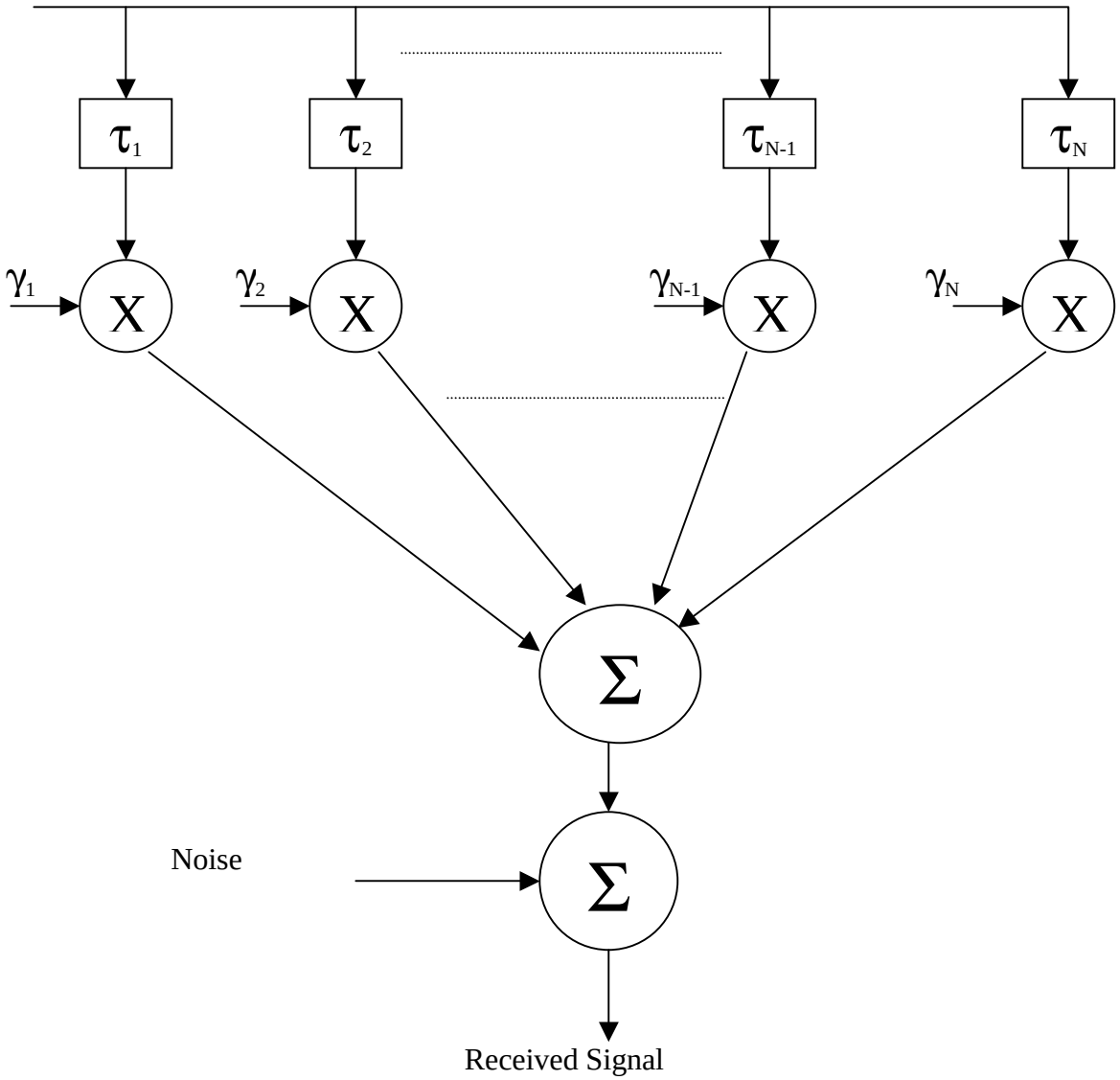

Figure 2.8 Block diagram of channel implementation.

2.7.4 Direction of Arrival (DoA)

When smart antennas are used in a system, the DoA of the signals plays an important role in resource allocation and resource management. There are different models suggested in the literature for modeling the DoA. There are geometrically based vector channel models and statistically based vector channel models. The statistical models rely on signal parameters obtained directly from some statistical distribution. The user is free to

choose from any statistical models, providing maximum flexibility in modeling the channel. In contrast, the geometric channel models provide a compact way of representing the AoA spread in the system, at the expense of decreased flexibility. For example, in the circular channel model that is described below, the AoA statistics are completely specified by the transmitter-receiver separation and the radius of the scatterers. However, the system does not model the channel effects when there are scatterers at other locations.

There are two geometrically based models – the elliptical channel model proposed by Liberti *et al.* [25] and the circular channel model proposed by Petrus *et al.*[24]. The elliptical channel model is suitable for modeling the propagation conditions in a microcell. It assumes that the base station and the mobile are at the foci of an ellipse and the scatterers are located at the periphery of the ellipse. The circular channel model is suitable for modeling a macrocell. The circular channel model considers a system in which the BS is at a greater height than the MS and the scatterers. The scatterers are assumed to be in a circle around the mobile station. We will look at the circular channel model in greater detail since we have used it in the vector channel modeling of our system.

2.7.4.1 Geometrically Based Singular Bounce Circular Model

In circular channel model proposed by Petrus *et al.* [24], the base station is assumed to be at a higher altitude than the mobile and all the scattering occurs in the vicinity of the mobile. This is shown in Figure 2.9. The radius of the scatterers characterizes the AoA profile of the system. All the scatterers fall within the maximum radius specified, and multipath occurs due to scattering from objects within this radius.

The main assumptions in the circular channel model are [28,29,30]:

- The signal reaching the base station may be modeled as plane waves from the horizon, hence there is only azimuth angle variation. In circular co-ordinates, only the angle ϕ varies, θ remains constant at 90^0.
- The scatterers are uniformly distributed within a circle around the mobile.

- Each scatterer is an omni-directional re-radiating element. This means that the signal arriving from the mobile is reflected towards the base station. The other scatterers do not influence the reflection.
- All scatterers have equal scattering coefficients with random phases.

The geometrical representation of the circular channel model is shown in Figure 2.9. The scatterers lie inside a circle of radius R. From the geometry of the figure, the AoA at the BS after reflecting from a scatterer at a distance r is given in equation 2.7

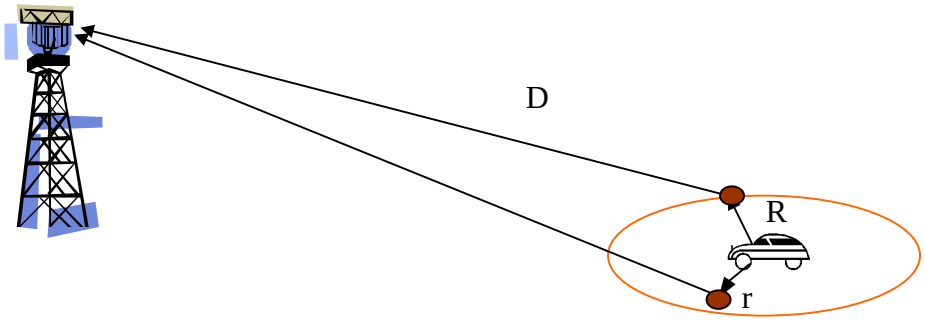

Figure 2.9 Physical Model for geometrically based single bounce circular model.

$$\theta_a = \tan^{-1}\left(\frac{\sin(\theta_d)}{D - r\cos(\theta_d)}\right) \qquad 2.7$$

The maximum angle of arrival at the base station is given by equation 2.8

$$\phi_{\max} = \sin^{-1}\left(\frac{R}{D}\right) \qquad 2.8$$

Hence, the maximum angle of arrival at the BS will depend on the distance between the BS and the mobile. The farther the mobile from the base station, the larger the AoA variation is.

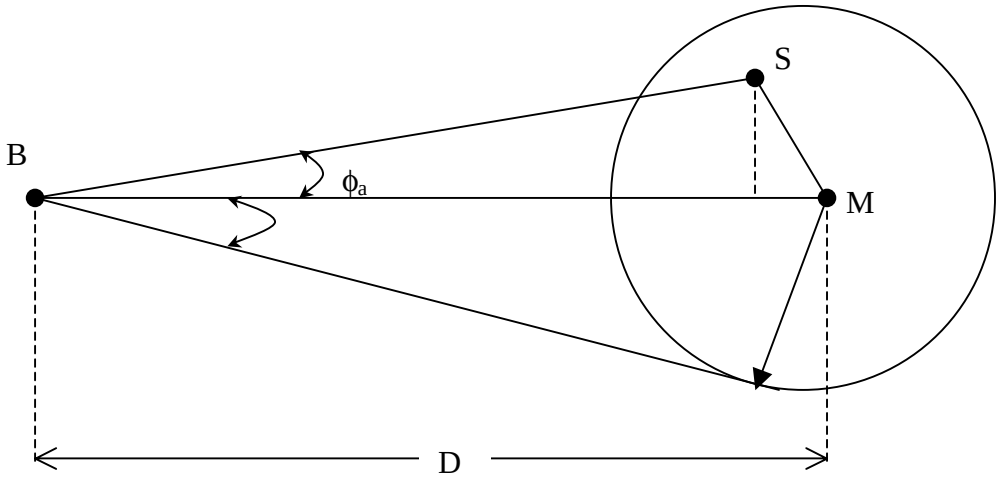

Figure 2.10 Geometry for the computation of AoA

From the geometry of Figure 2.10, an approximate closed form pdf for the AoA of the received multipath has been computed in [24]. This pdf can be used for generating the AoA of the received multipath and is given in Equation 2.9.

$$f_{\theta a}(\theta_a) = \begin{cases} \dfrac{\pi}{4.9\theta_{a\max}} \cos\left(\dfrac{\pi}{2}\dfrac{\theta_a}{\theta_{a\max}}\right)^{0.475} & -\theta_{a\max} \le \theta_a \le \theta_{a\max} \\ 0 & otherwise \end{cases} \qquad 2.9$$

The distribution of the AoA is shown in Figure 2.11.

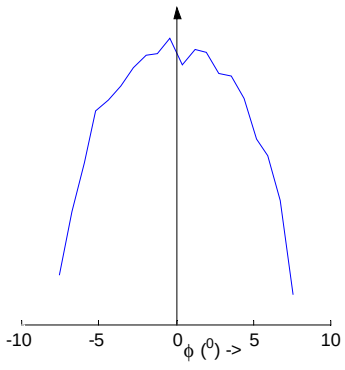

Figure 2.11 Probability distribution of AoA.

In the integrated system model, the location of the user is generated as described in section 2.4 and the radius of the scatterer distribution is a parameter in the definition of the channel. The AoA of the multipath at the receiver is computed by finding the Line of Sight (LOS) angle between the transmitter and the receiver and adding the computed AoA due to scattering to this computed value. This is given in Equation 2.10.

$$\phi = \tan^{-1}\left(\frac{y}{x}\right) + \phi_a \qquad 2.10$$

An important parameter relating to the channel characteristics is the radius at which the scatterers are distributed near the mobile. Measurement studies [29] have been conducted for finding the AoA statistics. The AoA at the receiver from a transmitter at a known location has been measured; the radius of scatterers is found to be in the range of 50-200m [29]

2.8 Chapter conclusion

In this chapter we discussed the various subsystems in our model. We explained the QoS parameters for a 3G system from an end-to-end perspective and concentrated on the parameters relevant to our study. Since the users in the system are mobile, we explained the models used to characterize their location and movement. A brief overview of the physical layer structure of the WCDMA system is given. The vector channel model that we have used in our simulation studies is explained. In the next chapter we will look into the transmitter and receiver details of the system as described by 3G standards.

Chapter 3 PHYSICAL LAYER MODEL

3.1 Introduction

We are interested in studying the impact on the upper layers in the protocol stack when smart antennas are deployed at the base station. For this purpose, the transmitter and receiver of the communication system have to be modeled. Additionally, the system that we model should adhere to a standard and be feasible to implement. In the present work we consider the 3G standard. The WCDMA physical layer can be modeled in two parts – uplink and downlink. In the present study we consider transmission from the MS to the BS, since in practice the capacity of a system is uplink limited.

The functionality of the uplink can be split into two parts – the transmitter section in the mobile station and the receiver at the base station. Directional antennas are deployed at the base station and hence the receiver has a two-dimensional (2-D) rake receiver. In our study, we look into three layers in the Open Systems Interconnect (OSI) model. Smart antenna is a physical layer implementation issue, whereas MAC and Radio Resource Control (RRC) are higher layer issues. Hence, we look at these layers and interfaces between them for the present study.

Data transfer between the MAC layer and the physical layer takes place using of transport channels. The data channels are logically divided into different physical channels that as covered in Section 3.4. Section 3.5 will give details about the transmitter and section 3.6 will cover the receiver model.

3.2 Interfaces to the Physical Layer

The function of the physical layer (Layer 1, L1) is to provide data transport services to the higher layers. The physical layer communicates with the RRC and the MAC layers. This interfacing is shown in Figure 3.1[31].

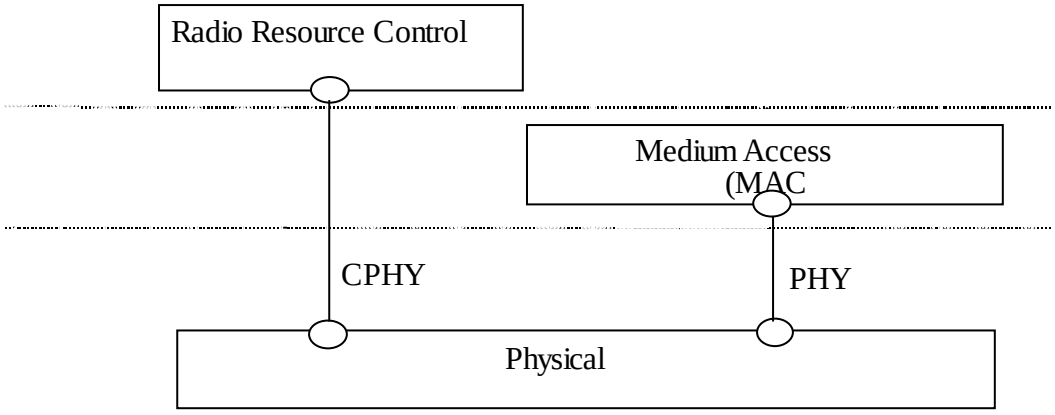

Figure 3.1 Interface of the physical layer with upper layers [31]

3.2.1 Interface to MAC Layer

The physical layer offers data transmission services to the MAC layer. The communication between the physical layer and MAC layer occurs through PHY primitives. The definition of the PHY primitives is done in an abstract way that does not constrain the implementation. The main functions performed by the PHY primitives are: (i) to transfer the transport blocks over the radio interface and (ii) to indicate the status of the layer 1 to layer 2.

3.2.2 Interface to RRC

The physical layer acts as an interface between the RRC entity in the User Equipment (UE) and in the network. Communication is performed in an abstract way using CPHY primitives. The primitives exchange functions to control the configuration of the physical layer.

3.3 Transport Channels

Transport channels are defined by the MAC layer. The corresponding transport format controls the coding, interleaving, rate matching etc. of the transport channel. Layer 1 can multiplex several transport channels together to form a Coded Composite Transport Channel. In this case, the Transport Format Combination Indicator (TFCI) fields uniquely identify the transport formats used by the individual transport channels [31]. Table 3.1

lists the different transport channels defined by the 3G standards for Uplink (UL) and Downlink (DL). The combination of transport channels forms a transport block. The allowed transport block combinations are listed in [31].

Table 3.1 Transport Channels defined in WCDMA standard

Channel	Expanded Name	UL/DL	Function
DCH	Dedicated Channel	UL and DL	- Only dedicated channel - Fast rate change - Fast power control - Inherent addressing of UEs
BCH	Broadcast Channel	DL	- Broadcast system and cell specific information - Transmitted over entire cell - Low fixed bit rate
FACH	Forward Access Channel	DL	- Transmitted over entire cell using omni directional antennas or part of cell using beam forming antennas - Uses slow power control
PCH	Paging Channel	DL	- Transmitted over entire cell - Associated with the transmission of paging indicator in the physical layer
RACH	Random Access Channel	UL	- Received from the entire cell - Open loop power control - Limited size data field - Risk of collision
CPCH	Common Packet Channel	UL	- Bursty data traffic - Contention based
DSCH	Downlink Shared Channel	DL	- Shared by several UEs - Associated with a DCH

3.4 Physical Channels

The transport blocks obtained from the upper layer are mapped to logical physical channels by layer 1. The physical layer follows exact timing of 10 ms for the radio frames. A transport block is generated every 10 ms or multiple thereof. The physical channel consists of a layered structure of radio frames and time slots. A radio frame in 3G is a processing slot consisting of 15 time slots [32]. The number of bits/time slot depends on the physical channel.

The different physical channels defined in the 3G standard are listed in Table 3.2. The wireless system capacity is usually uplink limited, hence in our study we look into the uplink only. In addition we look into dedicated resource allocation – so dedicated physical channels in the uplink are studied. In the following sub-sections we will give a description of the dedicated uplink physical channels – DPDCH and DPCCH.

Table 3.2 Physical channels in the 3G standard

Channel	Expanded Name	UL/DL	Description	TRCH
DPDCH	Dedicated Physical Data Channel	UL	- Dedicated channel - Carries data generated by Layer 2 and above	DCH
DPCCH	Dedicated Physical Control Channel	UL	- Dedicated channel - Carries control information generated by layer 1 in the Q-channel	DCH
PRACH	Physical Random Access Channel	UL	- Common Channel - Slotted ALOHA used for channel access	RACH
PCPCH	Physical Common Packet Channel	UL	- Common channel - Uses Digital Sense Multiple Access (DSMA-CD) with fast acquisition indication	CPCH
DPCH	Dedicated Physical Channel	DL	- Dedicated channel - Control and data information are time multiplexed.	DCH
CPICH	Common Pilot Channel	DL	- Common channel - Fixed rate (30 kbps, SF=256) - Carries a pre-defined bit/symbol sequence. - Two types – Primary CPICH and Secondary CPICH - Used as phase reference	CPCH
P-CCPCH	Primary Common Control Physical Channel	DL	- Common channel - Fixed rate	BCH
S-CCPCH	Secondary Common Control Physical Channel	DL	- Common channel - Multiple rates possible	FACH PCH
SCH	Synchronization Channel	DL	- Common channel - Used for cell search	DSCH
PDSCH	Physical Downlink Shared Channel	DL	- Common channel - Shared by users based on code multiplexing	DSCH
AICH	Acquisition Indicator Channel	DL	- Common channel - Used to carry Acquisition Indicators (AI)	DSCH
PICH	Page Indicator Channel	DL	- Common channel - Fixed rate - Carries Page Indicators (PI)	DSCH

3.4.1 DPDCH

DPDCH is the dedicated uplink channel used to carry the data in DCH. The DPDCH is multiplexed into the I and Q channels. There may be zero, one or several uplink DPDCHs on each connection. The channelization codes used for the DPDCHs depend on the spreading factor. The DPDCH Spreading Factor (SF) can vary from 256 down to 4. In addition, multi-code operation is possible for the uplink dedicated physical channels. In such a case, several parallel DPDCH are transmitted using different channelization codes.

The frame length of DPDCH is of duration 10 ms and is divided into 15 slots. Each 10 ms frame has 38400 chips, leading to a chip rate of 3.84 Mcps. The frame format is shown in Figure 3.2. The channel bit rate, SF, bits/frame, bits/slot and data bits in each frame are given in Table 3.3.

Table 3.3 DPDCH fields [32]

Slot Format #I	Channel Bit Rate (kbps)	SF	Bits/ Frame	Bits/ Slot
0	15	256	150	10
1	30	128	300	20
2	60	64	600	40
3	120	32	1200	80
4	240	16	2400	160
5	480	8	4800	320
6	960	4	9600	640

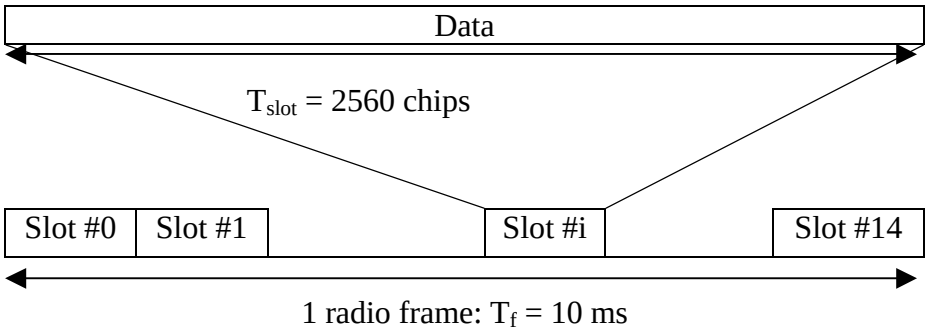

Figure 3.2 Frame format of DPDCH

3.4.2 DPCCH

DPCCH is the dedicated uplink channel used to carry the Layer 1 control information. The control information includes pilot bits, transmit power control (TPC) commands, feedback information (FBI) and an optional TFCI. The pilot bits are used to support channel estimation for coherent detection. The pilot bits can also be used to form the weights for tracking beam antenna arrays as described in [33].

There is only one DPCCH per Layer 1 connection and it is multiplexed into the Q-channel. The DPCCH has a constant data rate and uses the same spreading code for all the users. The frame format of the uplink control channel is shown in Figure 3.3.

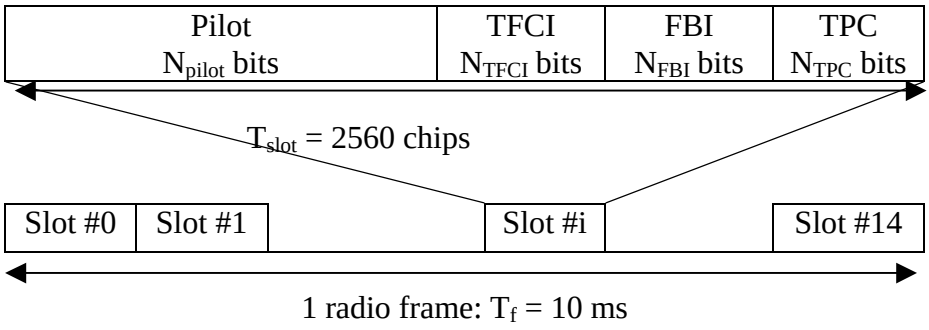

Figure 3.3 Frame format of DPCCH

3.5 Uplink transmitter

In this section we describe the physical layer at the MS supporting WCDMA standard. The MAC layer supplies the transport block sets to the physical layer at periodic intervals called Transmission Time Interval (TTI) [31]. The TTI is always a multiple of the minimum interleaving period. The TTI must belong to the set {10 ms, 20 ms, 40 ms, 80 ms}. For simplicity, we have limited the model to 10 ms transport block sets.

The data flow diagram for the WCDMA uplink transmitter is given in Figure 3.4. The data coming from the higher layers is segmented and sent to the convolutional encoder. The coded data is rate matched so as to get a pre-defined rate, and then this data is

interleaved. The interleaved data is mapped to physical channels. Depending on the physical channel used the data is spread and then scrambled prior to transmission.

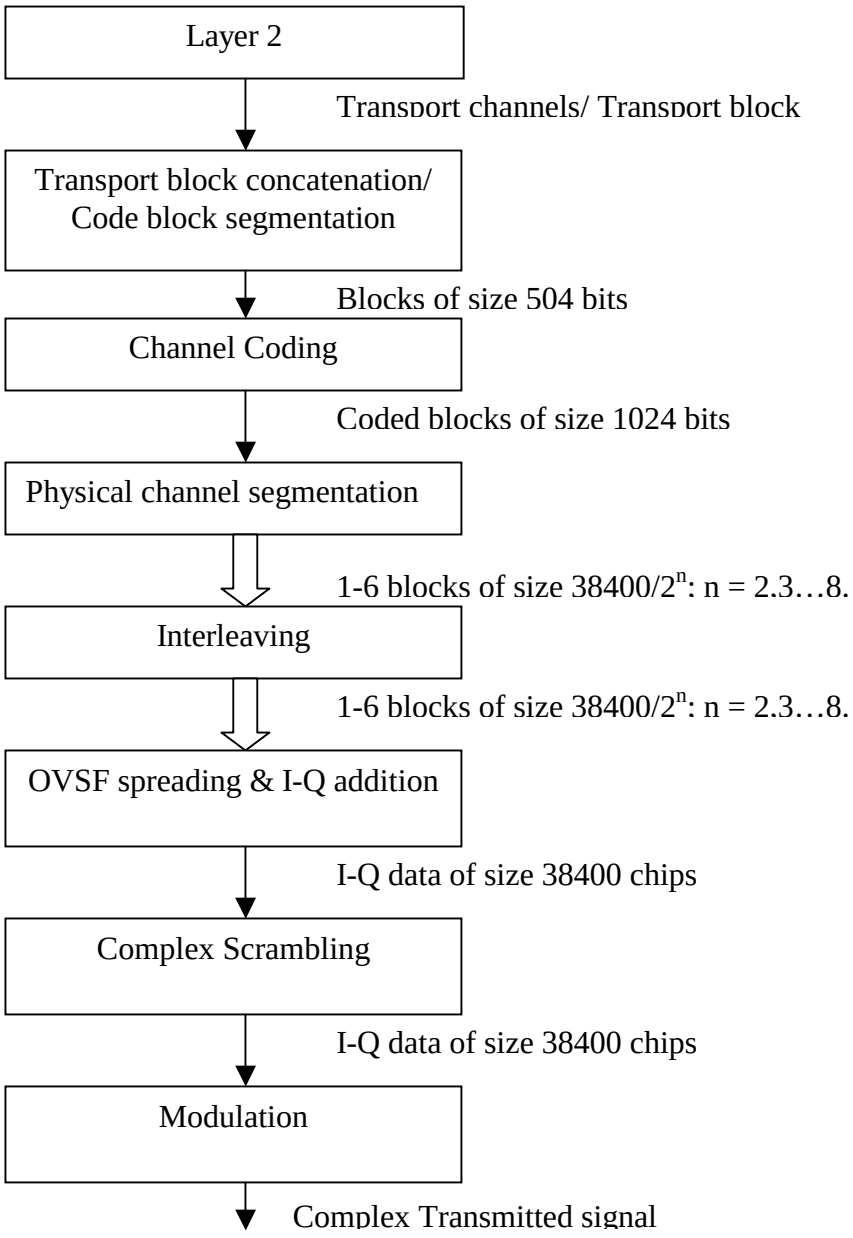

Figure 3.4 Data flow diagram for the uplink transmitter with 10 ms transport block size

3.5.1 Channel Concatenation and Code block segmentation

The transport channels contain a sequence of *X* data bits to be transmitted to the base station. There can be multiple transport blocks that are to be transmitted over a single

Transmission Time Interval (TTI). All the transport blocks to be transmitted over a TTI are serially concatenated. However the error correction coding applied to the transmitted data has set block sizes (C) as given in Table 3.4. If the number of bits in a TTI is larger than the code block size, then code block segmentation is performed to obtain constant length code blocks. If $X \neq nC$ where n is any integer, filler bits are added to the last block.

Table 3.4 Code block sizes for different coding schemes

Error control coding	**Code Block Size**
Convolutional coding	504
Turbo coding	5114
No coding	Unlimited

3.5.2 Channel Coding

In the WCDMA standard, three kinds of channel coding techniques are suggested – Rate ½ convolutional codes, rate 1/3 convolutional codes, and rate ½ turbo codes [34]. The coding scheme used for transmission is specified in the transport channel. The data channels can use any of the coding schemes listed or transmit uncoded information. We have implemented and studied two of the coding schemes in the present system. These two coding techniques are described below.

3.5.2.1 Convolutional Coder

The connection diagram of the coder is shown in Figure 3.5 and Figure 3.6. The coder has a block length of 9 and uses a block size of 504. Eight tail bits are added to flush the coder, resulting in a coded block length of 1024 for rate ½ coder or 1520 for rate 1/3 coder. The coders start with the all the registers initialized to zeros. The coded bits are sent to the interleaver before transmission.

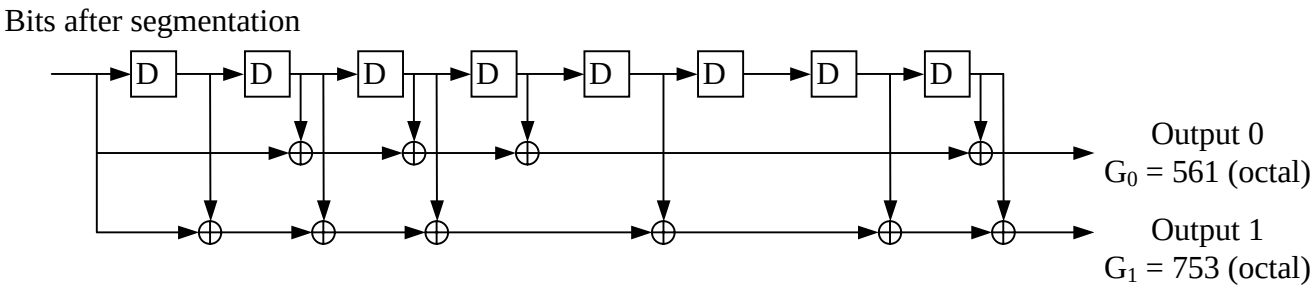

Figure 3.5 Connection diagram of rate 1/2 convolutional coder

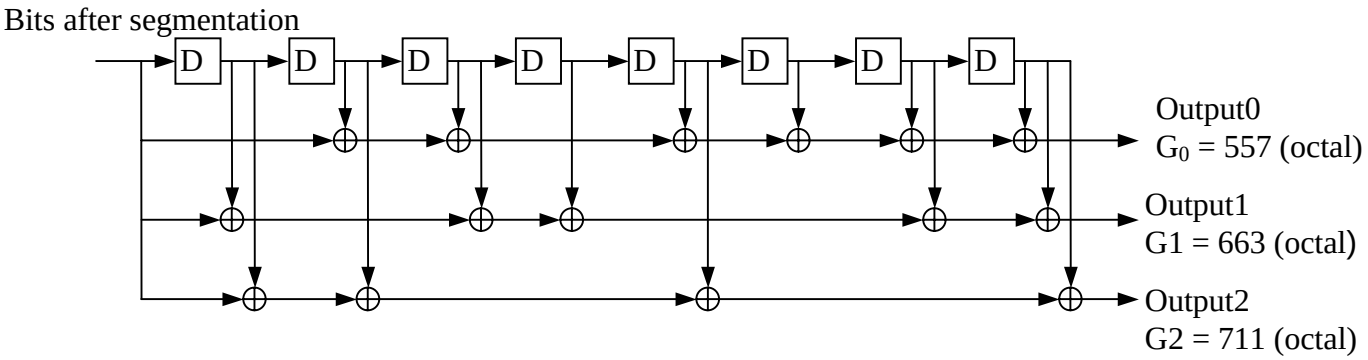

Figure 3.6 Connection diagram of rate 1/3 convolutional coder

The data rates supported by the system for the two different convolutional coding schemes are shown in Table 3.1 and Table 3.6 respectively.

Table 3.5 Data rate calculation for rate ½ coder

Final Chip Rate	SF	# of Channels	Coded Bits Per Frame	# of Code Blocks	Coded Bits from Encoder	Bits to Encoder + Trailing Zeros	Data Bits	Data Rate
38400	256	1	150	1	150	75	67	6700
38400	128	1	300	1	300	150	142	14200
38400	64	1	600	1	600	300	292	29200
38400	32	1	1200	1	1024	512	504	50400
38400	16	1	2400	2	2048	1024	1008	100800
38400	8	1	4800	4	4096	2048	2016	201600
38400	4	1	9600	9	9216	4608	4536	453600
38400	4	2	19200	18	18432	9216	9072	907200
38400	4	3	28800	28	28672	14336	14112	1411200
38400	4	4	38400	37	37888	18944	18648	1864800
38400	4	5	48000	46	47104	23552	23184	2318400
38400	4	6	57600	56	57344	28672	28224	2822400

Table 3.6 Data Rate calculation for Rate 1/3 coder

Final Chip Rate	SF	Number of Channels	Coded Bits Per Frame	# of Code Blocks	Coded Bits from encoder	Bits to Encoder+ Trailing bits	Data Bits	Data Rate
38400	256	1	150	1	150	50	42	4200
38400	128	1	300	1	300	100	92	9200
38400	64	1	600	1	600	200	192	19200
38400	32	1	1200	1	1200	504	496	49600
38400	16	1	2400	1	1512	504	496	49600
38400	8	1	4800	3	4536	1512	1504	150400
38400	4	1	9600	6	9072	3024	3016	301600
38400	4	2	19200	12	18144	6048	6040	604000
38400	4	3	28800	19	28728	9576	9568	956800
38400	4	4	38400	25	37800	12600	12592	1259200
38400	4	5	48000	31	46872	15624	15616	1561600
38400	4	6	57600	38	57456	19152	19144	1914400

3.5.3 Physical Channel Segmentation

The input to the physical channel segmentation block is the output of the rate-matching block. Rate matching is applied to the transmitted sequence as per the command of the higher layers. If the data rate is high, then multiple physical channels, DPDCH, are used and the bits are divided among the different Physical Channels. If the input data is denoted by x_1, x_2, $x_3 \ldots x_Y$ where Y is the number of bits input to the physical channel segmentation block, P is the number of physical channels, and U is the number of bits in one radio frame for each physical channel, then the number of bits in one radio frame is given by Equation 3.1.

$$U = \frac{Y}{P} \qquad 3.1$$

The bits after physical channel segmentation are given by

$u_{1k} = x_k$ k = 1,2,…U

$u_{2k} = x_{k+U}$ k = 1,2,…U

$u_{pk} = x_{k+(p-1)U}$ k = 1,2,…U

3.5.4 Interleaving

Interleaving is performed to protect the code from block errors. Convolutional coding is robust against random errors but breaks down for burst errors. Introducing an interleaver in between is an effective technique for spreading the errors. There are two stages of interleaving specified in the standard. The second interleaver stage[1] will interleave the data as specified in Table 3.7

Table 3.7 Second Interleaving pattern.

Number of column C_2	Inter-column permutation pattern
30	{0, 20, 10, 5, 15, 25, 3, 13, 23, 8, 18, 28, 1, 11, 21, 6, 16, 26, 4, 14, 24, 19, 9, 29, 12, 2, 7, 22, 27, 17}

[1] The first interleaving occurs for transport block sets having TTI $\in$ {20, 40,80}

3.5.5 Spreading

Once the data is segmented into physical channels and interleaved, it has to be spread so as to achieve a final transmitted chip rate of 3.84 Mcps. For a 10 ms frame, the number of chips/frame is

$$Nchips = (3.84 \times 10^6) \times (10 \times 10^{-3}) = 38400 \ \ chips / \ frame$$

To accommodate different bit rates coming into the spreading block, the spreading length must be different. When physical channels are multiplexed into the same frame, the codes should be orthogonal to each other so as to separate them at the receiver. The technique of using orthogonal codes to separate physical channels in the same frame is termed channelization. The spreading codes also provide spreading gain to the transmitted information. Hence the function of the channelization codes is three fold - (i) to obtain a constant bit rate for transmission regardless of the data rate; (ii) to obtain spreading gain; and (iii) to accomplish channelization.

Orthogonal Variable Spreading Factor (OVSF) codes are used for spreading. The OVSF codes can be explained using the code tree given in Figure 3.7. In the figure, the codes are represented as $C_{ch,k,n}$. The subscripts uniquely describe a code word in the code tree. The channelization code has 3 subscripts (ch, k, n). The first subscript "ch" denotes that the code is a channelization code. The second subscript (k) is equal to the length of the code. The third subscript (n) gives the specific code in the channelization sequence.

The first bit transmitted is the leftmost bit in the sequence. Each level in the code tree defines spreading codes of length SF. All codes in the same level (same value of k) are orthogonal to each other. Two codes in different levels are orthogonal to each other if one of the codewords is not the mother (root) code of the other. This will lead to the restriction that a station cannot simultaneously use two codes, where one code is the mother of the other [35].

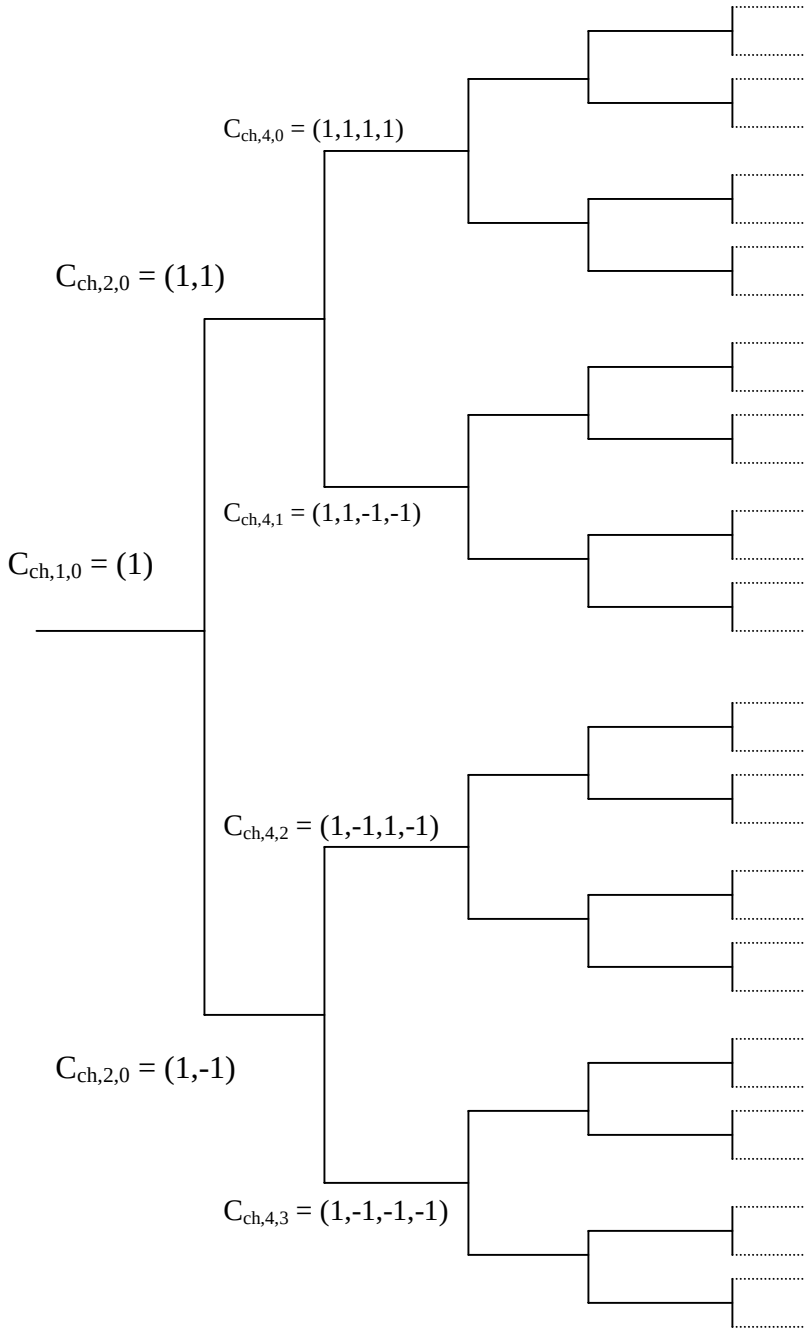

Figure 3.7 Code tree used for the generation of OVSF codes

In many cases the spreading and de-spreading is carried out in software. In this case, the OVSF codes can be generated iteratively. For this purpose a matrix representation of the OVSF codes can be used.

$$C_{ch,n,x} = \begin{bmatrix} C_{ch,n-1,x} & C_{ch,n-1,x} \\ C_{ch,n-1,x} & -C_{ch,n-1,x} \end{bmatrix}$$

where $C_{ch,1,0}$ = [1]. In many signal processing applications, this matrix can be created using Hadamard transforms.

The spreading factor required can be determined from the raw data rate by using equation 3.2.

SF = 38400 / (raw data rate in bps* 10 ms) 3.2

For uplink transmission, DPCCH has a data rate of 150 kbps, and a spreading factor of 256 is used. The OVSF code $C_{ch,256,1}$ is used by the control channel. All the channels having the same data rate are allotted the same spreading code in the uplink and the code is denoted by $C_{ch,k,n}$ where k= length of the code, n = branch of the tree.

The codes for the different channels are allotted based on the following rules [36]:

1. The DPDCH channel is always spread by $C_c = C_{ch,256,0}$
2. When only one DPDCH exist, it is spread by $C_{d,1} = C_{ch,SF,k}$ where SF is the spreading factor and $k = SF / 4$.
3. For multiple DPDCH, all DPDCH have spreading factor $SF = 4, C_{d,n} = C_{ch,4,k}$ where $k = 1$ if $n \in \{1,2\}, k = 2$ if $n \in \{5,6\}, k = 3$ if $n \in \{3,4\}$

3.5.6 Scrambling

After channelization using the spreading codes, the code sequence will have 38400 chips/frame. The DPDCH/DPCCH may be scrambled using either long or short spreading codes. We use long spreading codes in our implementation.

The long scrambling codes are Gold codes, generated using the position wise modulo-2 sum of 38400 chip segments of two binary m-sequences of degree 25. The primitive polynomials for the generation of the m-sequences are given by equation 3.3

$$G_1(X) = X^{25} + X^3 + 1$$
$$G_2(X) = X^{25} + X^3 + X^2 + X + 1 \quad 3.3$$

If $x_n(i)$ and $y_n(i)$ denote the two m-sequences generated using the above polynomials, the binary Gold sequence z_n is given by using equation 3.4

$$z_n(i) = x_n(i) + y_n(i) \quad , i = 0,1,2,....2^{25} - 2 \quad 3.4$$

From this the real valued gold sequence $z_n(i)$ is computed by Equation 3.5

$$Z_n(i) = \begin{cases} +1 & if\ z_n(i) = 0 \\ -1 & if\ z_n(i) = 1 \end{cases} \quad for\ \ i = 0,1,\ldots,2^{25} - 2. \quad 3.5$$

The real-valued long scrambling sequences are defined by Equation 3.6 and Equation 3.7.

$c_{long,1,n}(i) = Z_n(i),\ i = 0, 1, 2, \ldots, 2^{25} - 2$ 3.6

$c_{long,2,n}(i) = Z_n((i + 16777232) \text{ modulo } (2^{25} - 1)),\ i = 0, 1, 2, \ldots, 2^{25} - 2.$ .. 3.7

And the complex valued long scrambling sequence $C_{long,n}$ is defined as

$$C_{long,n}(i) = c_{long,1,n}(i)\left(1 + j(-1)^i c_{long,2,n}\left(2\lfloor i/2 \rfloor\right)\right) \quad 3.8$$

where $i = 0, 1, \ldots, 2^{25} - 2$ and $\lfloor\ \rfloor$ denotes rounding to nearest lower integer. Figure 3.8 shows the configuration of the scrambling code generator.

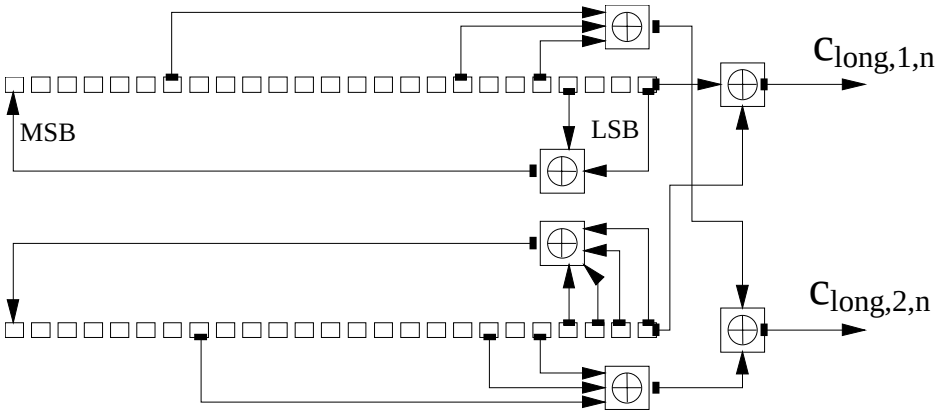

Figure 3.8 Configuration of uplink scrambling sequence generator [36]

3.5.7 Modulation

There are two modulation schemes defined for the WCDMA standard. The transmitted symbols in the downlink are BPSK modulated and in the uplink they are QPSK modulated. The data bits after scrambling are QPSK modulated before transmission.

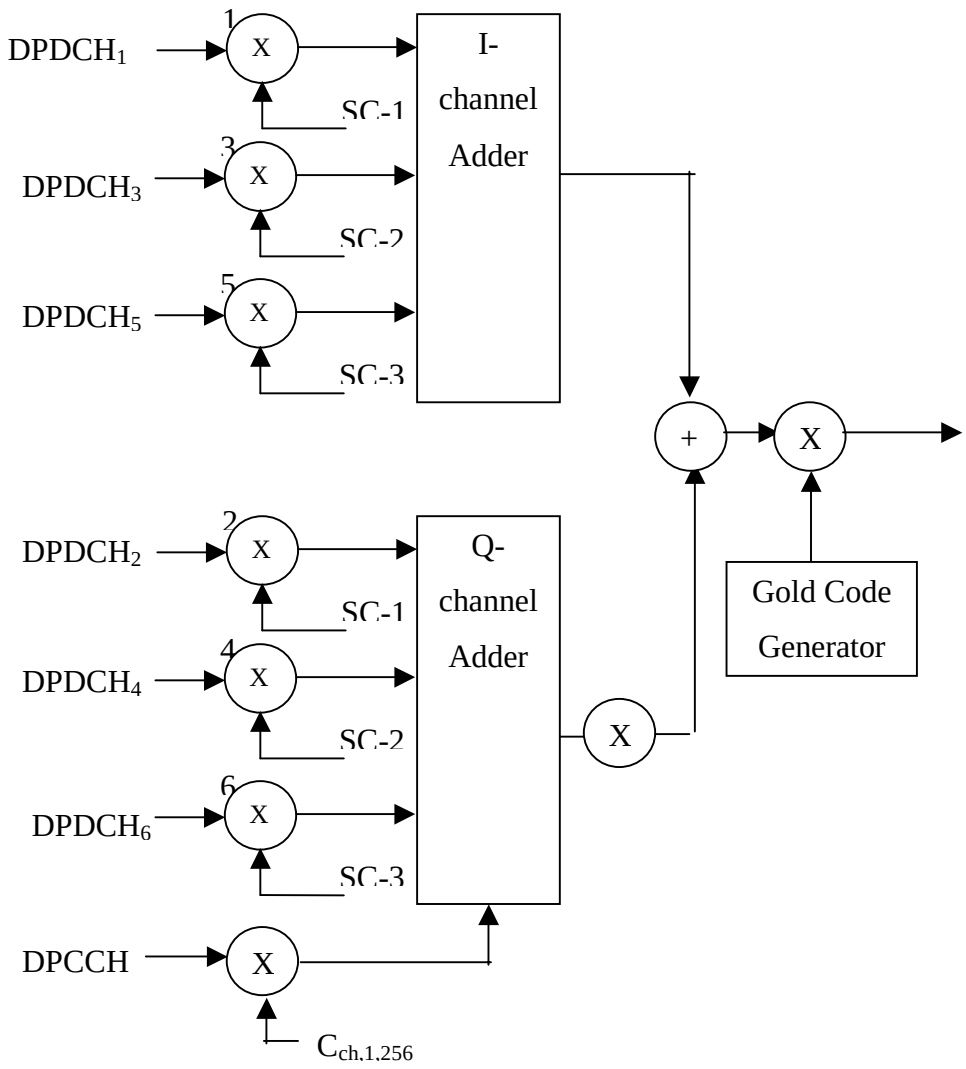

Figure 3.9 Spreading and scrambling of the uplink transmitted sequence

3.6 Uplink Receiver

The transmitted signal passes through a vector channel that introduces large scale and small scale fading and Additive White Gaussian Noise (AWGN) in the received signal. A rake receiver can be used to combine multiple copies of the same signal that may arrive at the receiver. The use of beam forming antennas (smart antennas) at the receiver will add another dimension to the signal processing, leading to the use of Two Dimensional Rake (2D-Rake) receivers. The output of the 2D-Rake is an optimal or sub-optimal combination of the received signal. The output of the 2-D Rake receiver is fed to the receiver, whose data flow diagram is shown in Figure 3.10

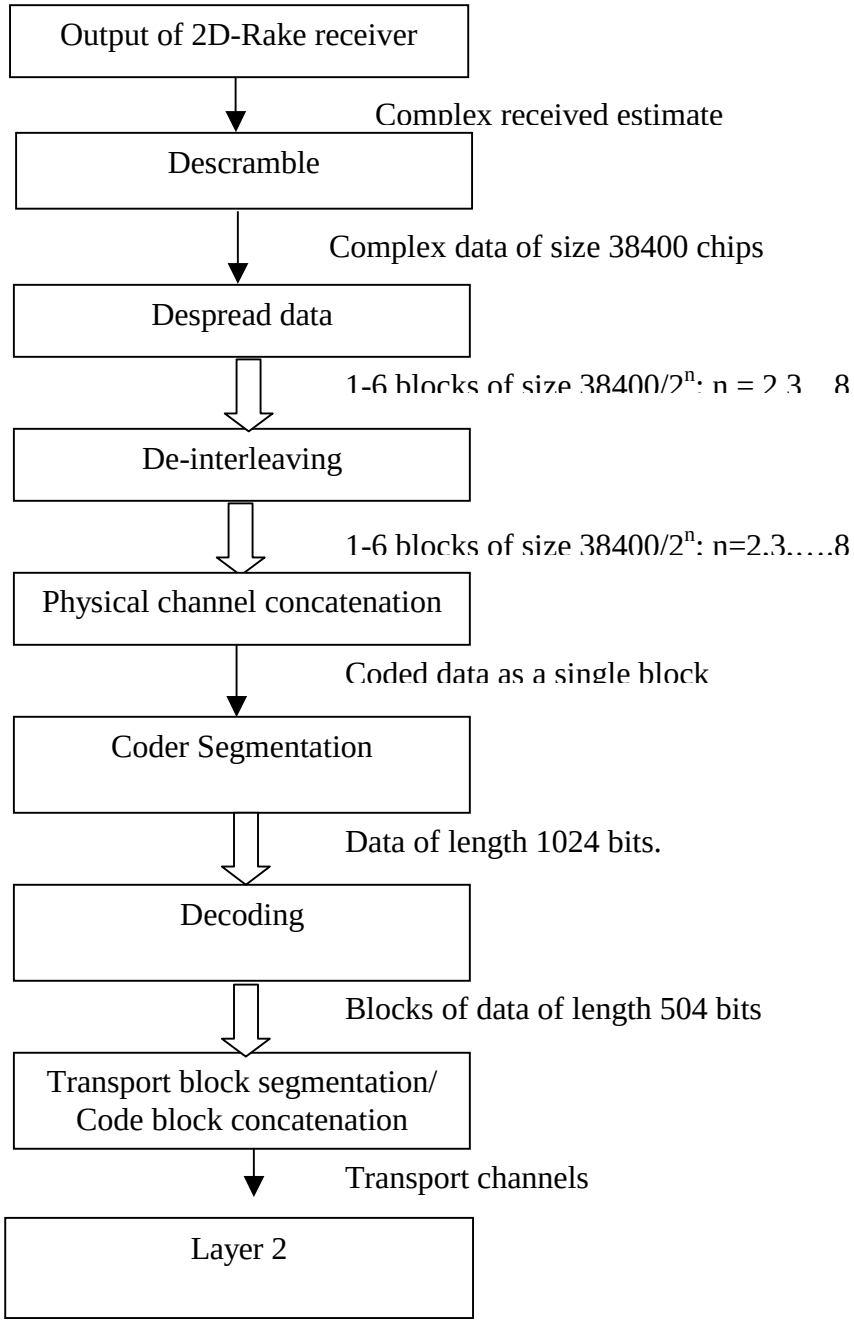

Figure 3.10 Data flow diagram at the receiver

3.6.1 Rake Receiver

In a CDMA system, the received signal has resolvable multipath components, providing temporal diversity. Rake receivers exploit multipath scenario by coherently combining the energy in the different multipath components. The time delay of each multipath component is estimated and coherently received. All the multipath components are added together to obtain the received signal. This is shown in Figure 3.11.

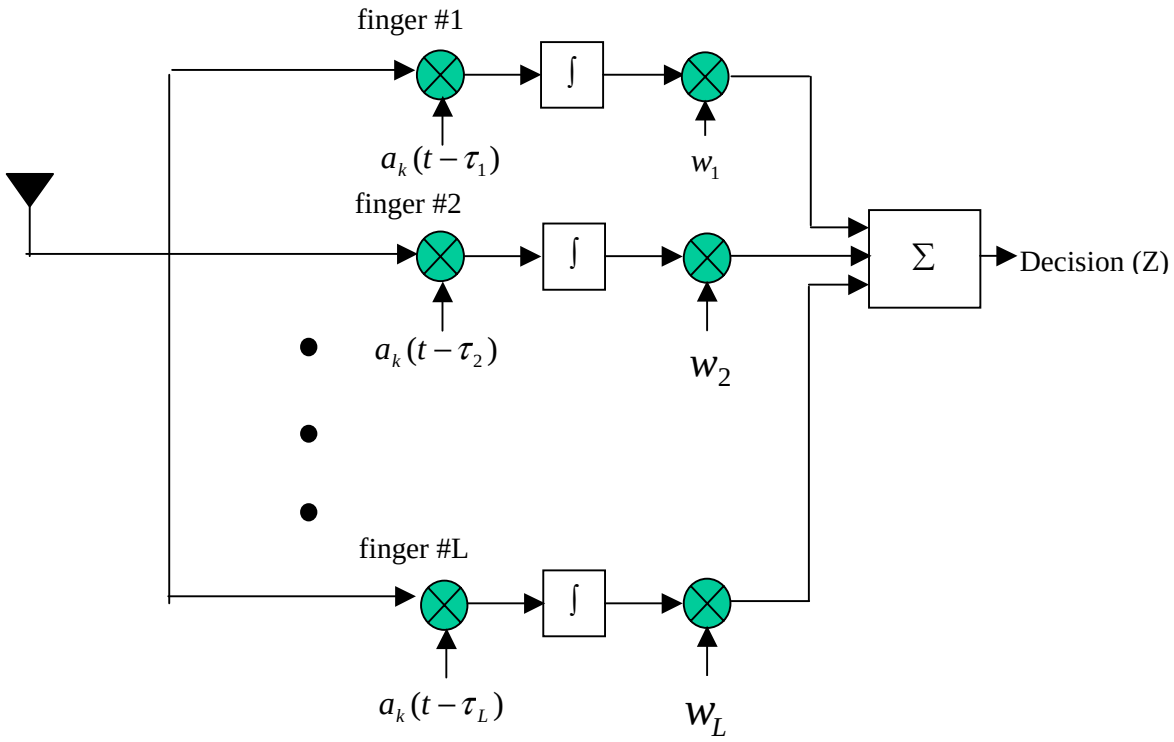

Figure 3.11 Block diagram of a rake receiver

In the diagram, τ_i is the delay of the i^{th} multipath, a_k is the scrambling code, w_i is the weight of each branch. Depending on the relationship of the weights, there are different types of combining schemes, including among others:

(i) Selection combining

(ii) Equal Gain Combining (EGC)

(iii) Maximal Ratio Combing (MRC)

Of these approaches, MRC gives the best performance [37]; in our simulation model we use a MRC rake receiver for temporal combining.

The performance advantage of a rake receiver depends on the number of rake fingers and the relative power of the multipath components. For instance the user of a rake receiver will yield more benefits for an indoor channel with fewer resolvable multipath components. This is shown in Figure 3.12.

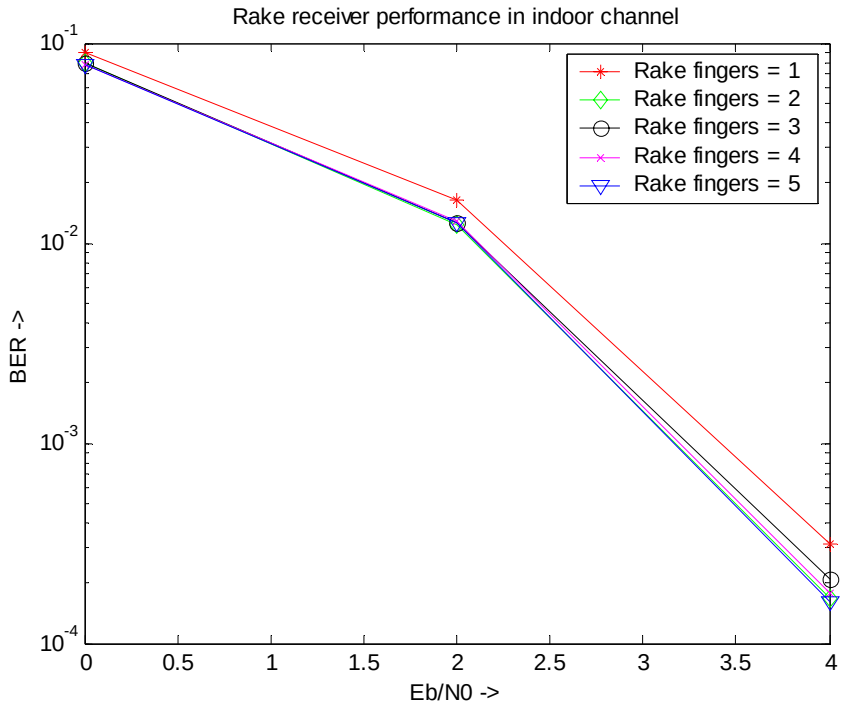

Figure 3.12 Rake receiver performance in indoor channel

From Figure 3.12, it can be observed that for an indoor channel the performance does not increase significantly as we increase the number of rake fingers beyond 2 fingers. This is due to the fact that in the channel we are modeling, there are only two significant multipath components that can be resolved.

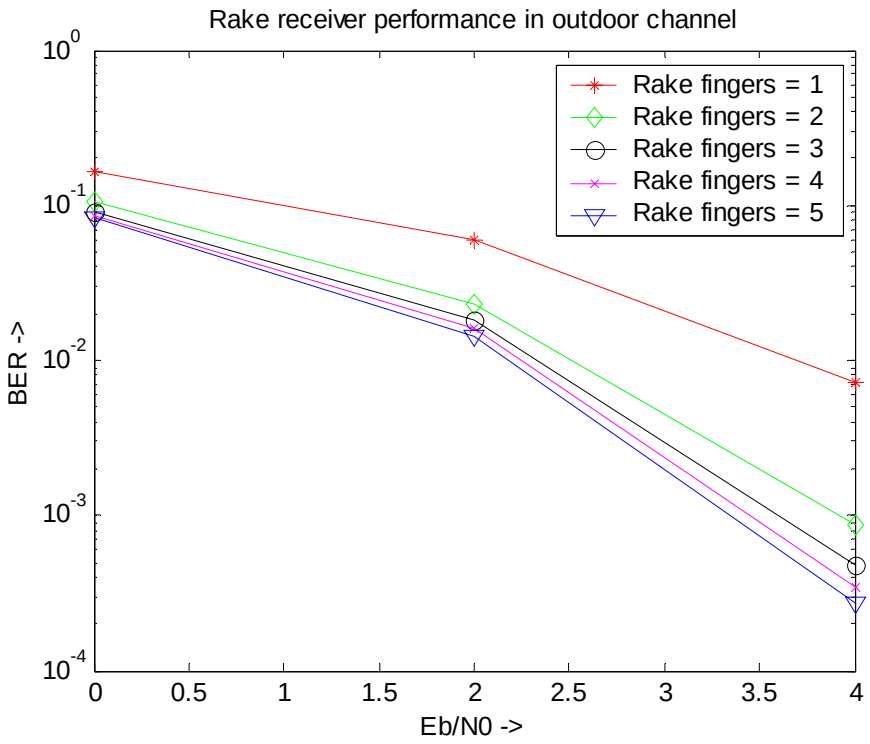

Figure 3.13 Rake receiver performance in outdoor channel

From the BER plot for the outdoor channel, we can see that the BER decreases as the number of rake fingers increases. However the performance improvement is not very significant beyond 4 rake fingers. This shows that the rake receiver is more effective in an outdoor channel.

In our system we assume perfect channel estimation, meaning that the channel coefficients are known and not estimated. This is the ideal case; the effect of errors due to channel estimation can be found in [38].

3.6.2 Beamforming

Smart antennas provide higher capacity and range extension to a cellular communication system. The smart antenna system consists of an array of low gain antenna elements connected by a combining network [39]. However, in practical systems we use identical antenna elements arranged with equal spacing. A baseband complex envelope model of a

Linear Equally Spaced (LES) array is shown in Figure 3.14. It can be seen from the array geometry that the same signal will be arriving at array element l after a time delay Δt. For a narrow band assumption for the received signal, the time delay can be modeled as a simple phase shift [37]. Another simplifying assumption is to consider that the antenna elements are isotropic. The received signal z(t) can be represented by equation 3.9 [39]

$$z(t) = \sum_{k=1}^{K} w_k u_k(t) = As(t) \sum_{k=1}^{K} w_k \exp(-j\beta d_k \cos\phi \sin\theta) = As(t) f(\theta, \phi) \qquad 3.9$$

$f(\theta, \phi)$ is called the array factor. The array factor is a function of the azimuth and elevation angles of arrival, the weights of the antenna elements, the separation of the array elements and the wavelength of the received signal. The minimum separation between the elements should be at least half wavelength [37]. i.e.,

$$\Delta x \geq \frac{\lambda}{2} \qquad 3.10$$

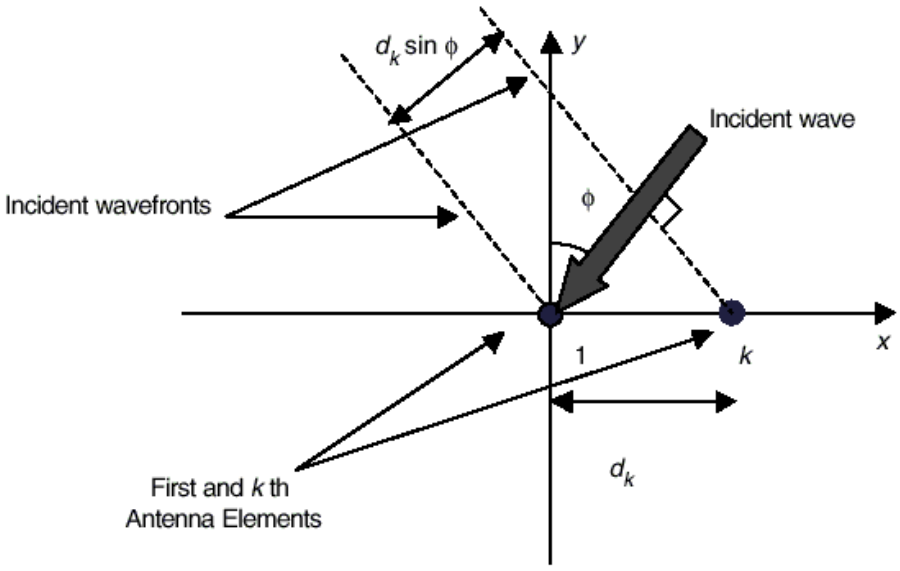

Figure 3.14 Geometry of a LES antenna array [37]

If the smart antennas are deployed at the BS, the wave is incident in the x-y plane so that the elevation angle is $\frac{\pi}{2}$. Then, the arrays factor becomes a function of the azimuth angle of arrival only. Considering the minimal spatial separation for the antenna array, the array factor can be simplified and is represented in Equation 3.11

$$f(\theta,\phi) = \sum_{m=1}^{M} w_m \exp(-j\pi m \cos\phi) \qquad 3.11$$

The beam can be made to point in any direction by changing the weights w_m.

So, changing ϕ_0 will point the beam to different directions. Figure 3.15 shows the plot when $\phi_0 = 45^0$.

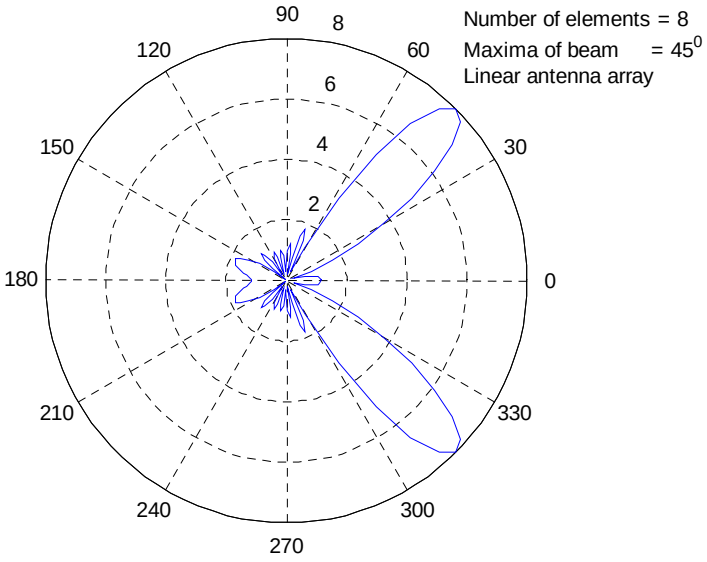

Figure 3.15 Array factor of a linear antenna array with maxima at 45^0

From Figure 3.15 It can be seen that the antenna pattern is symmetrical. This is because the linear antenna array is single dimensional. A two-dimensional antenna array will

provide more flexibility to the beam pattern. The array factor of a circular antenna array is given in Equation 3.12.

$$f(\theta,\phi) = \sum_{m=1}^{M} I_m \exp(j\alpha_m)\exp(j\beta\rho_m^{'}\sin\theta\cos(\phi-\phi_m)) \quad 3.12$$

I_m is the current excitation of the mth element located at $\phi = \phi_m$, α_m is the associated phase excitation and $\rho_m^{'}$ is the radial distance of each element center from the origin. For cophasal excitation, the antenna weights are given by Equation 3.13

$$\alpha_m = -\beta\rho_m^{'}\sin\theta_0\cos(\phi_0-\phi_m) \quad 3.13$$

where θ_0 and ϕ_0 are the desired position of the main beam maximum.

We consider a circular antenna array having constant response in the Z-axis and having maxima at 90^0 and equally spaced at half wavelength from the origin. The current excitation is assumed to be 1Amp. i.e.,

$$f(\theta,\phi) = f(\phi) \quad 3.14$$

$$\theta = \frac{\pi}{2} \quad 3.15$$

$$\rho_m^{'} = \frac{\lambda}{2} \quad 3.16$$

$$and \quad \beta = \frac{2\pi}{\lambda} \quad 3.17$$

Using these assumptions, the beam pattern for the circular antenna array can simplified as Equation 3.18.

$$f(\phi) = \sum_{m=1}^{M}\exp(-j\pi\cos(\phi_0-\phi_m)).\exp(j\pi\cos(\phi-\phi_m)) \quad 3.18$$

The beam pattern for circular antenna array is plotted in Figure 3.16.

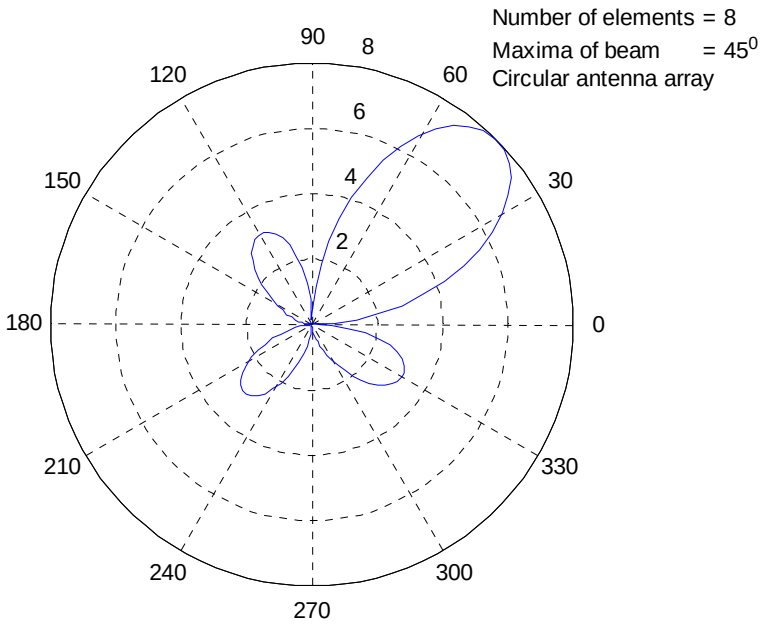

Figure 3.16 Array factor of circular antenna array

If the weights are static, we have a fixed beam antenna array. A Beam Forming Network (BFN) can be used to produce M beams from M elements. Hence, by using an 8-element antenna we can obtain 8 beams. If the smart antenna system uses only the fixed BFN, a switch can be used to select the best beam to receive a particular signal. The best signal output from the set of beamformer outputs can be chosen for a user.

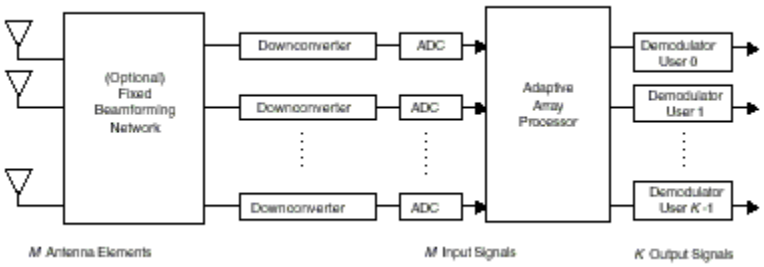

Figure 3.17 Fixed beamforming network[37]

The antenna weights are updated to maximize the quality of the signal that is available to the demodulator. In the case of adaptive antenna arrays, the maxima of the beam will shift so as to point to the desired user's direction of arrival. The weights are updated so as to converge to the desired user. There are various techniques for beam forming. These can be found in [37,39].

Either adaptive antenna arrays or switched beam arrays can be used for beam forming. In a CDMA system there are many users using the same channel, hence forming nulls towards all the interferers will become computationally very complex. Studies [1] have shown that the performance of a switched beam is only slightly less than that achieved by an adaptive antenna array.

In our system we use a simple switched beam circular antenna array. The advantage of the circular array is the presence of a single major lobe as opposed to two lobes in the linear array. If the symmetric beam pattern of a linear array is used, there will be interference from non co-located users. Using the circular antenna array simplifies the resource allocation since there is no high interference from non co-located users.

Switched beam arrays have lower implementation complexity as compared to the tracking beam antenna array. If tracking beam arrays are used, the issue becomes two-fold – weight determination for beamforming and resource management. In addition, a BS with finite number (M) of antenna elements, can form only M beams. If the number of users in the cell is greater than M, then beams cannot be formed towards all users. Hence other techniques like multi user detection or overloaded array processing will have to be used along with beam forming. Hence we use a switched beam antenna array in our system.

3.6.3 2D-Rake Receiver

In the present system we have both time diversity and space diversity. Different multipath signals from the users will be arriving at the receiver with different AoA. A space-time RAKE receiver structure consists of a spatial combiner for each of the

multipath components followed by a temporal RAKE receiver. We can use any of the combining techniques for the spatial combining and the temporal combining. Therefore we can have EGC, MRC or selection combining for the spatial combiner and the same or different combining schemes for the 1-D Rake receiver. This type of combined space and time combining is called 2D-Rake receiver. A block diagram of the 2D-Rake receiver is given in Figure 3.18.

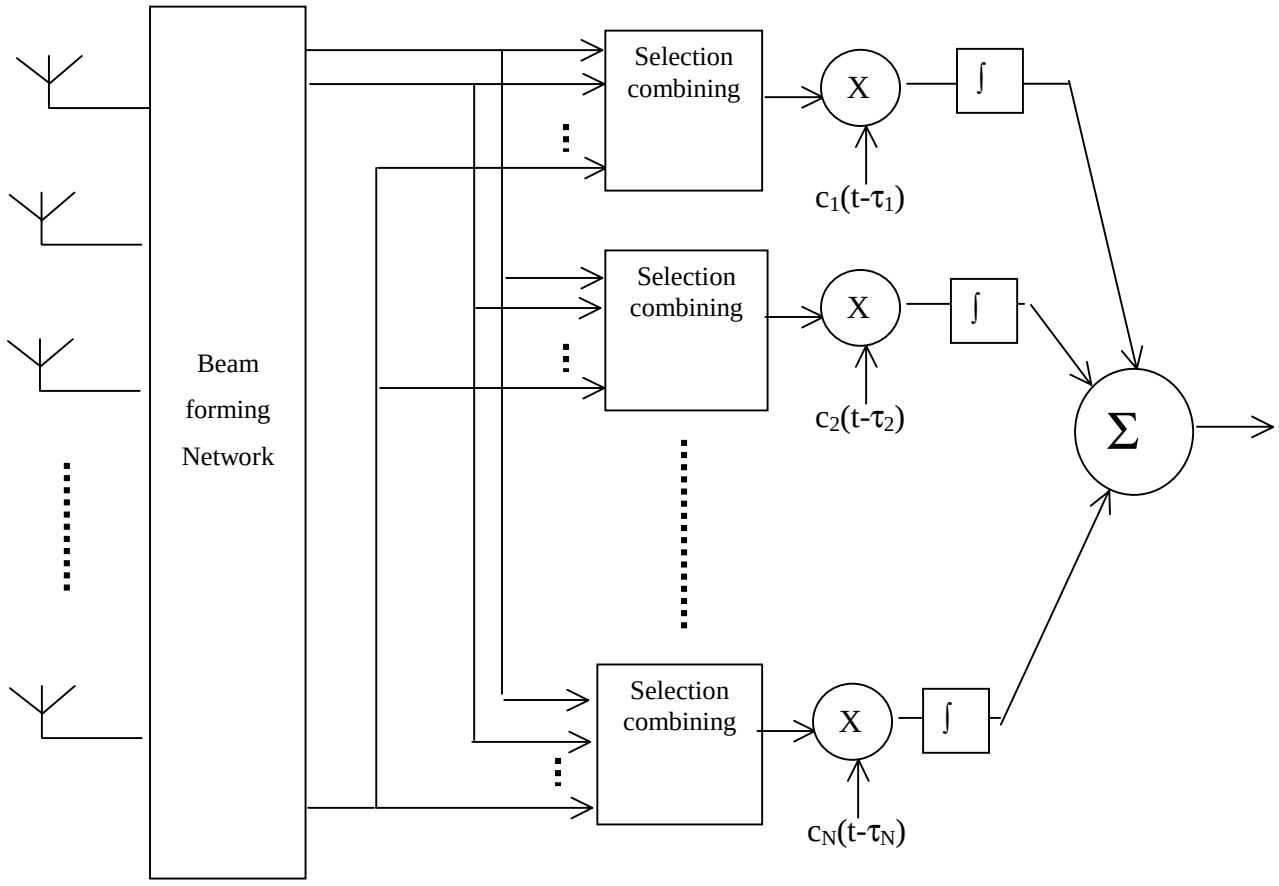

Figure 3.18 Two-dimensional RAKE receiver decoding for a single user

In our system we use selection combining for the spatial combining and MRC for the temporal combining. Hence each antenna selects the best signal at the beam former

output for each multipath. The different multipath components are co-phased and combined by the 1-D rake receiver to give a single estimate of the received signal.

3.6.4 De-scrambling and De-spreading

The signal received from the 2D-Rake receiver has the scrambling code and the spreading code superimposed to it. The first step is to de-scramble the received signal with the scrambling code. The higher layers assign the scrambling codes and the receiver has prior knowledge of the scrambling code. The de-scrambled data is split into the I and Q channels and multiplied with the corresponding spreading codes. The receiver knows about the spreading codes through the pilot bits in the control channel.

3.6.5 De-Interleaving

The data from the individual receiver antenna is de-interleaved prior to further processing. The de-interleaving reverses the process performed by the interleaver in the transmitter section. The de-interleaved sections are passed to the Viterbi decoder, which performs the decoding operation.

3.6.6 Convolutional Decoder

A Viterbi decoder is used for decoding the transmitted signals. The estimate of the received signals is passed through the decoder, which performs maximum likelihood sequence estimation. The convolutional coder and decoder will provide a coding gain to the transmitted sequence. Hence the BER performance of a system with coding will be better than that for an uncoded system. The BER of a coded and uncoded system in an Additive White Gaussian Noise (AWGN) is plotted in Figure 3.19.

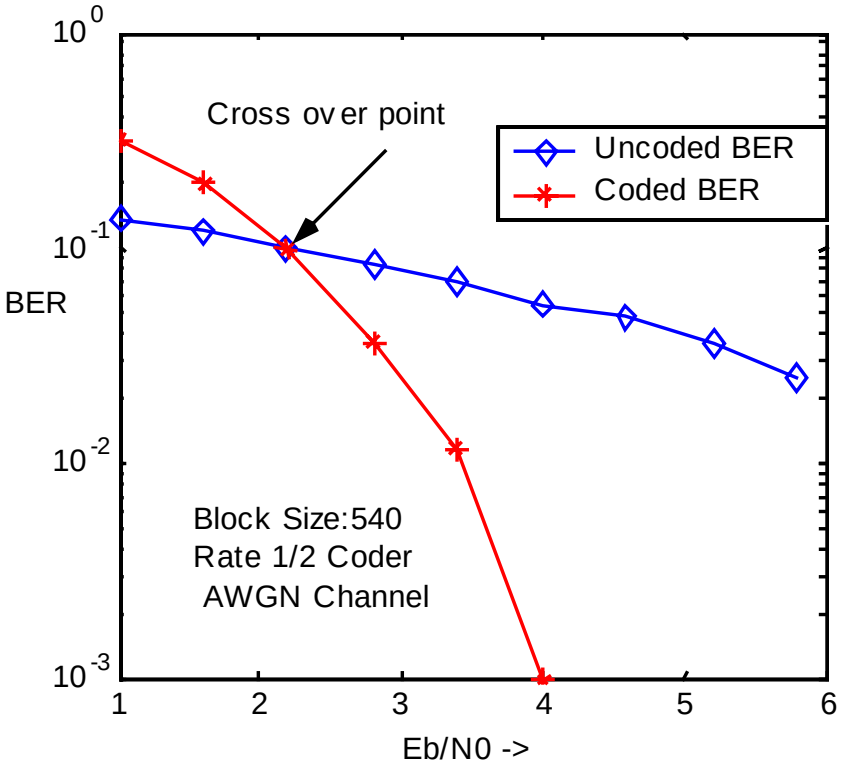

Figure 3.19 BER of convolutional coded and uncoded system.

The output from the decoder is the estimate of the uncoded data, which is used in the BER estimation.

3.7 Chapter Conclusion

In this chapter we discussed the details of the physical channel simulated in our work, which forms the test bed for the resource allocation and management algorithms. The characteristics of WCDMA standard relevant to our study are discussed in detail. A description of the transmitter used in the base station is provided. A description of the base station deploying smart antennas is also discussed in detail.

Chapter 4 RESOURCE MANAGEMENT FOR A SMART ANTENNA NETWORK

4.1 Introduction

In a 3G communications system all the users share the same resource – namely the power allowed in the cell. Depending on the channel conditions and the net available resource, the users are allowed to transmit at a maximum allowed power level that ultimately determines the QoS that will be experienced by the user. Resource management algorithms aim at enhancing the effective capacity subject to power constraints. Call admission control and resource control for the existing calls form the major tasks of resource management. In this chapter we explore the effect of smart antennas on the resource management of a cellular system. We propose some algorithms for resource management in a cellular system supporting heterogeneous users.

Section 4.2 presents the relationship between power and data rate. The elasticity of users introduced in chapter 2 is presented in greater detail in section 4.3. We first describe the resource allocation strategy for an omni-directional antenna system in section 4.5. The proposed algorithm for resource allocation are provided in section 4.6; a modified resource allocation algorithm is given in section 4.7. Finally, the resource management algorithms for a smart antenna system are given in section 4.8. Section 4.9 gives an insight into how the to support the requirements from the 3G framework.

4.2 Differentiating services

The total power that can be received by the base station remains constant due to the power limitation of the BS. In addition, with multiple users in the cell, each user acts as interference to other users. Increasing the power level of one user will decrease the SINR of the other users and hence degrade other users' BER. Therefore we have two bounds on the total power in the system – the limitation imposed by the BS characteristics and the SINR requirement of each of the other users. We note that error correction coding can be employed to address increases in BER; however, this is only effective up to a limit.

Varying the spreading factor of the transmitted sequence differentiates the data rate provided to each user. The lower data rates will have higher spreading factors and thereby higher processing gain leading to better BER performance. The higher data rate users will tend to have worse BER performance.

We can increase the transmitted power for the high data rate users in order to compensate for the disadvantage in the processing gain. The power level for the different data rates in order to obtain the same performance for all the data rates can be derived. Consider two flows transmitted at rates R_1 and R_2 with power P_1 and P_2 respectively. The spreading gain associated with the rates is G_1 and G_2. In order to obtain equal performance at the receiver, the energy per bit after de-spreading should be the same:

$$P_1 G_1 = P_2 G_2 \quad (4.1)$$

However, spreading gain G_1 is proportional to spreading factor SF_1. So, equation 4.1 can be written as

$$P_1 SF_1 = P_2 SF_2 \quad (4.2)$$

$$P_1/P_2 = SF_2/SF_1 \quad (4.3)$$

Since power in the cell is the limiting factor for a CDMA system, allotting different power is equivalent to assigning different bandwidth for the calls in a bandwidth limited environment.

Figure 4.1 shows the BER plot for different data rate users in the system with different processing gains and different transmitted power levels. The BER is almost equal for different spreading factors, thereby demonstrating the principle outlined in equation 4.3.

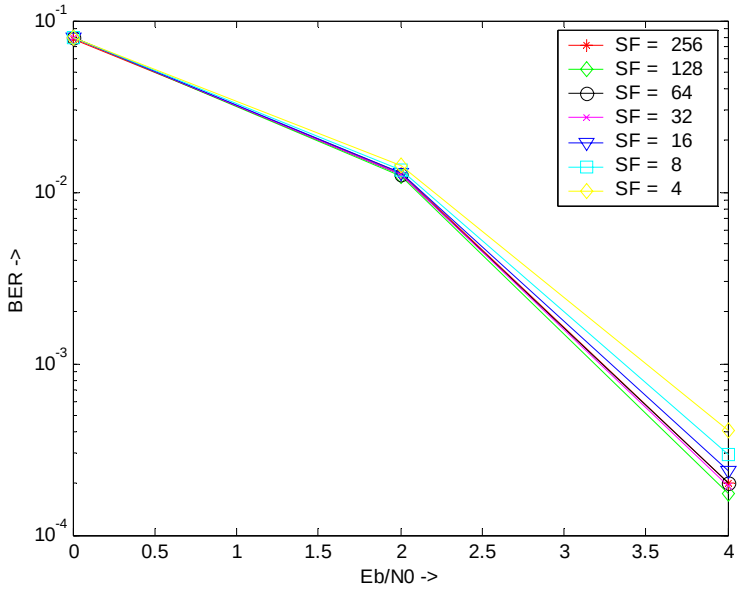

Figure 4.1 BER for different spreading factors with normalized power

4.3 User Elasticity and Satisfaction Index

When differentiated services are provided, the user may be given the choice of accepting a range of services with different "satisfaction" indices associated with the services. This is a feasible alternative since a user may desire a data rate of 1 Mbps for a file download, but he will be satisfied with a rate of 56 Kbps rather than losing the connection when the channel conditions are poor. However a very low rate of 1 Kbps will not be acceptable. This leads to the concept of a minimum rate acceptable to the user. In addition all rates may not be possible, leading to a range of data rates that can be handled by the user. This concept is called user elasticity.

The user will not be equally satisfied with all the classes he is prepared to accept. A metric to measure the user satisfaction should be defined for this purpose. The type of service allotted to the user depends on the present cell conditions. In addition, the services provided to the user are dynamic, possibly varying for the duration of a single call. Hence we require a metric to define the user satisfaction, which provides an indication of the services provided to the user in relation to the services requested.

Different metrics have been suggested to measure the user satisfaction. A definition of utility function as a function of expended energy (since this is related to the battery life time), SINR ratio at the receiver (this decides the error probability of the received signal) and the total number of data bits before encoding is given in [42]. This complexity of this definition is valid for studying the performance of a power control algorithm, but the complexity is not warranted for our work. A quantitative mapping between the resources allocated and requested resource is described in [43] termed as the benefit function. The instantaneous benefit, total benefit and average benefit are of importance. The aim of the resource management should be to increase the total benefit, but the frequency of benefit variation should be limited. Though the definitions in that paper are in the context of real-time systems, some of the same assumptions hold in our work since the final services offered to the users are compared.

In our work, we define a simple metric - Satisfaction Index (SI), a parameter that varies between 0 and 1: 1 corresponds to the best service and 0 to no service being allotted to the user. For a group of traffic flows with similar coding schemes, we adopt a simple definition of the SI as

SI = (Allotted Data Rate)/(Maximum Requested Data Rate) 4.4

We compute the average SI in the system and in the present context we do not consider the frequency of SI variation. Note that the SI is a simplified model of user *utility*, the benefit that a user derives from a given service. Utility is a widely used metric in the design and evaluation of pricing mechanisms for networks that support service differentiation.

Through the duration of the call, the SI can vary depending on cell conditions. If a call by another user ends, this frees up resources that can be re-allocated to continuing flows, increasing the SI. If a new call arrives, part of the resources is given to the new call, reducing the SI of the current users. This kind of adaptive resource management scheme

is proposed in [43] and can be deployed in a system that uses omni-directional antennas as well as one deploying smart antennas.

4.4 Requirements of Resource Management

4.4.1 Resource Management in a cellular system with omni-directional antennas

In a cellular system with omni-directional antennas, the users may move between cells requiring that the call be handed over from one BS to the next. A good resource management algorithm will maintain the QoS guarantees in a cost-effective manner. The hand off algorithms can be centralized or distributed. The BS handling the call can be chosen as the BS that is closest to the user or the BS receiving the maximum power from the user. There are many variables that can be used as inputs (handoff criteria) to the handoff algorithm, including received signal strength, signal-to interference ratio, distance, transmit power, velocity, etc.

4.4.2 Intra-cell handoff in a smart antenna system

The presence of narrow beams in a cell due to smart antennas gives rise to the condition where the users move across multiple beams during the holding time of one call. This will lead to intracellular hand off, leading to the need for resource management within the cell. However, the channel between the BS and MS is a vector channel, meaning there is the additional dimension of angle in the received signal. Hence, the beam selection will depend on the AoA of the multipath components of the signal. The AoA can change due to user movement or due to channel conditions. The effect of user movement on AoA will be more pronounced when the MS is in the vicinity of the BS. The AoA variation due to scattering gives a stochastic distribution for the AoA. The AoA variations of two kinds of users are shown in Figure 4.2 and Figure 4.3.

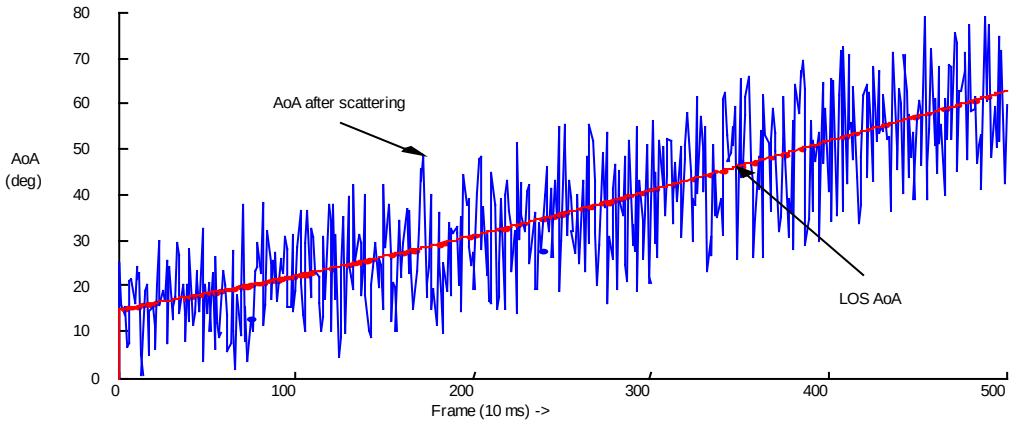

Figure 4.2 AoA of a user moving with a velocity of 120 kmph near the base station

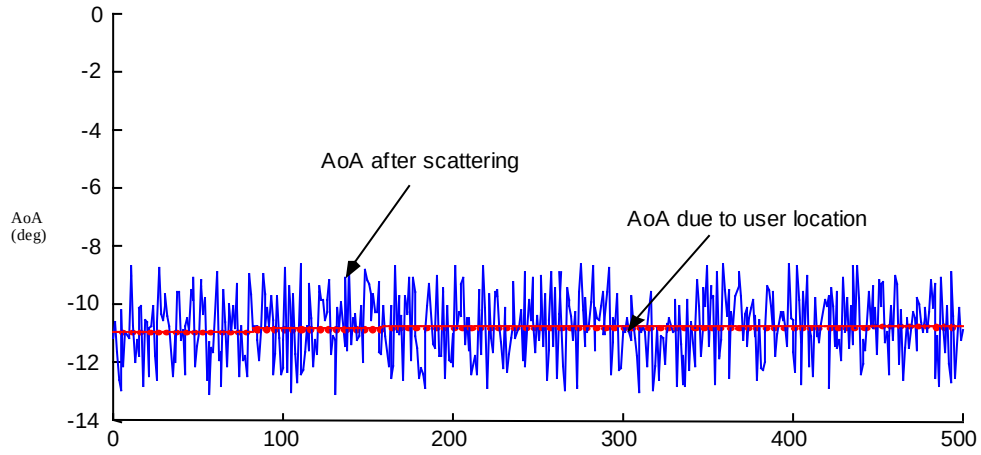

Figure 4.3 AoA of a user moving with a velocity of 120 kmph in the periphery of the cell

The intracell handoff can be handled similarly to intercell handoff by using traditional handoff techniques. However, there are other issues associated with intracell handoff: (1) the same BS handles the call even after the intra cell hand off; (2) depending on the beam pattern, the user continues to have an impact on the beam from which it has been handed off. These two conditions facilitate the use of a centralized resource management algorithm in the cell.

4.4.3 Utilizing user elasticity for resource management

The ability of the user to accommodate different QoS and power levels is defined as the user elasticity. The QoS experienced by the user can change dynamically during the hold time of a single call. This will give additional flexibility to the resource management problem. The QoS provided to individual users can be changed dynamically by varying the power of individual users. Hence, if the power level of a beam exceeds the maximum allowed, the power level of the individual users can be reduced. This will prevent call outage, though at the cost of lower QoS for the users.

If the user moves to an area serviced by an under utilized beam, the user power can be increased. Hence the user will achieve a better QoS. Hence depending on the channel conditions the QoS of the user can be varied to fully utilize the available resources and to prevent call outage.

Since the AoA depends on multiple parameters such as the angular location of the user, distance of the user from the BS, radius of scatterer, and channel conditions, the resource management should be adaptive. This means that the cell should be monitored at sufficient time intervals and resources should be reallocated as necessary. If the time interval used for this adaptation is very large, it can lead to dropped calls and under utilization of resources. On the other hand, frequent adaptation may lead to significant processing costs.

In the following sections the resource allocation and management algorithms will be discussed in greater detail. We first describe a generic resource allocation algorithm for a BS with omni-directional antennas and move on to describe a resource allocation algorithm for a smart antenna network. A modification of the resource allocation algorithm that will reduce the number of blocked calls is discussed next and finally we present a resource management algorithm for continuously monitoring the calls in a smart antenna network.

4.5 Resource allocation for an omni-directional antenna system

A first come first serve basis for adaptive resource allocation is considered for the case of a base station with an omni-directional antenna. Resources are allotted to the users based on the current availability of bandwidth under the constraint that the net power does not exceed a pre-defined value. The maximum power permitted in a cell is dependent on the BER requirement of the users. The system supports an arbitrary number of QoS classes, and each class is characterized by a target data rate and coding scheme. Each user defines an ordered list of QoS classes (from least to most desirable) that would meet the user's performance requirements. The power contribution of the user in the cell is predicted by measuring the received power through the control channels. The data rate of the control channel in WCDMA is 15 kbps. Using this information and equation (4), the power level for an arbitrary data rate can be predicted. The algorithm steps are explained below.

4.5.1 Symbol Definitions:

TC_i : Traffic Class requested by the user

P_{pilot} : Received Pilot power

R_{pilot} : Pilot Channel data rate

R_{Tci} : Traffic Class raw data rate

P_{new_Tci} :Predicted received power for the traffic class TCi.

P_{cell} : Present Cell power

P_{cell_accept} : Cell power if the new call request is accepted

P_{cell_max} : Maximum Cell power

4.5.2 Algorithm:

1. User transmits class requests – [TC_1 TC_2…TC_n] through the control channels. TC_n is the most preferred class.
2. Base station receives the request and measures the received pilot power. The received power is the summation of all the multipath powers.
3. Set the Call Rejected parameter to true.
4. Set i to n.

5. Calculate the required raw data rate (R_{Tci}) of the class TC_i (depending on the channel coding used).
6. Predict the received power of the class TC_i

$$P_{new\_TCi} = P_{pilot} * R_{Tci} / R_{pilot}$$

7. Calculate the received power in the cell if the class TC_i is admitted.

$$P_{cell\_accept} = P_{cell} + P_{new\_TCi}$$

8. If $P_{cell\_accept} < P_{max}$
    - Admit traffic class TC_i, set Call Rejected parameter to False.
    - Inform the user regarding the admitted traffic class.
    - Exit from the loop.
9. Else set i to i-1 and loop to step 5.
10. If no class can be accepted, reject the call.

The flow chart describing this algorithm is shown in Figure 4.4.

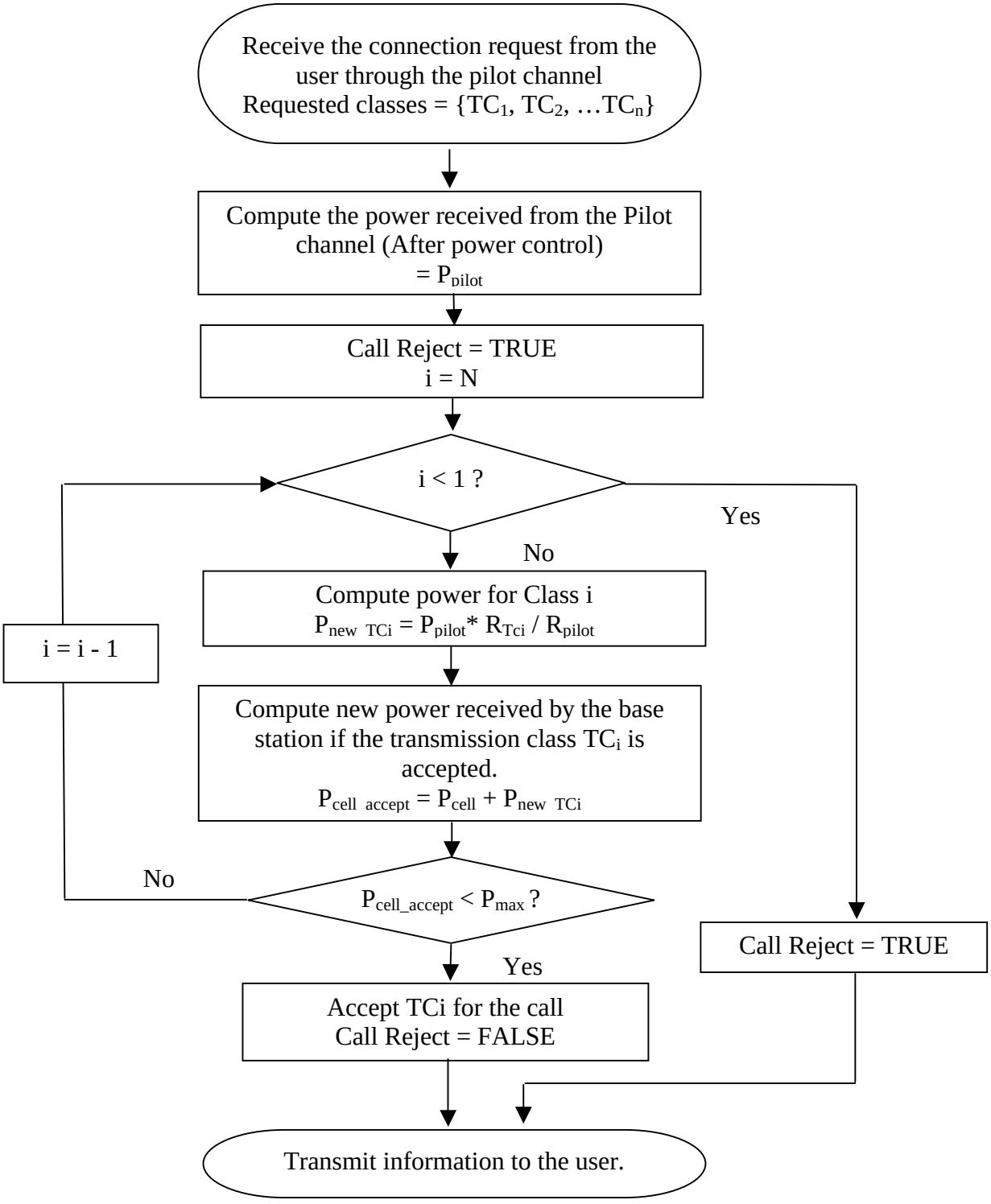

Figure 4.4 Flow chart for simple resource allocation for omni-directional antennas

4.6 Initial resource allocation for a smart antenna system

In a cell with omni-directional antennas, all the users in the cell act as interferers to the rest of the users in the cell. The effect is worsened due to the presence of multipath components, which have the effect of increasing the interference. In contrast to that, the primary impact of smart antennas on resource admission strategies is due to the direction of arrival of the multipath components. The multipath components from a user can arrive from any direction. The angle of arrival can depend on multiple factors – microcell/macrocell, distance between the base station and the mobile, scatterer radius etc. Depending on the channel conditions, the multipath components can impact the same beam or multiple beams. The effect of the multipath components on the beams is computed from the received pilot channel. Using this information and the power ratio of the required traffic class to the pilot channel, the impact of each traffic class on the beams can be computed. A class that will provide an interference level within the acceptable bounds is accepted. The previous algorithm for the call admission control can then be modified to the one outlined below.

4.6.1 Constants

M : Number of switched beam antennas

4.6.2 Symbol Definitions:

TC_i : Traffic Class requested by the user

R_{pilot} : Pilot Channel data rate

R_{Tci} : Traffic Class raw data rate

$P_{pilot\ beam\_m}$:Received Pilot power at antenna m

$P_{new\_Tci\_beam\_m}$:Predicted received power for the traffic class TC_i at antenna m.

P_{beam_m} :Present antenna receive power

$P_{accept\_beam\_m}$: Received power at antenna m if class TC_i is accepted

$P_{max\_beam\_m}$: Maximum receive power for antenna m

4.6.3 Algorithm Description:

1. User transmits class requests – [TC_1 TC_2…TC_n] through the control channels. TC_n is the most preferred class.
2. Base station receives the request and measures the received pilot power $P_{pilot\_beam\_m}$ at each of the antennas.
3. Set the Call Rejected parameter to true.
4. Repeat the following steps for n down to 1.
5. Calculate the required raw data rate (R_{Tci}) of the class TC_i (depending on the channel coding used).
6. Iterate steps (a) and (b) for all antennas, m = 1…M
    a. Predict the received power of the class TC_i

$$P_{new\_Tci\_beam\_m} = P_{pilot\_beam\_m} * R_{Tci} / R_{pilot}$$

    b. Calculate the received power in the antenna if the class TC_i is admitted.

$$P_{accept\_beam\_m} = P_{beam\_m} + P_{new\_Tci\_beam\_m}$$

7. If $P_{accept\_antenna\_m} < P_{max\_antenna\_m}$ for all m = 1…M
    - Admit traffic class TC_i, set Call Rejected parameter to False.
    - Inform the user regarding the admitted traffic class.
    - Exit from the loop.
8. Else loop to step 4
9. If no class can be accepted, reject the call.

The flow chart for this algorithm is given in Figure 4.5

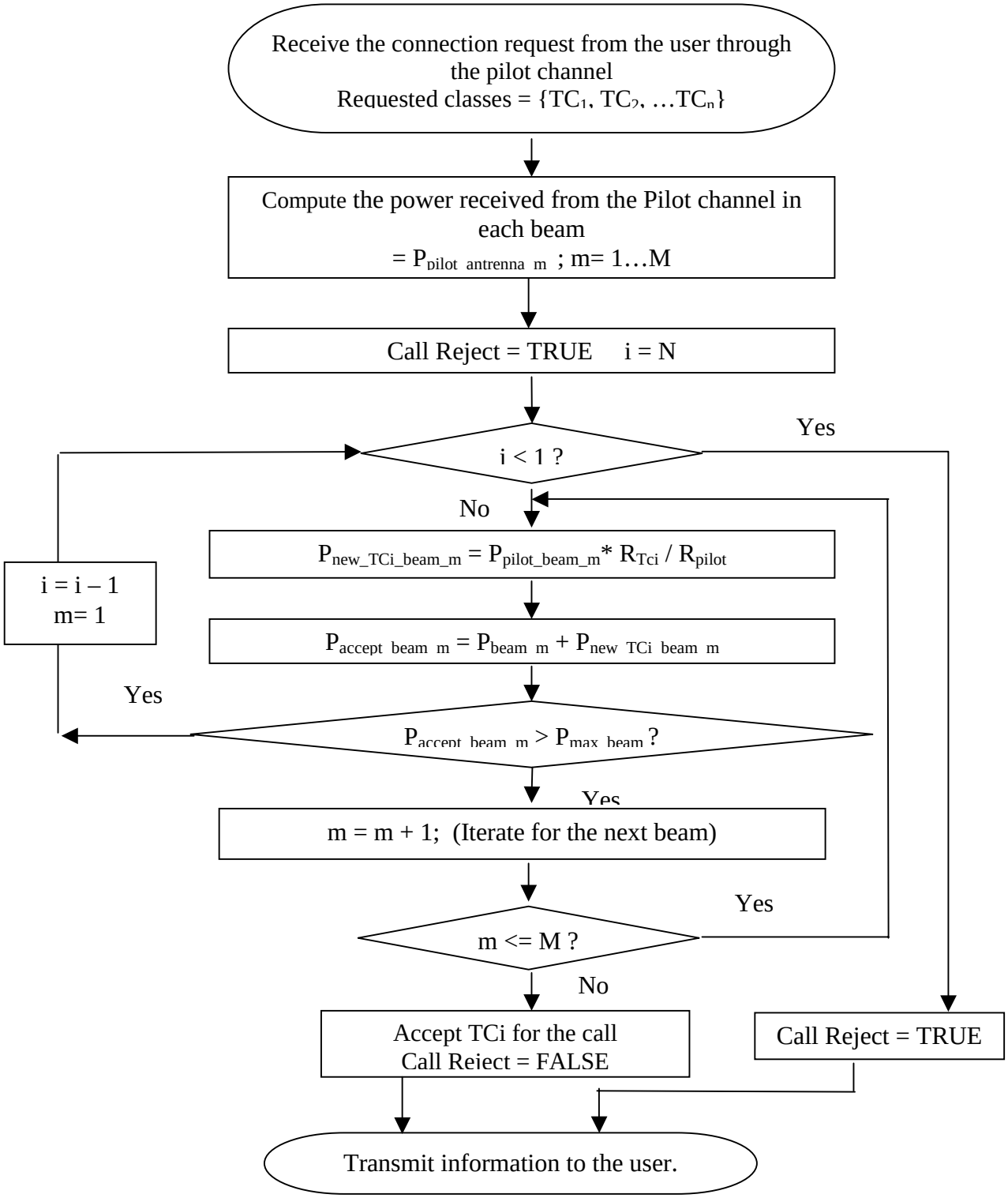

Figure 4.5 Flow chart for resource allocation for a smart antenna system

4.7 Modified Resource allocation for smart antenna system

In the previous section, we discussed the resource allocation for a smart antenna system. However, the elasticity of the existing users is not utilized when the decision for accepting a new user is taken. We can downgrade some of the existing users and thereby decrease the number of rejected calls. This will also bring up the aggregate throughput in the system in addition to decreasing the blocking probability. However, the trade-off here is the decrease in the SI of the accepted users. We describe the modified resource allocation algorithm below:

4.7.1 Symbol Definitions:

TC_i : Traffic Class requested by the user

R_{pilot} : Pilot Channel data rate

R_{Tci} : Traffic Class raw data rate

$P_{pilot\ beam\_m}$:Received Pilot power at beam m

$P_{new\_Tci\_beam\_m}$:Predicted received power for the traffic class TC_i at beam m.

P_{beam_m} :Present beam receive power

$P_{accept\_beam\_m}$: Received power at beam m if class TC_i is accepted

$P_{max\_beam\_m}$: Maximum receive power for beam m

4.7.2 Algorithm Description:

1. User transmits class requests – [TC_1 TC_2…TC_n] through the control channels. TC_n is the most preferred class.
2. Base station receives the request and measures the received pilot power $P_{pilot\_beam\_m}$ at each of the beams.
3. Set the Call rejected parameter to *true*.
4. Repeat the following steps for n down to 1.
5. Calculate the required raw data rate(R_{Tci}) of the class TC_i (depending on the channel coding used).
6. Iterate steps (a) and (b) for all beams, m = 1…M
    a. Predict the received power of the class TC_i

$$P_{new\_Tci\_beam\_m} = P_{pilot\_beam\_m} * R_{Tci} / R_{pilot}$$

b. Calculate the received power in the beam if the class TC_i is admitted.

$$P_{accept\_beam\_m} = P_{beam\_m} + P_{new\_Tci\_beam\_m}$$

7. If $P_{accept\_beam\_m} < P_{max\_beam\_m}$ for all m = 1…M
    a. Admit traffic class TC_i, set Call Rejected parameter to *false*.
    b. Inform the user regarding the admitted traffic class.
    c. Exit from the loop.
8. If the call cannot be accepted at the present data rate, find the beams that will exceed the power limit if the new user is accepted.
9. Repeat the following steps for all beams that will cause problems.
    a. Sort in descending order the received power of all the existing users in the selected beam
    b. Repeat the following steps for all sorted users u = 1…U.
        i. Find the alternate classes to which user u can be degraded to accept a new call.
        ii. For each lower alternate class, predict the received power in all the beams if user u is degraded and the new user is accepted.

$$P_{new\_Tci\_beam\_m} = P_{pilot\_beam\_m} * R_{Tci} / R_{pilot}$$

$$P_{new\_beam\_m} = P_{beam\_m} - P_{user\_u\_beam\_m} (1 - R_{Tc\_alternate}/R_{present})$$

$$P_{accept\_beam\_m} = P_{new\_Tci\_beam\_m} + P_{new\_beam\_m}$$

        iii. If the new computed power is less than the received power for all beams, degrade user u and accept the new user. Transmit this information to the degraded user through the control channel
        iv. Set the call reject to false.
10. Transmit the call accept/reject information to the new user.

The flow chart for this resource allocation is shown in Figure 4.6.

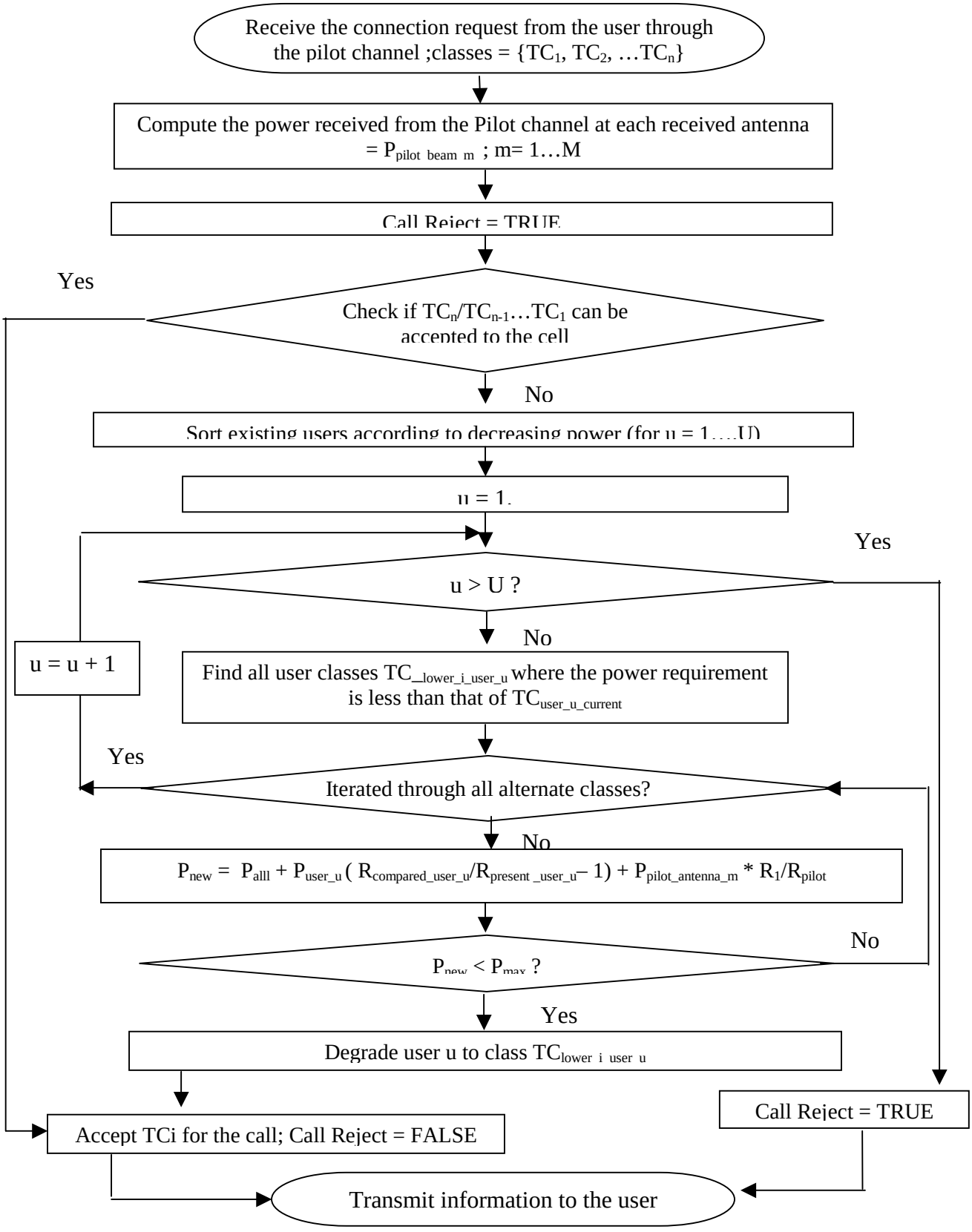

Figure 4.6 Modified resource allocation for a system with smart antennas

4.8 Resource management for a smart antenna system

The need for continuing resource management occurs in a smart antenna in a similar manner to the requirement for hand-off in a multi-cellular system. The users are allotted power levels depending on the pilot channel strength at the time of arrival of a call; however, the AoA and impact on the antenna array vary as the user moves about in the cell. So if a call is in progress for a sufficient amount of time, two users who were not interacting may start interacting. In a voice oriented network this can cause the call to be dropped. However, for data services, the problem can be circumvented by allotting lower data rates and thereby reduced power to these users when they start interacting. In other words, it is clearly advantageous to have a resource management system that allows for graceful degradation of QoS, rather than a hard decision to drop existing calls. Also note that it is possible that the movement of the users will yield a beneficial effect on system quality, whenever a user moves into an area that ends up generating lower interference to other users. The resource management scheme that we propose acts as outlined below. The flow charts for this algorithm are given in Figure 4.7 and Figure 4.8.

4.8.1 Constants

M – Number of beams

U – Total number of users at time of resource management

I - Total number of classes requested by the user

4.8.2 Symbol Definitions

TC_i : Traffic Class requested by the user.

$R_{u\_current}$: Current data rate of user u.

$R_{\_u\_compared}$: Data rate of the class being compared.

R_{Tci} : Alternate Traffic Class raw data rate

$P_{new\_Tci\_beam\_m}$:Predicted received power for the traffic class TC_i at beam m.

P_{beam_m} :Present beam receive power

$P_{accept\_compared\_m}$: Received power at beam m if class TC_i is accepted.

$P_{max\_beam\_m}$:Maximum receive power for beam m.

$P_{user\_u\_beam\_m}$ Power received from user u by beam m.

$P_{no\_user\_u\_beam\_m}$ Power at beam m if user u is absent

$P_{beam\_m\_all\_users}$: Collection of $P_{user\_u\_beam\_m}$ having non-zero received power at beam m.

$TC_{\_lower\_i\_user\_u}$:Traffic classes having a lower data rate than the present Traffic class for user u.

$TC_{\_higher\_i\_user\_u}$: Traffic classes having a higher data rate than the present Traffic class for user u.

4.8.3 Algorithm Description:

4.8.3.1 Class degradation

1. Iterate steps 2 – 11 for all beams m = 1…M.
2. Compare the received beam power, P_{beam_m} to maximum beam power $P_{max\_beam\_m.}$
   IF ($P_{beam\_m} > P_{max\_beam\_m}$) continue ;
   Else go to step 1.
3. Find the power contribution of all users at beam m.
   $P_{beam\_m\_all\_users} = [P_{user\_1\_beam\_m}, P_{user\_1\_beam\_m}, \ldots\ldots\ldots P_{user\_U\_beam\_m}]$
4. Sort $P_{beam\_m\_all\_users}$ with user 1 contributing the maximum power.
5. Iterate steps 6 – 11 for all users u in $P_{beam\_m\_all\_users}$
6. Find the power in the beam if user u is absent
   $P_{no\_user\_u\_beam\_m} = P_{beam\_m} - P_{user\_u\_beam\_m}$
7. Find all the classes requested by the user - R_{TCi}, having a rate $R_i < R_{u\_current}$. This gives the set $TC_{\_lower\_i\_user\_u}$
8. Sort $TC_{\_lower\_i\_user\_u}$ in the descending order of data rates.
9. Iterate steps 10-11 for all the classes in $TC_{\_lower\_i\_user\_u}$
10. Find the new power if user u is degraded to a lower traffic class.
    $P_{accept\_beam\_m} = P_{no\_user\_u\_beam\_m} + P_{user\_u\_beam\_m} * R_{\_u\_compared}/R_{\_current}$
11. If $P_{max\_beam\_m} < P_{accept\_beam\_m}$
    a. Reallocate the user to the new class $TC_{\_lower\_i\_user\_u}$
    b. Compute the new power in all beams–

$P_{\_beam\_mm} = P_{beam\_mm} - P_{user\_u\_beam\_m} + P_{user\_u\_beam\_mm} * R_{\_u\_compared}/R_{\_current}$

Use this newly computed values for subsequent calculations

c. Add user u to the list of degraded users.

d. Continue from Step 1.

Else loop to step 9.

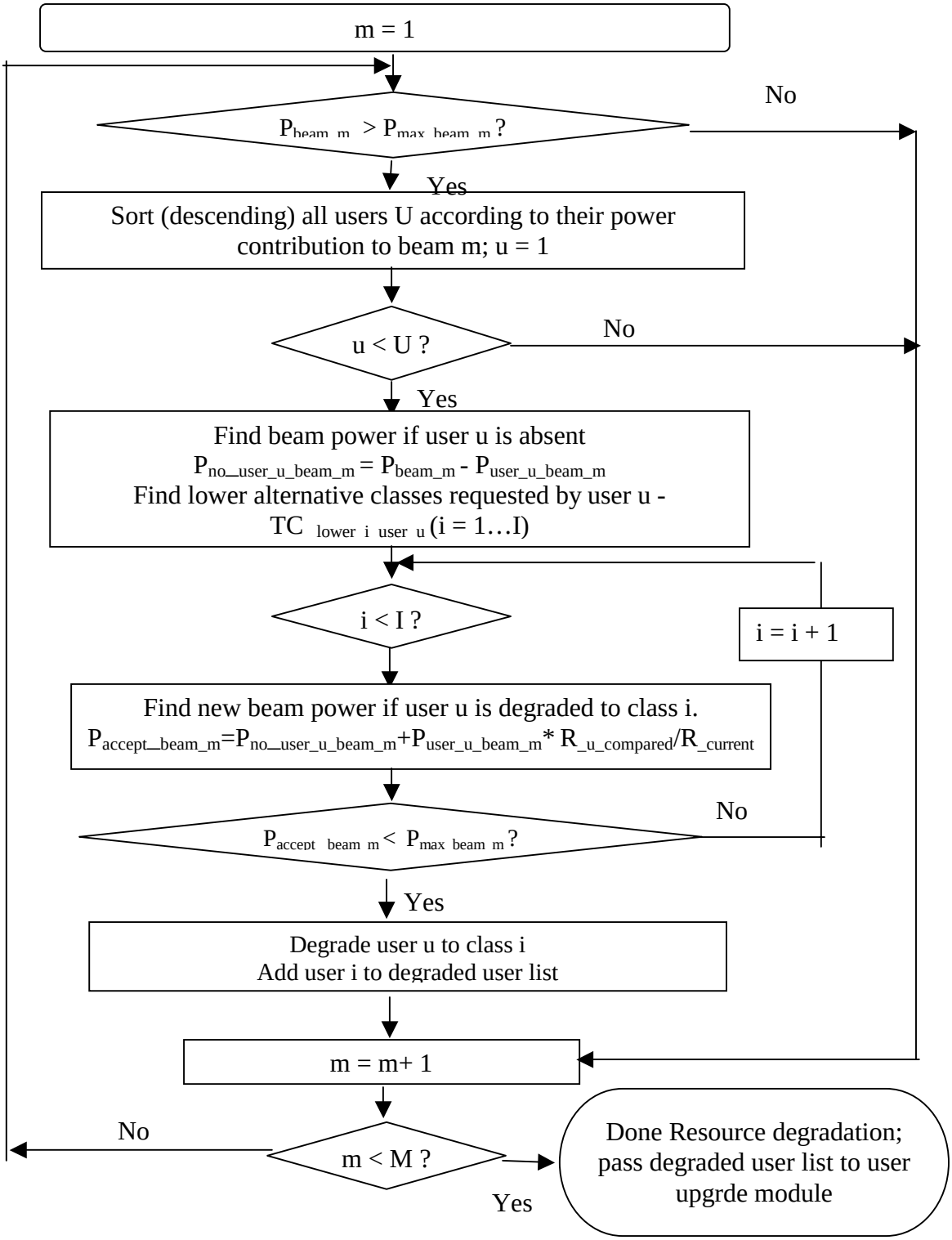

Figure 4.7. Flow chart of resource degradation section of resource management

4.8.3.2 Class up-gradation

1. For all users not in the degraded user list, perform the steps 2 to 7
2. Find all the classes requested by the user - R_{TCi}
3. Eliminate all classes having a rate <= $R_{u\_current}$. This step yields $TC\_higher\_i\_user\_u$
4. For all TC_i having $R_i > R_{current}$ perform steps 5- 8
5. Find the received power in the beam if TC_i is allotted instead of TC_{allot}
6. For all beams 1…m, compute

$P\_compute\_beam\_m = P_{beam\_m} - P_{user\_u\_beam\_m} + (P_{user\_u\_beam\_m} * R_i / R\_current)$

7. If $P_{max\_beam\_m} < P\_compute\_beam\_m$ for all m,
    a. upgrade the user to the Traffic class TC_i
    b. Continue step 1 for the next user.

    Else continue from step 4.

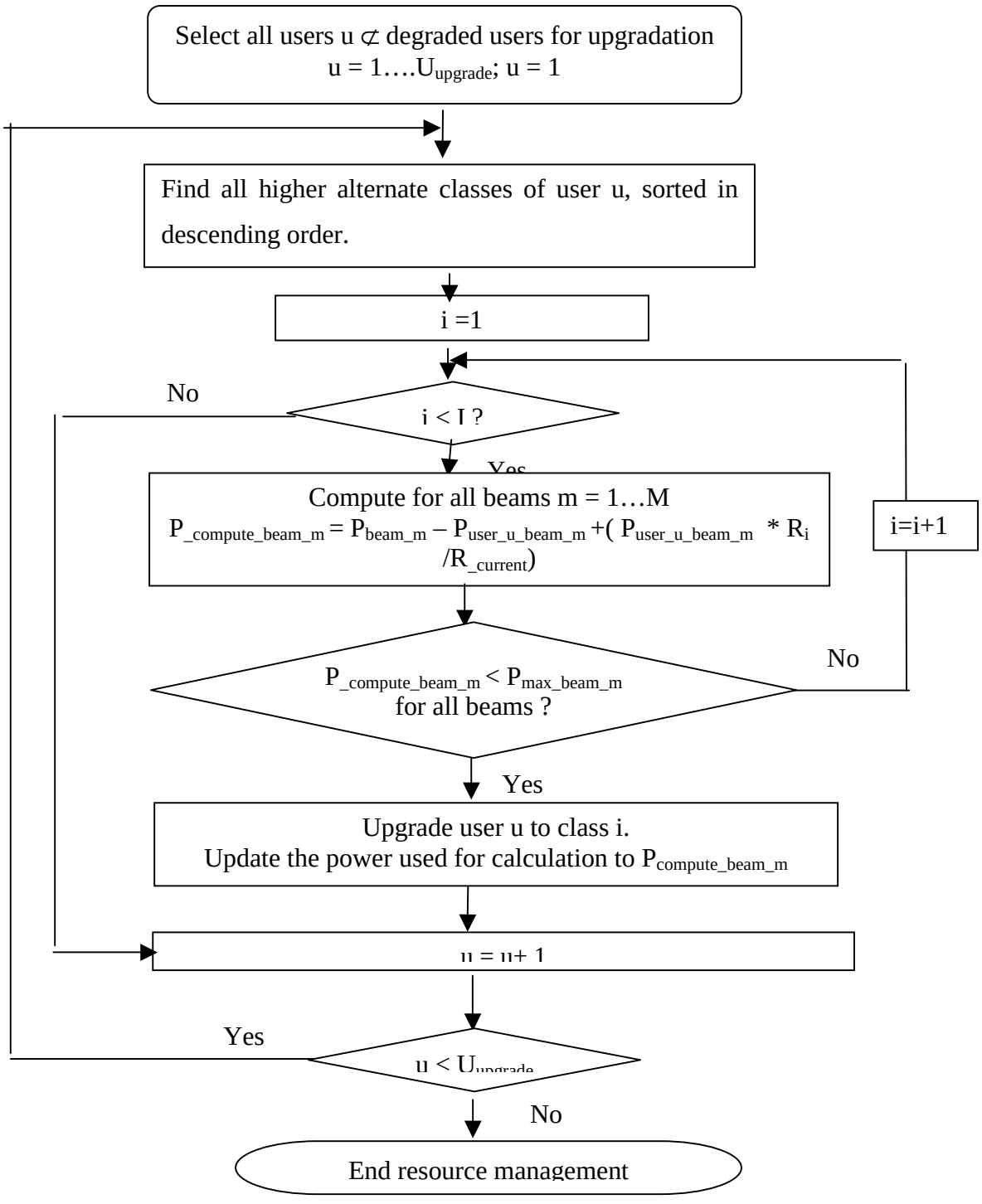

Figure 4.8 Resource up-gradation section of resource management algorithm

4.9 Support of services

The parameters required for resource management are computed at the physical layer and must be sent to the MAC layer. 3G standards specify the parameters that are to be measured by the MS and the BS. One of the parameters measured and transmitted to the RRC layer is the power level. This information can be passed to the upper layers periodically or event based. For implementing the proposed algorithm, a periodic transfer of the power level information is desirable between the physical layer and RRC. CPHY primitives can be used for this purpose.

The second service condition that has to be addressed is the dynamic nature of the spreading factor and spreading codes. The decision about the codes is made by the BS and has to be transmitted to the MS for use during the next transmission slot. Both in-band control signaling and out of band control can be used for this purpose. In using the in band control signaling, the control information will be multiplexed with the user data, reducing the data rate. The spreading code to be used is uniquely specified by the spreading code length and branch number. However, in the uplink all codes with the same spreading factor use the same spreading codes. This means that only the new spreading factor has to be transmitted to the user, which can take values from the set {4, 8,16,32,64,128,256,512}. Hence three bits can be used to specify the spreading code. The rate information layer can be used to relay this information as discussed in [45].

4.10 Chapter Conclusion

In this chapter we discussed the resource management requirements for smart antenna systems. The elasticity of users and the index of user satisfaction are explained. The resource allocation and management algorithms for omni-directional and smart antenna systems are presented. We conclude the chapter with a discussion on how the different parameters can be computed and the support provided by 3G for these services.

Chapter 5 SIMULATION RESULTS AND DISCUSSION

5.1 Introduction

In the previous chapters we presented the QoS requirements, physical layer parameters, channel modeling and resource management algorithms for a cellular system employing smart antennas. In this chapter we will look at the model validation and the effect of system conditions on the QoS parameters considered. The parameters related to a heterogeneous user population with elastic users are measured using simulation.

The first part of the chapter deals with the simulation results of multi-rate users in a WCDMA system. The BER in the system for different rate users, mix of multiple data rates and effect of channel coding are studied. The second part of the chapter deals with the simulation details of the proposed resource management algorithms and an assessment of system capacity.

5.2 Effect of heterogeneous users in a cellular system

The BER performance of the users in a cellular system depends on the SINR of the received calls. The SINR depends on the received signal power and the noise power. In a homogenous user system, the interference from other users is directly proportional to the number of other users in the cell. However, for a heterogeneous user system, the signal power of the user depends on the raw transmitted data rate. This means that the SINR of the user cannot be directly related to the number of users in the cell, but on the combined power level in the cell. . However, the level of interference in the cell depends on the location of the user, the multipath profile etc. As an example, a snap shot of the power level, BER and number of users of a heterogeneous user system with omni-directional antenna is shown in Figure 5.1.

It can be seen from the figure that the BER of the calls deteriorate when the power level in the system is high (time between 10 seconds and 20 seconds). The number of users at this time is low. However at a time of 100 seconds, the power level is lower, the number

of users is high but the BER is low. This shows the direct relation between the net power level in the cell and the BER of users.

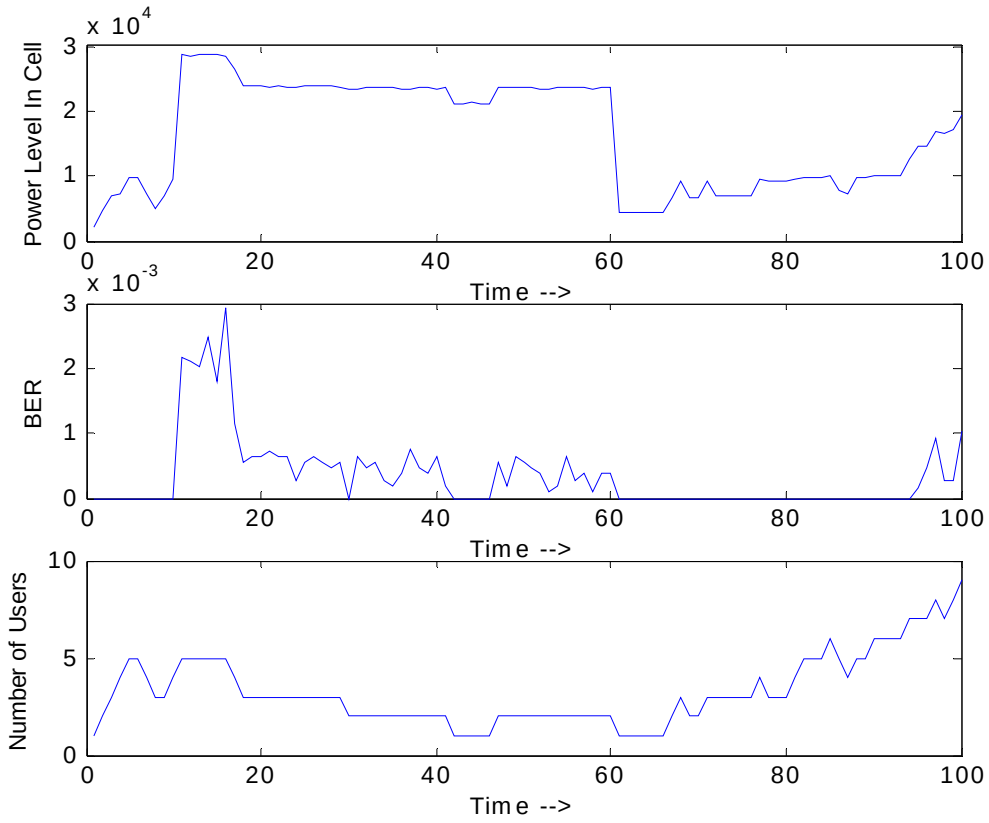

Figure 5.1 Power level plot of heterogeneous users in a WCDMA system

5.2.1 Cell Capacity with different data rates

For a heterogeneous user population, the total capacity in a cell can be defined as the aggregate data rate that can be supported in the cell at an acceptable BER. Hence a plot showing the BER of different number of users is a measure of the capacity of the cellular system. We present the results for two different cases with users of a similar kind existing in the system. The two conditions studied are

(i) Homogenous users with rate = 30 Kbps

(ii) Homogenous users with rate = 120 Kbps

The BER plots for the two cases are shown in Figure 5.2. It can be observed that the BER increases with the number of users in both cases. In the case of the higher data rate (120 Kbps) users, the BER increases at a faster, since the interferers have higher power and therefore the SINR deteriorates faster as compared to the case of lower data rate users.

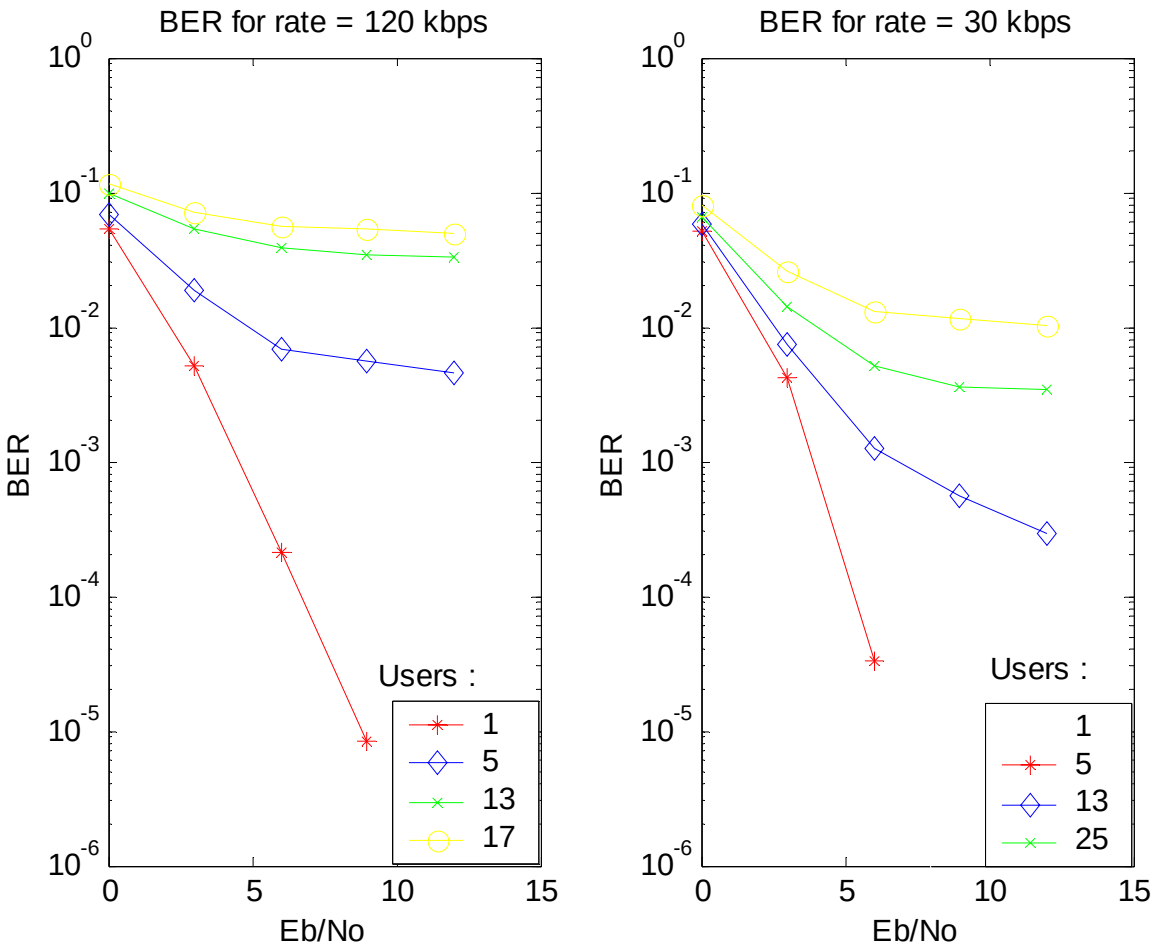

Figure 5.2 BER plots for homogenous users with rate = 120 Kbps and 30 Kbps

5.2.2 Cell Capacity in different channels

The BER performance of the users will depend on the channel conditions, due to differences in the multipath profiles of distinct types of channels. The outdoor channel

has a higher number of multipath components as compared to the indoor channel. This will help in the performance of the rake receiver, but will deteriorate the performance of the other users in the system. We observe from Figure 5.3 that the BER performance in an outdoor channel is worse than that in the indoor channel. The detrimental effects of a high data rate user on other users will be greater in an outdoor channel than for an indoor channel. This is attributed to the presence of more multipath components in the outdoor channel.

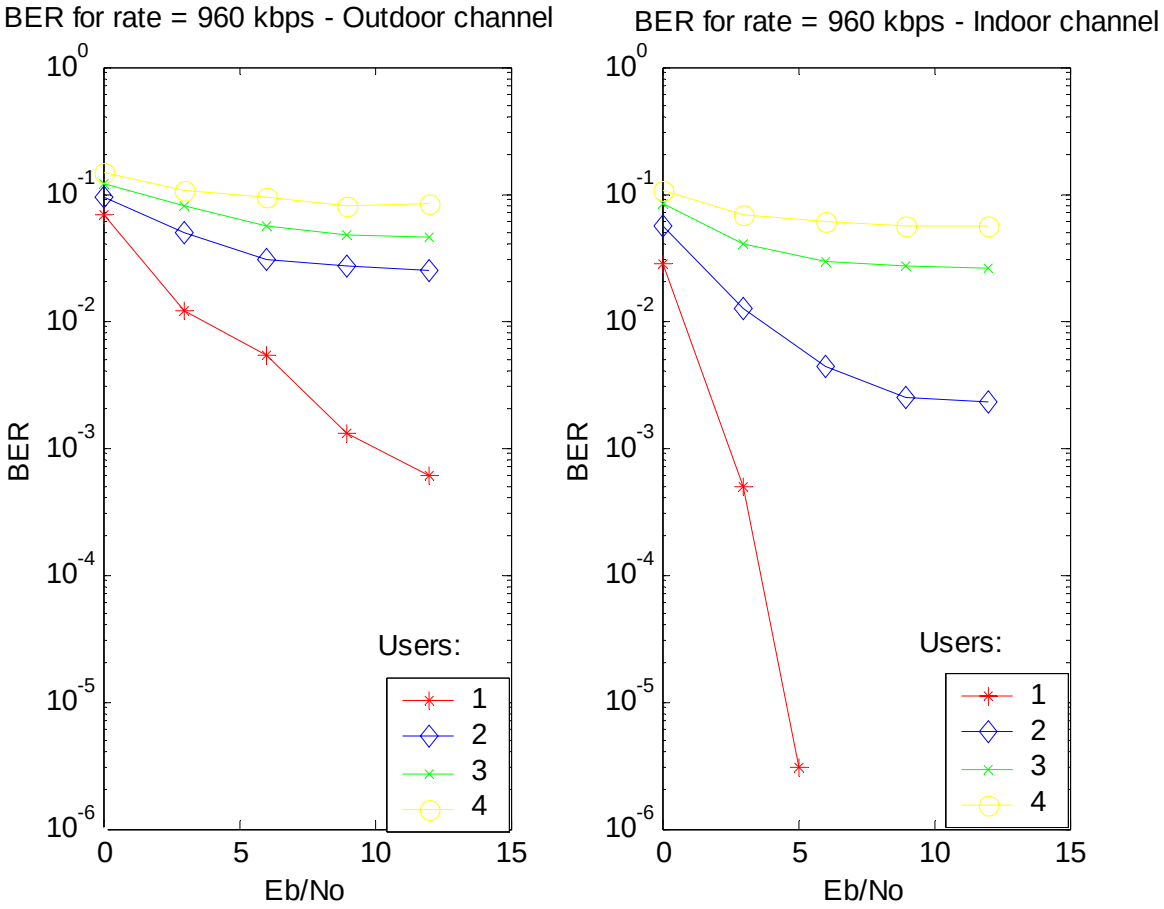

Figure 5.3 BER of users with SF = 4 (Rate = 9600 Kbps) in outdoor and indoor channels

5.2.3 Cell capacity with heterogeneous users

When heterogeneous users are present in a system, the number of users that can be supported will depend on the data rates and ratio of different users in the system. This is shown in Figure 5.4. In this case a traffic mix of two classes of users is considered. Class I users have a data rate of 30 Kbps and class II users have a data rate of 120 kbps. Varying the ratio of class I and class II users, we can see that the BER becomes lower for a higher ratio of class I users, as expected.

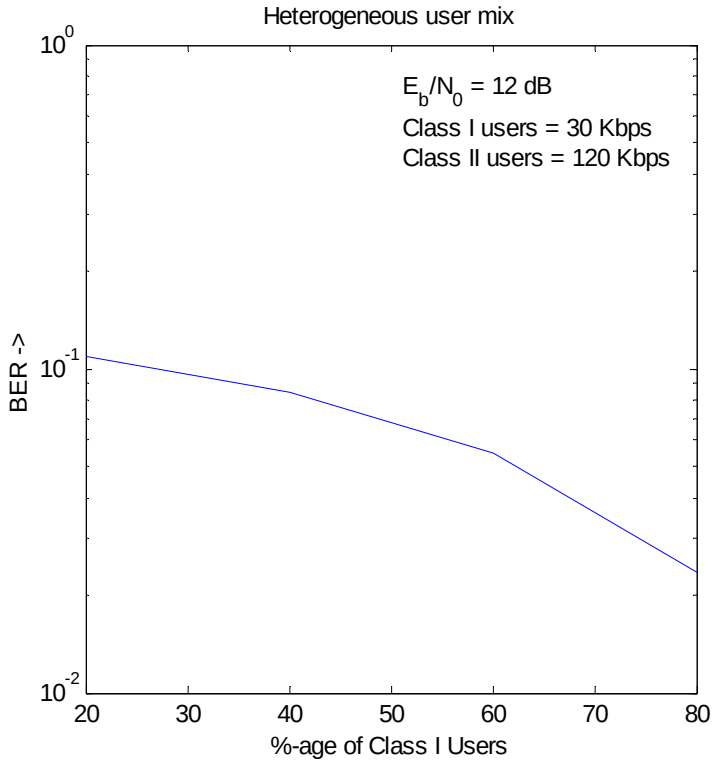

Figure 5.4 BER in a system with heterogeneous users

5.3 Effect of convolutional coding

The parameters we are studying in order to ensure QoS for the users are the data rates and BER. One method to improve the BER of the users is to employ channel coding. Having a channel coder in the system will yield coding gain for moderate to low BER. However, if the uncoded BER is higher than a certain threshold, the coder will be ineffective and the BER with coding will be higher than that for the uncoded scheme. Since the number

of errors in the uncoded system is large, the decoder continues in the wrong path without remerging to the correct one.

Figure 5.5 shows the effect of convolutional coding in a predominantly interference limited case. Users with a raw data rate of 120 Kbps are considered. As the number of users increases, SINR decreases and the coded and uncoded BER increase. At one point, the coded BER becomes higher than the uncoded BER. From this point onwards the additional complexity of a coder does not yield any coding gain.

In the case when very high data rate users co-exist, the situation becomes worse. For a data rate of 3.84 Mbps, the degradation is more rapid. The coded and uncoded BER can be seen in Figure 5.6. For a single user, the BER without coding is in the order of 10^{-3}. This is attributed to the multipath fading. However the convolutional coder is effective in this case and the coded BER is close to zero. However, when one more user is added to the cell, the noise floor goes up and the BER without coding will be of the order of 0.15 – 0.2. The convolutional coder is not able to perform well at this BER and this will cause the coded BER to be higher than the uncoded BER. The addition of a high data rate user (3.84 Mbps) is equivalent to adding 32 users having 120 Kbps. So, the sudden degradation of the BER is expected.

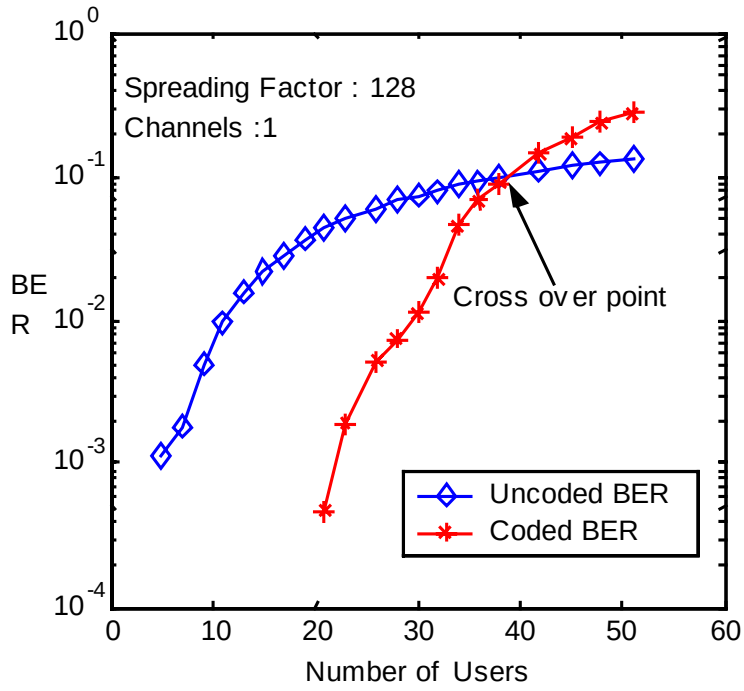

Figure 5.5 BER performance of the encoder for 120 kbps (Eb/N0 = 5 dB)

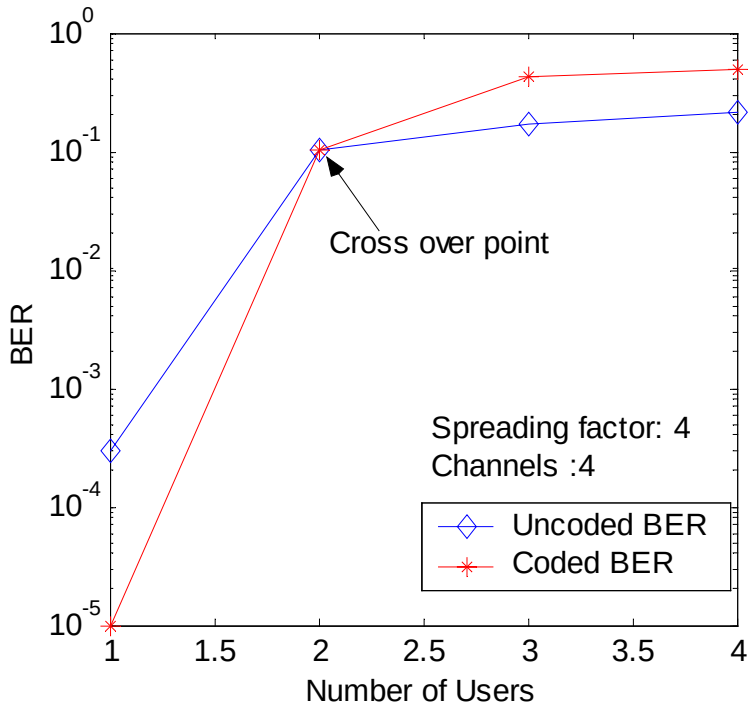

Figure 5.6 BER performance of the encoder for 3.84 Mbps (Eb/N0 = 5 dB)

5.4 Simulation time chart

In order to study the effect of the proposed resource allocation and management algorithms, we develop a simulation framework following the approach in [19]. There are three main events occurring in the system - call arrival, call departure and sampling of the system status. The call arrivals and call departures can occur at any time, but the status of the system is sampled at regular intervals. The arrival and departure rates are controlled by the mean call arrival rate (λ) and mean call departure rate (μ) respectively. The ratio of the call arrival rate and call departure rate will determine the load in the cell (A), measured in Erlangs.

$$A = \frac{\lambda}{\mu} \qquad 5.1$$

The resource management algorithm is run at multiples of the system sampling time. This simulation time chart in Figure 5.7 shows the different events occurring in the simulation.

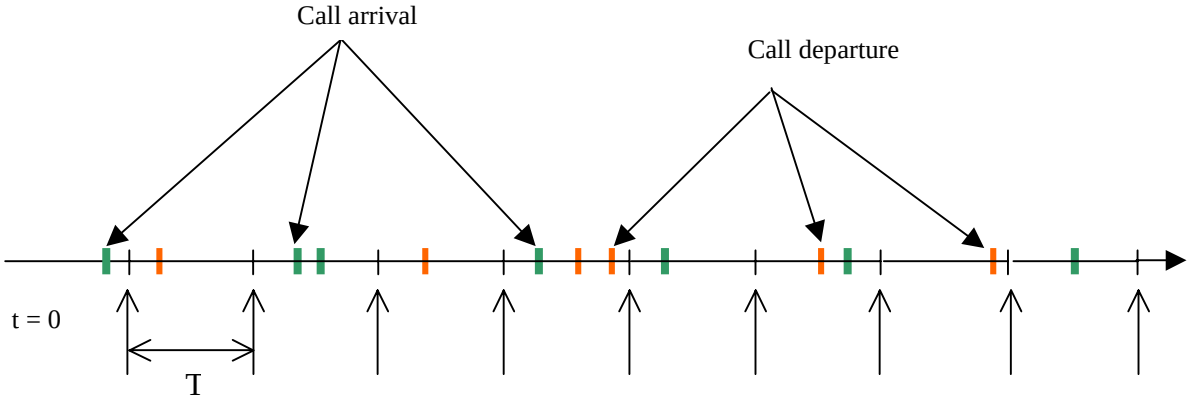

Figure 5.7 Time chart for the simulation

The next step is to choose proper values for the parameters in the simulation event. The departure rate determines the value of call hold time as given in equation 5.2.

$$Call\ Hold\ Time = \frac{1}{Departure\ Rate} \quad 5.2$$

As discussed in chapter 2, the hold time for each transmission class can be different. The call hold times are selected based on the nature of transmission. The call arrival times are adjusted so as to vary the load on the cell. One important aspect is that the call arrival rates can be higher than the call departure rates. In a conventional network queue, if the calls arrive at a faster rate than their departure, it will lead to buffer overflow and call blocking. However, in our case where we have a multi rate system, multiple low data rate calls can be accommodated in place of a single high data rate call. Hence the call blocking probability will not directly correspond to that predicted by the Erlang B formula.

The next parameter that has to be chosen is the simulation sampling time and the frequency of resource management. The WCDMA frames have a length of 10 ms. Hence the minimum sampling time for the simulation is 10 ms. However, having a sampling time of 10 ms would yield a very long simulation time. We choose a value of 1 sec for the simulation sampling period. The resource management update is performed at every simulation sampling period unless otherwise stated.

5.5 Drop probability for a system with smart antennas

The first part in the radio resource control is the allocation of suitable resources to the call depending on the present channel and cell conditions. At the time of allotment, the future location and future impact of the channel is not taken into account. However in a cell with beamforming, the resources required by the user keeps changing as he moves between the coverage area of different beams. This may lead to some calls getting dropped.

The power contribution of the user to each of the beams depends on the AoA of the multipath components at the BS. The AoA is dependent on the radial location of the user,

distance of the user from the mobile and the radius of the scatterers. The probability of the call getting dropped depends on the user velocity, scatterer radius etc. In Figure 5.8 we show the drop probability of calls in a system without resource management. The λ/μ ratio is 3 for all the simulations. Four conditions are studied – a system having only static users, a system with random walk users and a system with high-speed users moving in a constant direction and mix of all the three kinds of users (20% static, 50% random walk and 30% high-speed users).

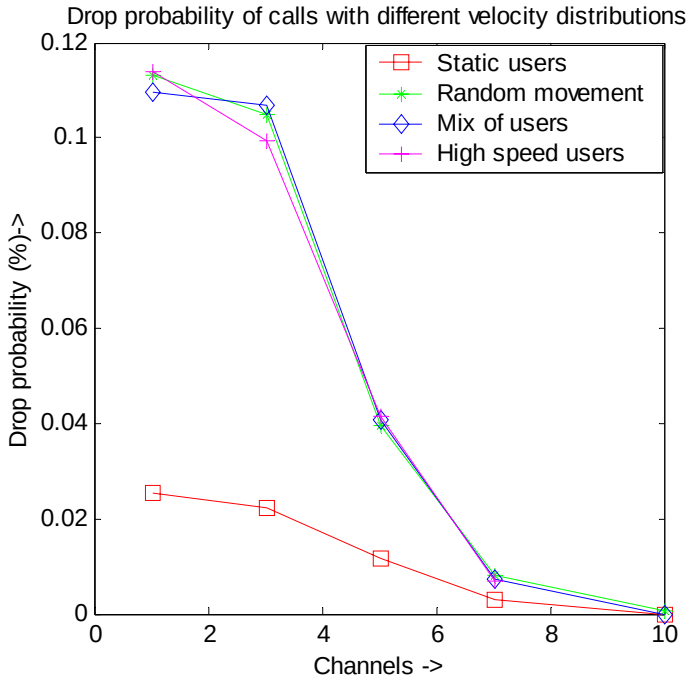

Figure 5.8 Call drop probability in a system with smart antennas (without resource management)

In the plot, we see calls drop even for a case with static users. This is attributed to the presence of scatterers in the cell, which will cause the AoA of the multipath components to vary even without any user movement. The call drop probability follows the same trend for the high speed, random walk and mix of user conditions.

A dropped call is very undesirable in a cellular system. Hence, the need for resource management in a smart antenna system is clear. For a managed system that takes into account user elasticity, reducing the data rate of the calls where the beam power exceeds the maximum power allowed can considerably reduce the call drop probability.

5.6 Resource management in an Omni-directional antenna network

Resource management can increase the throughput even in a system without smart antennas. In a system with resource management, the cell resources are fully utilized over time, whereas in a system without resource management, the cell power is left unused during some time. An existing call will be upgraded when another call ends, thereby using all the resources to the maximum extent.

The throughput of a system with and without resource management is shown in Figure 5.9. It can be observed that having resource management in the system enhances the throughput of the network.

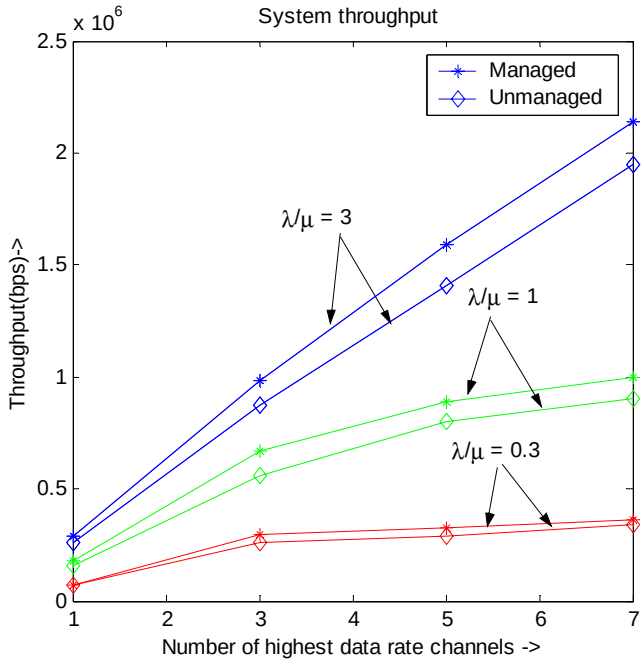

Figure 5.9 Throughput in an omni-directional antenna system with and without resource management

The call block probability for the system is plotted in Figure 5.10. From the plot it can be seen that the call blocking decreases with the increase in channels. This is a predictable condition since there are more resources available that can be allotted to the users. We can also see that the call blocking probability of the managed system is lower than that of the un-managed case. In a managed system employing the modified resource admission, new calls are admitted by lowering the allotted resources for the existing calls. Hence the call blocking probability decreases.

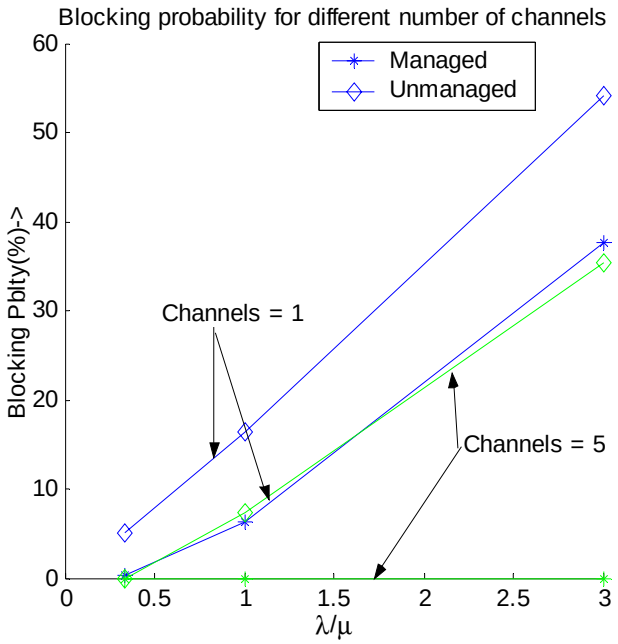

Figure 5.10 Blocking probability of an omni-directional antenna system for a managed and unmanaged system

Figure 5.11 shows the average satisfaction index of the users in the cell. The satisfaction index of users in a managed system is greater than that in an un-managed system. We also note that the SI decreases when the capacity in the cell increases (increasing λ/μ). Since the new calls are accepted by lowering the rates of the present calls, the call block probability decreases at the cost of the SI of the existing users.

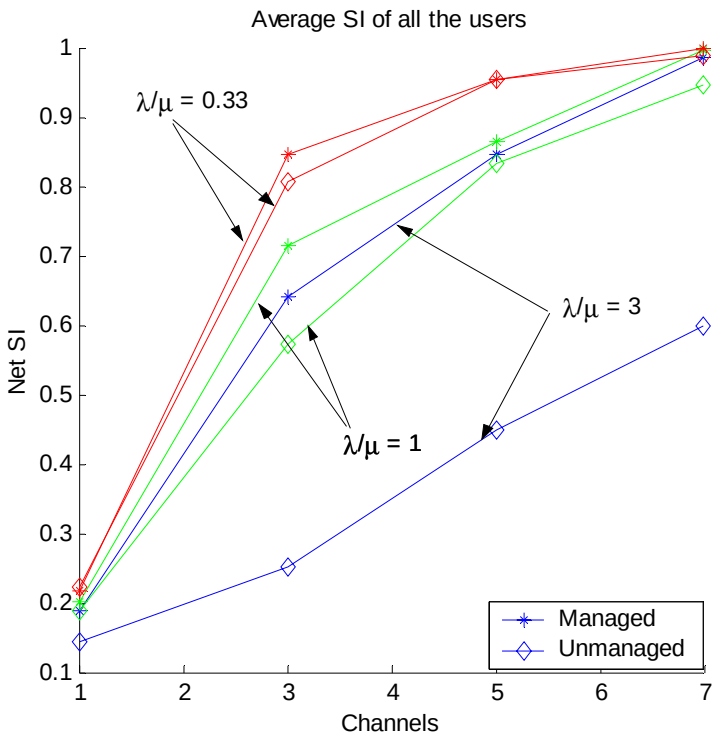

Figure 5.11 Satisfaction index of users with and without resource management

From these observations we can conclude that resource management can increase the aggregate throughput in a cellular system with omni-directional antennas. Added to this advantage is fact that resource management will also reduce the call drop probability. In the next sections we will discuss the performance advantage obtained using resource management in a smart antenna network.

5.7 Resource Management Mechanisms

The impact of the resource management algorithm in a smart antenna system can be explained with an example. Consider a cell having eight switched beams, having identical beam patterns. The major lobes have a 45^0 separation. The base station is located at the origin.

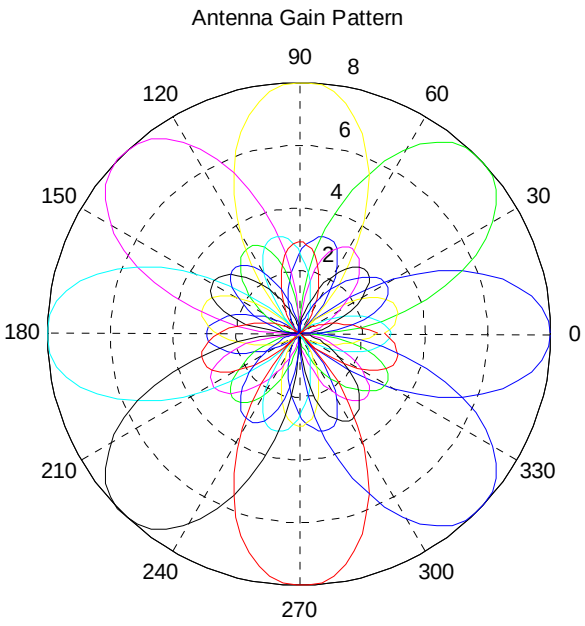

Figure 5.12 Beam pattern for the base station antenna

There are 3 users in the system, and their characteristics are given in Table 5.1. The SI of user U_3 is monitored. The plot of variation of SI with the location is given in. It can be seen that the SI increases as the user moves away from the 0^0 location – away from the collocated user U_1. At 45^0, U_3 still influences beam 1 due to the presence of side lobes. However, when the user approaches a position at 90^0, his SI increases to 1, since there are no other users influencing beam 3. When the user moves to the 180^0 position his SI decreases due to the presence of U_2. The effect of beam pattern can also be seen from this example. User U_1 is located at the area serviced by the major lobe of antenna 1which has a null at an angle 30^0; similarly antenna 3 servicing User U_2 and has a null at 30^0. This reduces the Multiple Access Interference (MAI) on user 3 at an angle 30^0, giving a high SI. At 45^0 antennas have significant side lobes, hence the presence of U_1 will impact the usable resources of U_3 at this location. If we have an antenna array having a beam pattern with reduced side lobes, SI will not be reduced when the user is in the locations 45^0 and 135^0.

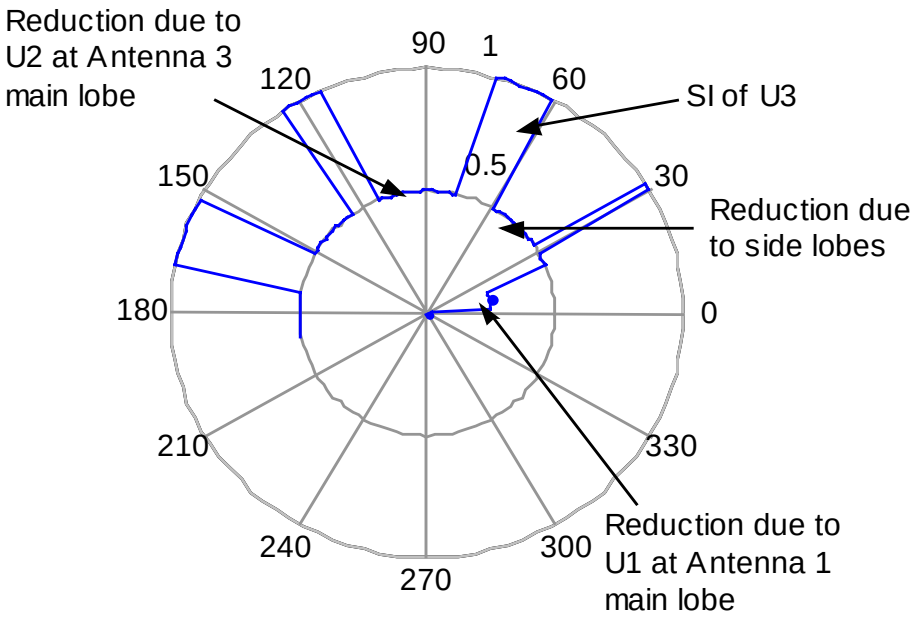

Figure 5.13 Plot of SI variation with location.

Table 5.1 User characteristics for the example in Figure 5.13

User	**Location (R,ϕ)**	**Velocity (km/hr)**	**Movement Type**	**Traffic Classes (No coding scheme is requested.)**
U_1	$(1414, 0^0)$	0	Stationary	(960 kbps)
U_2	$(1414,180^0)$	0	Stationary	(480 kbps)
U_3	$(1000,0^0)$	120	Circular	(960 kbps), (480 kbps), (240 kbps), (120 kbps), (60 kbps), (30 kbps), (15 kbps)

5.8 Application of resource management to smart antenna system supporting heterogeneous users

In this section we will explore the benefits of the resource management algorithm on a network with smart antennas. The parameters that we will study are the throughput, blocking probability and the satisfaction index of the users. In studying the satisfaction index, we consider the SI of all the users – hence the users whose calls got rejected will have an SI of 0 and the other users will have an SI varying from 0 to 1, which is the average SI for the entire duration of the call.

We will analyze the performance of the managed system as compared to an unmanaged system under different cases.

5.8.1 Fully elastic users

This case considers a situation in which all the users in the cell are fully elastic – meaning that they can take any rate in the set {15 Kbps, 30 Kbps, 60 Kbps, 120 Kbps, 240 Kbps, 480 Kbps, 960 Kbps}. The E_b/N_0 in the cell is 12 dB. The cell we have considered is a 3 km square cell. The scatterer radius is 200 m. There are 8 beams in the cell, formed using 8 beamforming antennas. Four rake fingers are used at the receiver for temporal combining.

The aggregate throughput in the cell is calculated by taking the sum of the throughput (in bits per second) of all users. This is plotted in Figure 5.14. Similar to the omni-directional antenna condition, the throughput of the system with resource management is greater than the throughput without resource management. However, in the present case the difference between the throughput with and without management increases as the system capacity increases.

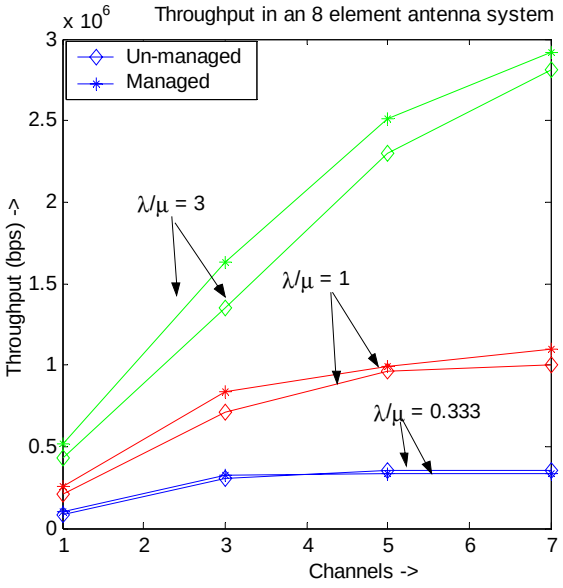

Figure 5.14 Aggregate throughput in the cell (fully elastic rates)

The blocking probability of the calls is shown in Figure 5.15. For the present simulation, monitoring the cell for 20,000 seconds, the managed system accepted all the calls that were generated. However in the un-managed system, the call blocking probability increases as the number of channels decreases.

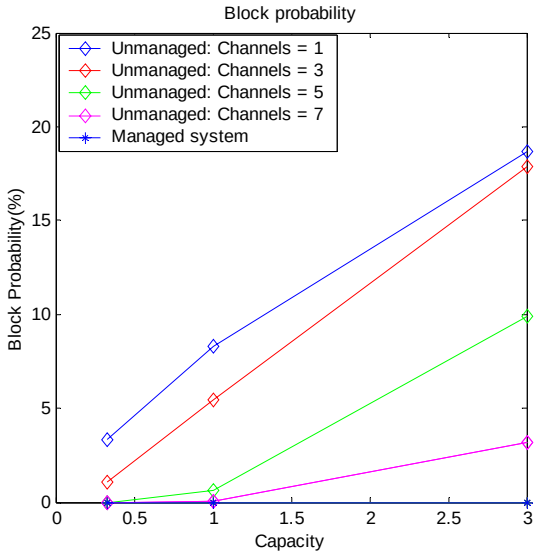

Figure 5.15 Blocking probability for the calls (fully elastic rates)

Figure 5.16 shows the drop probability of the calls. Drop of the calls occur due to the movement of the users between coverage areas of beams.

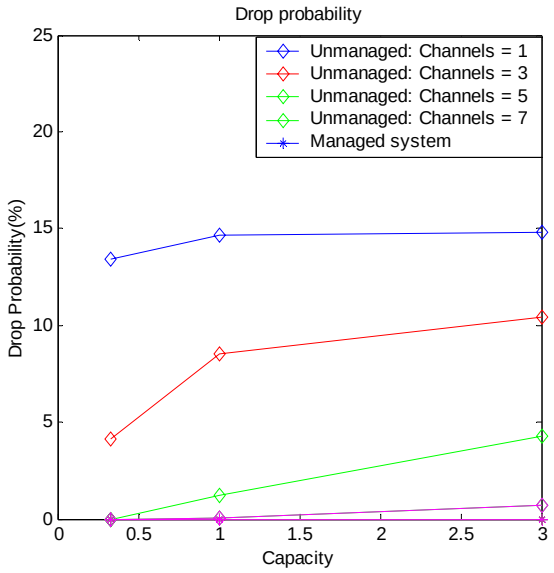

Figure 5.16 Drop probability for the calls (fully elastic rates)

The aggregate satisfaction index is given in Figure 5.17. The satisfaction index of the users is higher in a managed system. However with increasing capacity, the SI of the users decreases. Since the existing calls are degraded in order to accept new users into the system, the SI of the existing users decreases. This is seen in Figure 5.18 where the user the SI of the accepted users is plotted. The differential increase in SI with the use of resource management decreases for the users accepted into the cell. This is the price that we pay for reducing the call blocking rates.

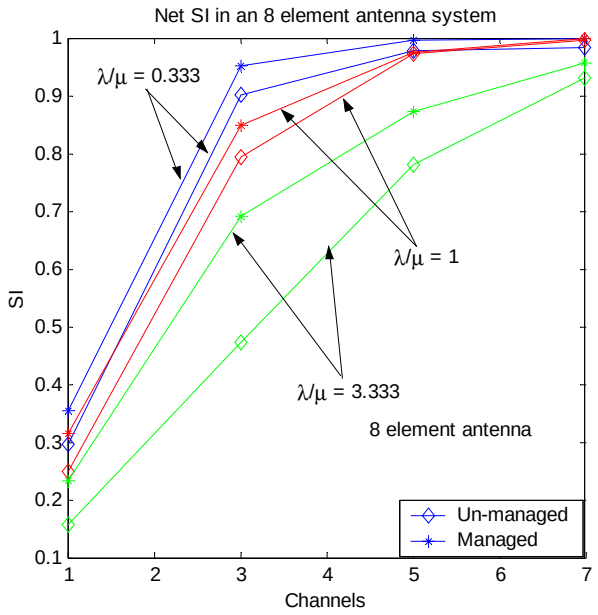

Figure 5.17 Net Satisfaction Index of the users (fully elastic rates)

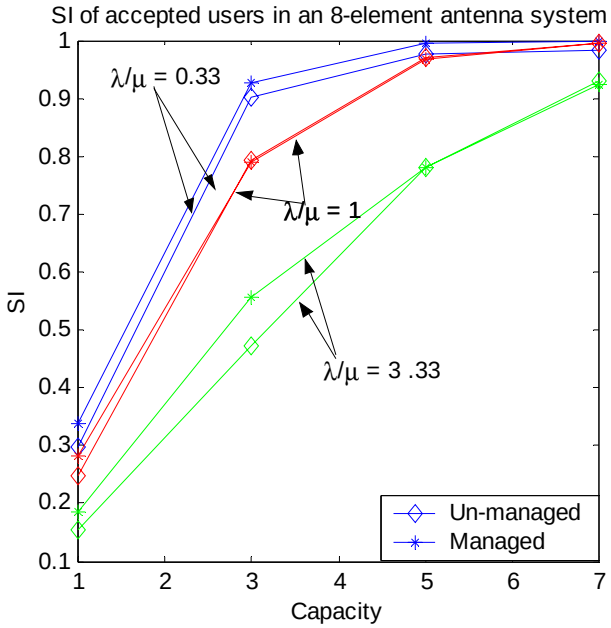

Figure 5.18 Satisfaction Index of accepted users (fully elastic rates)

5.8.2 Inelastic Users

In this section, we will consider the effect of resource management algorithm on users with different elasticity. We consider three transmission classes – one having full elasticity where the users can support data rates from the set {15 Kbps, 30 Kbps, 60 Kbps, 120 Kbps, 240 Kbps, 480 Kbps, 960 Kbps}; second having 4 step elasticity where the users can support rates from the set {15 Kbps, 60 Kbps, 240 Kbps, 960 Kbps}; the third can choose data rates from the set {15 Kbps, 960 Kbps}. The cell consists of only a single transmission class at one time. The simulation results for the throughput and SI is given in Figure 5.19 and Figure 5.20 respectively.

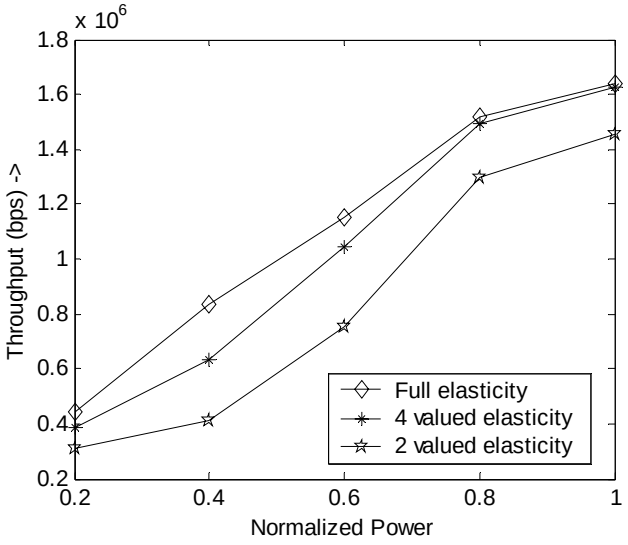

Figure 5.19 Aggregate throughput in the cell (in-elastic rates)

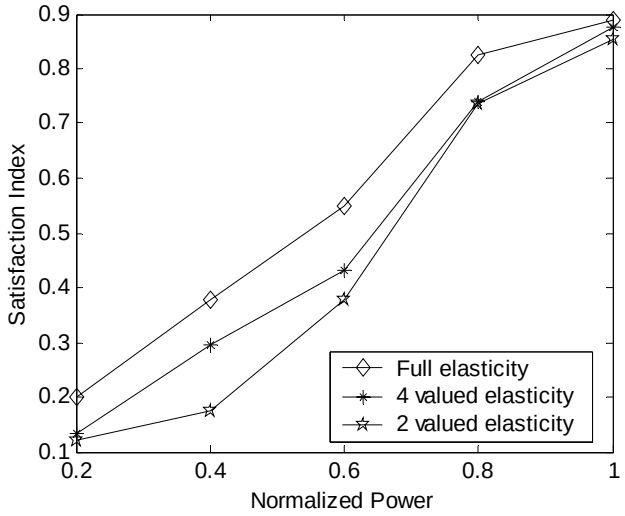

Figure 5.20 Satisfaction Index of the users (in-elastic rates)

We see that there is an increase in the aggregate throughput and average SI when the users have higher elasticity.

5.9 Effect of frequency of update

The resource management algorithm is adaptive. Hence, the frequency with which the algorithm is run will have an effect on the system. We conducted simulations with fully elastic users operating in a managed system varying the frequency with which the resource management is carried out. The resource management is applied in intervals of 1, 2 and 4. This means that when the resource management interval is 2, the resource management is done once every two simulation sample times.

The throughput for different resource management update intervals for three different capacity ratios is shown in Figure 5.21. From the figure it can be observed that the throughput in the cell decreases as the interval increases. The average SI of the users also follows the same trend. The call drop probability also increases as the interval increases. Since the resource management may not be applied at a time when the user moves from one coverage area to the other, the aggregate power in the beams will increase causing the call to be dropped. The call drop probability is plotted in Figure 5.23.

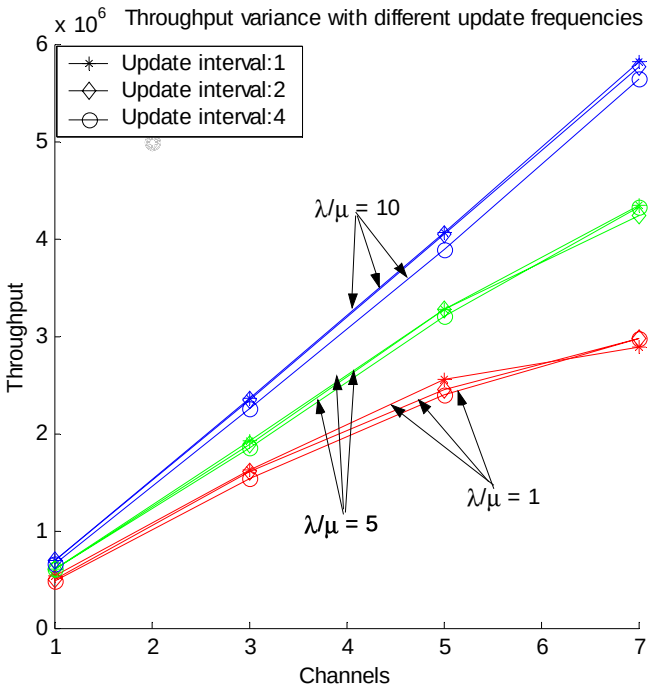

Figure 5.21 Throughput variation with different frequency for resource management

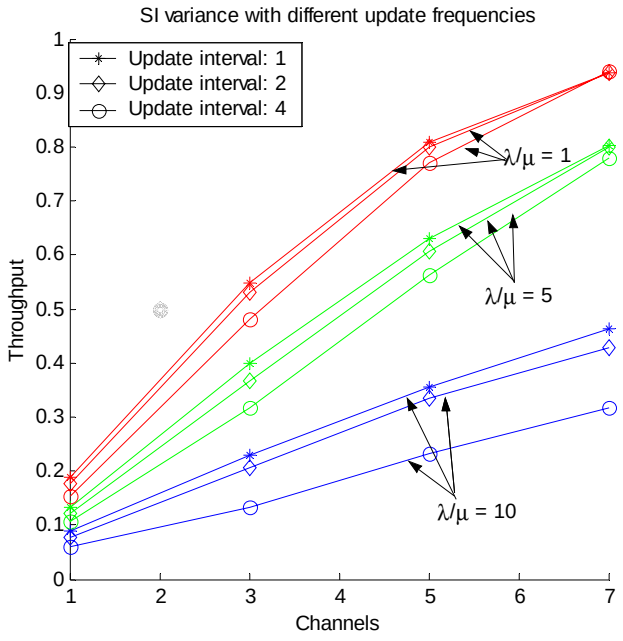

Figure 5.22 Satisfaction Index for different frequency of update for resource management

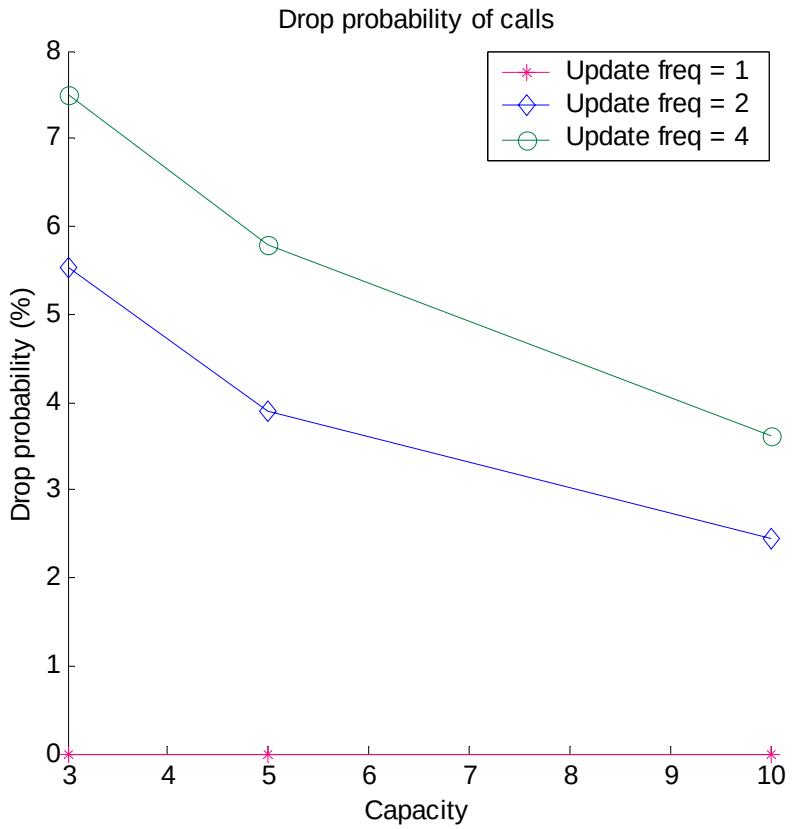

Figure 5.23 Variation in drop probability with different update intervals

5.10 Chapter Conclusion

We presented the simulation results obtained using the different resource management schemes in this chapter. First, we dealt with the simulation results applicable to a heterogeneous user system. The coding gain obtained using convolutional coding in a 3G system is presented next. The issues in radio resource management are discussed in section 5.5. The advantage of applying the resource management algorithm when applied to an omni-directional antenna system is shown in section 5.6. The performance advantage obtained by the application of resource management algorithm in a system that employs smart antennas is shown, and the effect of the frequency interval of update is presented in this chapter.

Chapter 6 CONCLUSIONS AND FUTURE WORK

In this chapter we present the summary of the work we have done, conclusions from the simulation studies we performed and areas for future research. The conclusions are based on the results presented in chapter 5. Primarily, we attempt to summarize the simulation model we have implemented and provide an overview of the proposed algorithms and the findings from the simulation studies. We also suggest some improvements that can be done to the algorithm in order to make it more suitable for other conditions.

6.1 Summary

This research aims at developing an algorithm that combines the beamforming parameters and multi-rate resource management parameters so as to maximize the aggregate throughput in the cell. With the demand for wireless data communications on the rise, it is anticipated that the need for adaptive QoS and deployment of smart antennas will be widespread.

3G systems will support both voice and data users. Some of these users are likely to be elastic in their demand for bandwidth, leading to additional flexibility in resource allocation and management. We model the QoS requests falling in different transmission classes – the transmission class is defined as requesting for a range of data rates with a specific BER requirement. The call arrival is modeled as a Poisson process and the inter-arrival time between calls has an exponential distribution. The transmitted signal is generated according to the 3G standards. The transmitted data is either uncoded or coded using rate ½ convolutional codes. OVSF codes are used for orthogonal spreading and for achieving a constant transmitted data rate. The users are differentiated using scrambling codes.

In order to develop a test bed for the algorithm, we modeled the cellular conditions applicable to a 3G-communication system. The primary external parameters that are modeled are the user mobility and the channel conditions. The interference level in the cell depends on the relative position of the users in the cell. In addition, changes in user location impact the resource management mechanism. Hence a model for user mobility is developed. For modeling the channel, the multipath profiles of the users depend on the distance of the user from the base station. The individual multipath components undergo Rayleigh fading. Since spatial diversity combining is also performed, the AoA of the received signal is important. The AoA is modeled using Petrus model, assuming scatterers to be distributed in a circular pattern around the user.

The resource allocation algorithm uses the parameters – power and AoA – measured from the pilot channel to make a decision about accepting a new user into the system. The power of other classes acceptable to the user is calculated and depending on the AoA of the multipath components, the call acceptance decision is made. The existing users may be degraded in order to accept the new user and thereby reduce the call blocking probability. The resource management algorithm continuously monitors the cell and reallocates the resources freed by an ended call. The management scheme takes advantage the elasticity of the users by bringing down the data rates in order to prevent, whenever possible, calls from getting dropped.

We studied the effect of channel conditions on the BER of the transmitted data. The effect of convolutional coding in interference-limited condition is also studied. We assess the performance of the algorithm under different load conditions. The conclusions drawn from the simulation results are listed in the next section.

6.2 Conclusions

From the study of the BER performance for heterogeneous users, the following conclusions can be drawn. Omni-directional antennas are used in this study.

- In a heterogeneous user system, the BER is not only related to the number of users in the cell but also to the data rate of the different users. A high data rate user in the system will significantly degrade the BER performance of other users in the system.
- Transmission of very high data rates in an outdoor channel renders very high BER as compared to transmission in an indoor channel. This is attributed to the higher number of multipath components present in an outdoor channel thereby detrimentally affecting the SINR of other users in the system.
- The use of a convolutional coder is not sufficient for a WCDMA system with multiple high data rate users.

We tested the performance of the proposed algorithms and compared the aggregate throughput, user satisfaction, call blocking probability and call dropping probability as compared to an unmanaged system. Our observations are listed below:

- The probability of the calls being dropped is high for a system with multiple beams and mobile users. Hence a mechanism to monitor the cell and manage the resources is essential for a smart antenna system.
- Even for a system without smart antennas, resource management provides an enhancement in the aggregate throughput. This can be attributed to the improved utilization of the resources by the system due to the reallocation of the resources that become free due to the calls that end.
- The SI of the users for a managed system is higher than that of an unmanaged system.
- The SI of the users is higher in a lower load condition. The decrease in SI arises due to the sharing of resources between multiple users in a higher load condition.
- In a smart antenna system with heterogeneous users, a managed system provides higher net throughput and higher SI for the users. The differential in the throughput increases as the load on the system increases. In other words, our proposed resource management algorithm provides greater benefit under high load conditions, as expected.

- The aggregate throughput in the cell increases when the users are fully elastic. The throughput and SI decreases when the elasticity of the users decreases.
- The aggregate throughput and user SI increase when the resource management is run at more frequent intervals. There is a tradeoff between the achievable benefit from the dynamic resource management and the overhead imposed by monitoring and adapting to current cell conditions very frequently.
- With the modified resource allocation algorithm, the blocking probability of the calls is reduced. However, this comes at the cost of the reduced SI of the accepted users in the system.
- The drop probability of the calls in a managed system depends on the frequency of update for the calls.

6.3 Future Research Directions

In this section we provide some pointers for further research in the area of resource allocation and management taking advantage of smart antennas deployed in the system. Some of the possible research areas are listed below:

- The resource allocation and management scheme can be modified to also include call hand off. In such a case, the user entering a cell from an adjacent cell will be treated in the same way as a user entering from the area serviced by another antenna.
- Resource reservation schemes for the users can be implemented. This will prevent QoS degradation when users have intra-cell and inter-cell handoffs.
- The resource management mechanism can employ prioritization of users and employ selective back off for lower priority users;
- The resource management algorithm proposed here can be adapted and tested for tracking beam antenna arrays. This will provide an added dimension of the beam former weights and decision on the users to be tracked.
- The resource management scheme can be expanded to incorporate more parameters such as modulation scheme, error correction mechanisms etc. in order to provide more stringent QoS guarantees to the users.

- This work can be adapted to incorporate recent wireless communication standards such as the Fourth Generation (4G) standards.

6.4 Chapter Conclusion

In this chapter we provided an overview of the work presented in this thesis and provided a list of the observations that we have drawn from the studies. Future research directions are also provided for the interested reader.

BIBLIOGRAPHY

[1] S. Choi, D Shim, T.K. Sarkar, "A Comparison of Tracking Beam Arrays and Switched-Beam Arrays Operating in a CDMA Mobile Communication Channel," *IEEE Antennas and Propagation Magazine*, Volume: 41 Issue: 6, Dec. 1999 pp 10-56.

[2] G. Song, K. Gong "Erlang capacity of a power controlled CDMA system with antenna arrays," *Vehicular Technology Conference Proceedings*, 2000.

[3] L. Jorguseski,E. Fledderus,J. Farserotu, R.Prasad "Radio resource allocation in third generation mobile communication systems," *IEEE Communications Magazine*, Feb. 2001, pp: 117 –123.

[4] T. Kwon, Y. Choi, C. Bisdikian, M. Naghshineh "Measurement-based Call Admission Control for Adaptive Multimedia in Wireless/ Mobile Networks," *Wireless Communications and Networking Conference*, 1999. pp: 540 -544 vol.2.

[5] L. Huang,S. Kumar, C. Kuo "Adaptive resource allocation for multimedia services in wireless communication networks," *Distributed Computing Systems Workshop 2001* pp: 307 –312.

[6] *Recommendation* 3G TS 23.107, "QoS Concept and Architecture," Third Generation Partnership Project Technical Specification Group Services and System Aspects, March 2000.

[7] S. Dixit, Y. Guo, and Z. Antoniou, "Resource management and Quality of Service in Third Generation Wireless Networks", *IEEE Communication Magazine*, vol. 39, no. 1, Feb. 2001, pp 125-133.

[8] S.K. Jong, and B. Kraimeche, "QoS Considerations on the Third Generation (3G) Wireless Systems," *Proc. Of Acadmia/Industry Working Conf. On Reasearch Challenges (AIWORC '00)*, 2000, pp. 249 –254.

[9] V. K. Garg, and O. T. W. Yu, “Integrated QoS Support in 3G UMTS Networks,” *Proc. IEEE Wireless Communications and Networking Conf. (WCNC 2000)*, vol. 3, 2000, pp 1187-1192.

[10] L. Bos, and S. Leroy, “Towards an all IP based UMTS Architecture,” *IEEE Network*, vol. 15, issue 1, Jan/Feb 2000, pp 36-45.

[11] T. Kuh, S. Levenson, and T. Walton, “End to End QoS Considerations for UMTS,” *IEEE Emerging Technologies Symp: Broadband Wireless Internet Access*, 2000.

[12] L.Z. Ribeiro and L.A. DaSilva, “Traffic demand characterization for multimedia mobile networks,” *Proc. IEEE Vehicular Technology Conf.*, Fall 2001, pp 620-624.

[13] L. Z. Ribeiro and L. A. DaSilva, “A Framework for the Dimensioning of Broadband Mobile Networks Supporting Wireless Internet Services,” accepted for publication in *IEEE Personal Communications Magazine*, 2002.

[14] B. Ahn, H. Yoon, and J-W. Cho, “Joint deployment of macrocells and microcells over urban areas with spatially non-uniform traffic distributions,” *Proc IEEE Vehicular Technology Conf.*, vol. 6, Fall 2000, pp 2634-2641.

[15] K.K. Leung, W. A. Massey, and W. Whitt, “Traffic models for wire-less communication networks,” *IEEE J. Select. Areas Communications*, vol. SAC-12, Oct. 1994, pp. 1353–1364.

[16] T. Tuna, and C. Ersoy, “Application of a Realistic Mobility Model to Call Admissions in DS-CDMA Cellular Systems,” *Proc. IEEE Vehicular Technology Conf.*, Spring 2001, pp 1047 – 1051.

[17] S. Tekinay, *Modeling and analysis of cellular networks with highly mobile heterogeneous Traffic sources*, Doctoral Dissertation, George Mason Univ., Fairfax, VA, 1994.

[18] M. Frodigh, “Performance bounds for power control supported DCA-algorithms in highway micro cellular radio systems,” *IEEE Trans. Vehicular Technology*

in highway micro cellular radio systems," *IEEE Trans. Vehicular Technology*, vol. 44, May 1995, pp. 238–243.

[19] P.Cardiari, *Resource Allocation and Adaptive Antennas in Cellular Communications*, Doctoral Dissertation, Virginia Polytechnic Institute and State Univ., VA, 1999.

[20] M.M. Zonoozi, and P. Dassanayake, "User Mobility Modeling and Characterization of Mobility Patterns," *IEEE J. Selected Areas of Communications*, vol. 15, pp 1239 – 1252, Sept. 1997.

[21] M. Rintamaki, I. Virtej, H. Koivo, "Two Mode Fast Power Control for WCDMA Systems," *Proc. IEEE Vehicular Technology Conf.*, Spring 2001. pp. 2893-2897.

[22] I. Virtej, M. Rintamaki, and H. Koivo, "Enhanced Fast Power Control for WCDMA Systems," *Symp. Personal, Indoor and Mobile Radio Communications (PIMRC 2000)*, 2000, pp 1435 –1439.

[23] S. Akhtar, S.A. Malik, and D.Zeghlache, "A Comparative Study of Power Control Stratergies for Soft Handover in FDD WCDMA System", *Proc. IEEE Vehicular Technology Conf.*, Spring 2001. pp. 2680-2684.

[24] P. Petrus, J.H. Reed and T.S. Rappaport, "Geometrically Based Statistical Channel Model for Macrocellular Mobile Environments," *Proc. IEEE Vehicular Technology Conf.*, Apr. 1996, pp. 844-848.

[25] J.C. Liberti, and T.S. Rappaport, "A geometrically based model for line-of-sight multipath radio channels," *Proc. IEEE Vehicular Technology Conf.*, 1996, vol.2, pp 844 –848.

[26] Alpha Concept Group, *Wideband Direct Sequence CDMA (WCDMA) Evaluation Document (3.0)*, SMG 905/97, Madrid, Spain, December 15-19, 1997.

[27] T. S. Rappaport, *Wireless Communications: Principles and Practice*, Prentice Hall, N.J., 1999.

Hall, N.J., 1999.

[28] P. Petrus, *Novel Adaptive Array Algorithms and Their Impact on Cellular System Capacity*, Doctoral Dissertation, Virginia Polytechnic Institute and State Univ., VA, 1999.

[29] R.B. Ertel and J.H. Reed, *Antenna Array Systems:Propagation and Performance*, Doctoral Dissertation, Virginia Polytechnic Institute and State Univ., VA, 1999.

[30] R.B. Ertel and J.H. Reed, "Angle and Time of Arrival Statistics for Circular and Elliptical Scattering Models," *IEEE Journal on Selected Areas In Communications*, vol. 17, no. 11, Nov. 1999, pp 1829 – 1841.

[31] *Recommendation* 3G TS 25.302, "Services provided by the Physical Layer," Third Generation Partnership Project Technical Specification Group Services and System Aspects, March 2000.

[32] *Recommendation* 3G TS 25.211, "Physical channels and mapping of transport channels onto physical channels," Third Generation Partnership project Technical Specification Group Radio Access Network,(FDD), December 1999.

[33] F.Alam, K. Zahid, B.D. Woerner and J.H. Reed**, "**Performance comparison between pilot symbol assisted and blind beamformer-rake receivers at the reverse link of third generation CDMA system," *Proc. IEEE Vehicular Technology Conf.*, Fall 2001, pp. 353-357.

[34] *Recommendation* 3G TS 25.212, "Multiplexing and Channel coding (FDD)," Third Generation Partnership project Technical Specification Group Radio Access Network,(FDD), December 1999.

[35] E.H. Dinan and B. Jabbari, "Spreading Codes for Direct Sequence CDMA and Wideband CDMA Cellular Networks," *IEEE Communications Magazin*e, vol. 36, September 1998, pp. 48-54.

[36] *Recommendation* 3G TS 25.213 V2.1.2, "Spreading and Modulation," Third Generation Partnership project Technical Specification Group Radio Access

Generation Partnership project Technical Specification Group Radio Access Network,(FDD), April 1999.

[37] J.H.Reed, *Software Radios: A Modern Approach to Radio Design,* to be published by Prentice Hall, N.J. 2002.

[38] J. Wang and J. Chen, "Performance of wideband CDMA systems with complex spreading and imperfect channel estimation," *IEEE J. Selected Areas in Communications*, vol. 9, no.1, Jan 2001, pp. 152 –163.

[39] J.C. Liberti and T.S. Rappaport, *Smart Antennas for Wireless Communications:1S-95 and Third Generation CDMA applications,* Prentice Hall, N.J. 1999.

[40] Y. Lei, *Resource Management with Smart Antenna in CDMA Systems,* Master's Thesis, Dept. of Electrical and Computer Engineering, Virginia Polytechnic Institute and State University, Blacksburg, VA, November 2001.

[41] K. Zahid, *Space-time Processing for the Wideband-CDMA System,* Master's Thesis, Dept. of Electrical and Computer Engineering, Virginia Polytechnic Institute and State University, Blacksburg, VA, Dec. 2000.

[42] D.Goodman, N. Mandayam, "Power control for wireless data," *IEEE Personal Communications*, April 2000.

[43] S.A.Brandt, "Performance analysis of dynamic soft real-time systems," *IEEE International Conference on. Performance, Computing, and Communications*, 2001. pp. 379 –386.

[44] *Radio Resource Management in Cellular Systems*, N. D. Tripathi, J. H. Reed and H.F VanLandingham; Kluwer Academic Publishers.

[45] T. Minn and K-Y Siu, " Dynamic Allocation of Orthogonal-Variable-Spreading-Factor Codes in W-CDMA," *IEEE Journal on Selected Areas in Communications*, vol. 18, no. 8, Aug. 2000, pp 1429 – 1440.

GLOSSARY OF ACRONYMS

2D Rake	:	Two-dimensional Rake receiver
2G	:	Second Generation
3G	:	Third Generation
3GPP	:	Third Generation Partnership Project
AICH	:	Acquisition Indicator Channel
AoA	:	Angle of Arrival
ATM	:	Asynchronous Transfer Mode
BCH	:	Broadcast Channel
BER	:	Bit Error Rate
BS	:	Base Station
CDF	:	Cumulative Distribution Function
CDMA	:	Code Division Multiple Access
CN	:	Core Network
CPCH	:	Common Packet Channel
CPICH	:	Common Pilot Channel
DCH	:	Dedicated Channel
DL	:	Downlink
DoA	:	Direction of Arrival
DPCCH	:	Dedicated Physical Control Channel
DPCH	:	Dedicated Physical Channel
DPDCH	:	Dedicated Physical Data Channel
DPDCH	:	Dedicated Physical Data Channel
DSCH	:	Downlink Shared Channel
FACH	:	Forward Access Channel
FDD	:	Frequency Division Duplexing
FDMA	:	Frequency Division Multiple Access
IP	:	Internet Protocol
ISI	:	Inter Symbol Interference

L1	:	Layer 1 – Physical layer
LOS	:	Line of Sight
MAC	:	Media Access Control
MAI	:	Multiple Access Interference
MS	:	Mobile Station
OSI	:	Open Systems Interconnect
P-CCPCH	:	Primary Common Control Physical Channel
PCH	:	Paging Channel
PCPCH	:	Physical Common Packet Channel
PCS	:	Personal Communication System
PDSCH	:	Physical Downlink Shared Channel
PICH	:	Page Indicator Channel
PRACH	:	Physical Random Access Channel
PRACH	:	Physical Random Access Channel
QoS	:	Quality of Service
RAB	:	Radio Access Bearer Service
RACH	:	Random Access Channel
RAN	:	Radio Access Network
RRC	:	Radio Resource Control
RRM	:	Radio Resource Management
S-CCPCH	:	Secondary Common Control Physical Channel
SCH	:	Synchronization Channel
SDMA	:	Space Division Multiple Access
SDU	:	Service Data Unit
SI	:	Satisfaction Index
SINR	:	Signal to Interference and Noise Ratio
SMS	:	Short Messaging Service
TC	:	Transmission Class
TDD	:	Time Division Duplexing
TDMA	:	Time Division Multiple Access
TE/MT	:	Terminal Equipment/Mobile Termination

TFCI	:	Transport Format Combination Indicators
UE	:	User Equipment
UL	:	Uplink
UMTS	:	Universal Mobile Telecommunication System
UTRAN	:	UMTS Terrestrial Radio Access Network
WCDMA	:	Wideband CDMA

Vita

Shakheela H. Marikar was born on December 1975 in Alleppey, India. She received her B.Tech degree from the College of Engineering, Trivandrum, India and was awarded the University gold medal for academic excellence. After her undergraduate degree she worked as a systems engineer in the industry for a period of two and half years. She worked as a research assistant in the Mobile and Portable Radio Group during her tenure in Virginia Tech.